RADIOCHEMICAL STUDIES ON ENVIRONMENTAL RADIOACTIVITY IN SUDAN

Adam Khatir Sam

B.Sc (Chemistry), M.Sc (Radioanalytical Chemistry), M.Sc (Radioecology).

A Thesis presented for the degree of Doctor of Philosophy in Radiochemistry

Department of Chemistry
Faculty of Science
University of Khartoum
1998

ACKNOWLEDGEMENTS

The work reported in this thesis has been carried out in Radiochemistry Laboratory at the Department of Radiation Physics, Lund University, Sweden under the external supervision of Professor Elis Holm through the financial support of International Atomic Energy Agency (IAEA). I am extremely grateful to Professor Elis Holm for accepting to act as my external supervisor, encouragement, fruitful suggestions, generous support through out the course of this work, and hospitality.

I am indebted most of all to my internal supervisor Associate Professor El Nigumi, Y. O. And co-supervisor Dr. Mustafa Mohammed Osman for their support and encouragement through out the study.

In preparing this work I have been assisted by and received advice from numerous individuals and institutions. I would like to detail and acknowledge:

I am sincerely grateful to Mrs Petersson , M. G., for reading and commenting upon the earlier versions of the thesis. Her fruitful suggestions greatly improved the quality of the final version.

I am under substantial intellectual debt to Dr. El Khangi, F. A., Director of Research and Services, Sudan Atomic Energy Commission (SAEC), whose sustained interest, assistance, stimulating discussions, constructive criticisms and scholastic philosophy, I acknowledge with special appreciation.

There are many persons who sacrificed much to make, even in the most difficult circumstances, that the institutional co-operation work. I so much respect that efforts from Omer I. El-Amin, Director General, SAEC and Dr. Shaddad, I. A., Head, Physics and instrumentation Department, SAEC.

Dr. Abdel Gadir El Hag, Vice Chancellor, the Red Sea University, Mr. Mohammed Al-Amin, Dean, Faculty of Marine Sciences and Fisheries and former college colleague Mr Ibrahim Ahamed Ali, Mr Madani El Hag M., Director, El Nile Petroleum Company, Port Sudan, Mr Omer Zakaria, Port Sudan Custom Laboratory, Capt. Mahmoud Sayed Ahamed, Maritime Administration Directorate, Mr Ahamed El-Toum, Sawakin Harbour, for giving me all the support without which it would have been impossible for me to conduct field work in the Red Sea. I am extremely unfortunate in receiving that help.

I acknowledge gratefully the assistance given to me by Dr. Roos P., Mr. Dan Josefsson, Mr. Mats Eriksson and Ms Johansson Lena, Radiochemistry Laboratory, Radiation Physics Dept., Lund University and the rest of the technical staff who help in one way or another for the accomplishment of this work.

Many thanks to my friends and colleagues in SAEC, and specially Ms Amal Ahamed who assisted me during sample collection and preparation.

Not the least, I extend many thanks to all those who positively contributed to my learning and to this research. For their names, I symbolically leave this space ...., and my sincere gratefulness.

Finally I would like specially to express my warm gratitudes to my wife, Nagwa, for a wonderful understanding during these years.

DEDICATION

I dedicate this thesis to the memory of my mother, my father, my wife and children, my sisters and brothers, to the soul of my late grandfather, all relatives and friends in El Fasher, to my best friend and former college colleague Mr Adam Moalim Yagoub.

TABLE OF CONTENTS

3. MATERIAL AND METHODS

PREFACE

The work upon which this thesis is based consists of three parts:

The first part deals with the assessment of terrestrial gamma- radiation in Sudan from the measurements of radionuclide activity concentrations in the soil. As a fact of nature, in the natural environment man is exposed to ionising radiation due to gamma-emitting radionuclides of uranium and thorium decay chains, and ^{40}Kwhich are present in the earth's crust, and to cosmic ray secondaries. Abnormal occurrences of uranium and its decay products in rock outcrops, soil and ground water, and thorium in monazite sands, are the main causes of high natural background areas that have been identified in several areas of the world (Roser et al., 1964). For instance, in southern Kerala and Tamil Nadu in India the absorbed dose rates in air reach 6000 nGy/h (UNSCEAR, 1988). Whereas, about 95% of the world's population live in areas of normal background radiation, with outdoor exposure ranging from 30 to 70 nGy/h (UNSCEAR, 1977). The occurrence of such anomalous background levels necessitates surveys on natural environmental radiation background and the evaluation of its contribution to the collective population dose. Furthermore, the progressive development of the nuclear industry and other contaminating technologies and the widespread and ever-increasing use of radiation in many aspects of life has made it necessary to conduct radiological surveys to evaluate the background of natural radiation in order to detect the level of man-made contamination, assess its impact, and implement appropriate countermeasures to protect the populace and the environment from radiation emergencies.

Interest in this kind of study has led to worldwide national surveys on natural radioactivity during the last decade (Yu-ming Lin et al. 1987; Myrick 1983; Leung et al. 1990; Quindos et al. 1993). The information obtained in the current study, is the only one in Sudan to date on the assessment of external exposure from terrestrial gamma- radiation. It is hoped that it will initiate a soil radiation map of the country (natural and man-made radionuclides) and provide a useful reference for the design

and development of a specific regional surveys related to the measurements of indoor and outdoor exposure in those areas with relatively higher levels of natural radioactivity. In a country where the development of the standards and the regulatory control action on radiation protection are under way, such data will provide a useful reference.

The second part deals with the radiological and chemical assessment of the Uro and Kurun rock phosphate deposits in the eastern part of the Nuba Mountains, western Sudan. The phosphate rock is the starting raw material for production of all phosphate products. It can be of sedimentary, volcanic or biological origin. The sedimentary phosphates usually have higher radioactivity than igneous phosphates. Concentrations of ^{232}Th and ^{40}K in phosphate rocks of all types are similar to those observed in soils, whereas the concentrations of ^{238}U and its decay products are high, which implies that the various radionuclides of the uranium decay series can be partitioned by physical and chemical means during phosphate mining and subsequent processing. Radium, a long-lived member of the ^{238}U series, with its half-life of 1600 years, can exist for long periods of time after separation from the parent. It is biologically available and is the immediate precursor of ^{222}Rn that has been implicated as potential inhalation hazard. Untreated ground rock phosphate have been used as plant fertilizers in many parts of the world at different rates of fertilization. The extensive use of rock phosphate fertilizers increases the external radiation exposure for the farmers and the α-activity of the food products via root uptake. The current study aims at evaluating the radioactivity level of the Uro and Kurun rock phosphates and assessing the additional external radiation exposure for the farmers when using these untreated ground rock phosphates as fertilizers. Visual inspection reflects lithological differences within the ore deposits which might be related to iron content or redox state. These differences were screened to provide a perspective on their relative contribution to ore radioactivity. In addition, investigations were undertaken to evaluate the exchangeable fraction of ^{226}Ra that contaminates the calcium source of the plants, maximum emanation power of the rock phosphate, exchangeable cations (Ca^{++}, K^{+}, Mg^{++}),

soluble phosphorus as well as pH and organic matter content. This study also considers the economic feasibility for using Uro and Kurun phosphate deposits as a feed material for uranium extraction.

The third part deals with the determination of radioactivity levels in marine sediments and marine organisms collected from the Sudanese coastal waters of the Red Sea. The occurrence of uranium and thorium and their decay products in marine environments has been a subject of study for many years, for a better understanding of oceanographic processes and phenomena, and the protection and management of the marine environment. The addition of man-made radionuclides to this pool of naturally occurring radionuclides, both from the atmospheric testing of nuclear weapons and from the authorized discharge of radioactive waste into coastal waters and the open sea, has led to worldwide research in marine radioactivity during the last decade especially in the developed countries. In developing countries there is a growing need for such studies in connection with the protection of their continental shelf and estuaries from land-based pollution and other types of anthropogenic impact on their marine and aquatic ecosystems. Sudan has c.853 km of coastline along the Red Sea which are of great economic, recreational and aesthetic value. To date no information is available on the radionuclide concentration levels (natural or artificial) in the different marine compartments (sediments, organisms, water). In a busy international water way like the Red Sea which is susceptible to accidental contamination, such lack of data impairs judgement on possible contamination of this environment, so it will be necessary to assess the levels of the existing radionuclides. In today's world, where transboundary accidents can occur such lack of data is unacceptable. Thus, measurements of activity concentrations of uranium and thorium isotopes, ^{226}Ra, ^{210}Po, ^{40}K and ^{137}Cs in sediments and marine organisms from the Sudanese Red Sea coast will be invaluable as base-line data help to define future research activities in marine radioactivity and as a monitor for determining unequivocally any future contamination.

The third part of the study programme was extended in order to look into the

behaviour of alpha-emitting isotopes of thorium and uranium in Port Sudan and Sawakin harbour sediments as well as to have a picture on the influence of terrestrial influx from the hinterland into the data. The naturally occurring alpha-emitting uranium isotopes, ^{238}U, ^{235}U and ^{234}U are present in large quantities in the world's oceans, due mainly to the formation of the very stable uranyl carbonate complex $[UO_2(CO_3)_3]^{-4}$ which results in a residence time in the oceans of nearly half a million years (Cochran, 1992)*. Although the $^{235}U/^{238}U$ activity ratio in seawater and coastal marine sediments is identical to what is often found in the continental crust, the $^{234}U/^{238}U$ ratio is greater than unity because of the preferential mobilization of ^{234}U during chemical weathering (Chen et al., 1986)* and to the scavenging from the water column into the sediments of ^{234}U produced *in-situ* from its recoil displaced progenitor ^{234}Th. The knowledge of isotopic ratios is important in constructing the geochemical balance of uranium and in understanding its behaviour in any domain of the system particularly the marine environment since the uranium isotopes ^{235}U and ^{234}U are parent isotopes for the particle reactive isotopes of ^{231}Pa and ^{230}Th respectively, which has recently proved to be of great value in sediment dating.

Thorium is known as one of the least soluble elements in seawater due to its tendency to hydrolyze and associate with particle surfaces. Indeed, ^{232}Th enters the oceans primarily in detrital form derived from continents, although Scott (1968)* has shown that there is some mobilization of thorium during weathering and soil formation. Unlike non-radiogenic ^{232}Th, other naturally occurring alpha-emitting thorium isotopes, ^{230}Th and ^{228}Th, have *in-situ* sources in marine environments resulting from the decay of conservatively behaving ^{234}U and ^{228}Ra parents, respectively. Owing to the particle reactive nature of thorium, the distribution of ^{230}Th and ^{228}Th in solution, suspended particles and sediments as well as the parent/daughter ratios have been used extensively to study the rate of sedimentation (Huh and Kadako, 1992) and mechanism of chemical scavenging in the oceans (Nozaki et al., 1981; Bacon and Anderson, 1982)*. Chemical scavenging is a process which is believed to be important in controlling the distributions and concentrations of many trace metals. In

open ocean scavenging is usually dominated by biogenic particles, and the short-lived ^{228}Th (5.7 years) is particularly useful in determining rates of cycling of these particles since its half-life is comparable to the scales of temporal variations in surface ocean processes (Murnane et al., 1990)*. The scavenging rates are not constant, however, but increase towards the shore (Bhat et al., 1969 and Kaufman et al., 1981)*.

There is a considerable body of literature on the concentration and behaviour of uranium and thorium isotopes in marine sediments from different regions of the world, but very few investigations have been carried out with sediments from the Red Sea (Ku, 1969), particularly from the Sudanese coastal region (Sam et al., 1996). In the present study, activity concentrations of alpha- emitting uranium and thorium isotopes have been determined in the sediments from harbours at Port Sudan and Sawakin and their behaviour is discussed in terms of isotopic concentration ratios, variation with depth and organic matter content.

*(Note: * these references are listed at the end of the bibliography list)*

ABSTRACT

Measurements of uranium and thorium isotopes, ^{226}Ra, ^{210}Po, ^{228}Ra, ^{40}K and fallout radionuclide ^{137}Cs in soil samples collected from different districts in Sudan, rock phosphate samples collected from the Uro and Kurun rock phosphate deposits in the eastern part of the Nuba mountains in western Sudan, and surface marine sediments and marine organisms collected from the Sudanese coastal waters of the Red Sea have been made using a high resolution gamma-spectrometry, radiochemical separation and α-spectrometry.

The external exposure due to γ-radiation from the ground has been calculated from the results of the measurements of radionuclide activity concentrations in the soil samples. The average exposure was found to be 45.4 ± 21.3 nGy/h, corresponding to the annual dose equivalent of 278 μSv/y. With the exception of the Arkuri and Dumper areas in the western part of the country, the calculated exposure falls within the global wide range of outdoor radiation exposure given in the UNSCEAR publications. The nation-wide average concentrations of ^{226}Ra, ^{238}U, ^{232}Th, ^{40}K and ^{137}Cs determined were 31.6 ± 27 , 20.1 ± 16.4, 19.1 ± 8.1, 280.3 ± 137.6 and 4.1± 4.3 Bq/kg, respectively. This shows that there is little contamination due to fallout radioactivity at survey sites. The exchangeable radium fraction constitutes 19 -24% of the total radium content.

The data show that ^{238}U and its decay products are the principal contributors of radioactivity in both phosphate deposits at Uro and Kurun. The highest activity concentrations were measured in grey coloured rock phosphate samples. The equivalent mass concentrations of uranium in the Uro rock phosphate fall within the range that could be economically recovered as the by-product of fertilizer industry. The mean activity concentrations weighted by the average agricultural consumption of 300 kg/ha of untreated ground rock fertilizer resulted in an annual distribution of 120.63 Bq Ra/m^2 , 0.22 Bq Th/m^2 and 1.77 Bq K/m^2 with Uro rock and 12.97, 0.21 and 4.24 Bq/m^2 respectively, with Kurun rock fertilizer. From these values the

external radiation exposure over agricultural areas was estimated under the assumption that the activity remains in the soil until removal by radioactive decay. This resulted in an additional external radiation exposure for the population of 23.41 x 10^{-9} Gy/h and 2.59 x 10^{-9} Gy/h at 1 m above ground level for Uro and Kurun rock phosphate fertilizers, respectively. These estimates show that the natural radionuclides contained in Uro and Kurun rock fertilizers contribute only little to the mean terrestrial radiation exposure of the population. However, the exposure rate (absorbed dose rate in air) 1 m above Uro and Kurun phosphate deposit areas as estimated using dose rate conversion factors reach 7108 and 402 nGy/h, respectively, which place them among high background radiation areas. The exchangeable radium fraction in rock phosphates constitutes 0.24% (Uro) and 0.08% (Kurun) of the total amount of the radium. Estimates of the maximum emanation have shown that the extent of contamination that could be expected for the calcium source of the plant from Kurun rock fertilizer is negligible compared with that of unfertilized soils. The total activity of the Uro rock phosphate was the highest as estimated using the radium equivalent index and compared with values from some other countries.

In marine sediments analysed, the maximum activity concentrations of ^{238}U, ^{226}Ra, ^{210}Po, ^{232}Th, ^{40}K and ^{137}Cs were found to be 53, 59.9, 94.7, 19.3, 515 and 10.1 Bq/kg dry weight, respectively. Comparison of the data on natural radionuclides from coastal marine sediments with those collected from 30 km off-shore (Sanganeb atoll) reveals that both anthropogenic and terrestrial influx from the hinterland into the data is negligible. However, values for ^{226}Ra and ^{210}Po are higher in the sediments from Port Sudan harbour relative to those from the adjacent fringing reefs. Uranium content is higher in shallow-water sediments and the authigenic fraction constitutes 12% on the average. The $^{228}Th/^{232}Th$ disequilibrium in sediments indicates a rapid rate of sedimentation at the sampling sites. The activity levels detected for ^{137}Cs in sediments collected from the Port Sudan harbour are fairly high as compared with values from other sampling areas. On the basis of individual data , the variations are insignificant with regard to the uptake of natural radionuclides by marine species considered in this

study. However, ^{137}Cs activity in algae ranged from 0.33 to 1.32 Bq/kg with *Sargassum* (brown algae) showing the highest level.

PUBLICATIONS

This thesis is based on the following papers:

1- Sam, A. K, M. M. O. Ahamed, F. A. El Khangi, Y. O. El Nigumi and E. Holm. Assessment of terrestrial gamma-radiation in Sudan, *Radiation Protection Dosimetry*, 71(2), 141-145 (1997).

2- Sam, A. K, M. M. O. Ahamed, F. A. El Khangi, Y. O. El Nigumi and E. Holm. Radioactivity levels in the Red Sea coastal environment of Sudan. *Marine Pollution Bulletin, in press* (1996).

3- Sam, A. K, M. M. O. Ahamed, F. A. El Khangi, Y. O. El Nigumi and E. Holm. Radiological and chemical assessment of Uro and Kurun rock phosphates. *J. Environ. Radioactivity, in press* (1997).

4- Sam, A. K, M. M. O. Ahamed, F. A. El Khangi, Y. O. El Nigumi and E. Holm. Concentrations and behaviour of uranium and thorium isotopes in some Red Sea sediments. *Submitted to the Journal of Environmental Radioactivity* (1997).

LIST OF TABLES

LIST OF FIGURES

Chapter 1

ENVIRONMENTAL RADIOACTIVITY

1.1 Introduction

Radioactive elements present in the environment can be classified into three groups according to their origin: terrigenous, cosmogenic and man-made. The terrigenous radionuclides include the three primordial actinide parent nuclides, ^{238}U, ^{232}Th and ^{235}U and their respective decay products; and the long-lived primordial nuclides of elements coexisting in the environment with stable counterparts. The important members in this later category include ^{40}K ($t_{1/2}$ = 1.25 x 10^9 y) and ^{87}Rb (half-live = 4.7 x 10^{10} y). ^{40}K has a natural abundance of 0.0118% and accounts for about 90% of the radioactivity of seawater. A unique feature of the three primordial nuclides, ^{238}U, ^{232}Th and ^{235}U and their respective decay products, is that each independent decay-series has chemically and physically dissimilar elements, with a wide range of characteristic half-lives. The two most important natural decay series, the uranium (4n +2) and the thorium (4n) series, are named after their parent nuclides (**Fig. 1.1-2**). The third series headed by ^{235}U is called the actinium series (4n+3). Any sample of natural uranium contains ^{235}U in a constant amount relative to ^{238}U isotope, viz. 0.72% (UNSCEAR, 1977; 1982; 1988). If the radionuclides in these series are left undisturbed, they attain a state of radioactive equilibrium in which the activity of each member of the series is the same as that of the parent. Due to chemical or physical separation processes, 100% radioactive equilibrium with the head of the series is rarely found. Aspects of radioactive equilibrium are important in environmental radiology since they can be used to monitor the effects of

chemical and geologic processes.

Both ^{40}K and ^{87}Rb are belong to the alkali metal group, so that they are dispersed widely over the whole environmental spheres, especially in the hydrosphere, due to their susceptibility to weathering. The radioactivity of ^{40}K thus represents over 90% of the total radioactivity of sea water, while that of ^{87}Rb corresponds approximately 1%. In a closed system the decay of ^{40}K and ^{87}Rb respectively to ^{40}Ar and ^{87}Sr provides the basis for geochronology (Fukai and Yokoyama, 1982).

The cosmogenic radionuclides, on the other hand, are produced continually in the upper atmosphere by interaction of cosmic radiation with gaseous atoms of nitrogen, oxygen and argon. At least 14 cosmogenic radionuclides are known. The important members of this group include:

^{3}H (Half-life: 12.3 y),

^{10}Be (Half-life: 2.5 My),

^{7}Be (Half-life: 53 days),

^{14}C (Half-life: 5730 y),

^{26}Al (Half-life: 7.2×10^{5} y),

^{32}Si (Half-life: ~ 560 y) and

^{36}Cl (Half-life: 3.1×10^{5} y).

^{14}C is rapidly oxidized to CO_2 in the biosphere maintaining a uniform global concentration ($^{14}C/^{12}C = 10^{-12}$). Atmospheric testing of nuclear weapons and emissions from nuclear power reactors and reprocessing plants have added considerable quantities of ^{14}C and ^{3}H to the natural pool (Andras, 1993 and Jaworowski, 1982). The presence of artificial ^{3}H and ^{14}C must be considered when using these nuclides as tracers. The long half-life and low abundance of ^{10}Be ($^{10}Be/^{9}Be < 10^{-14}$), ^{26}Al ($^{26}Al/^{27}Al < 10^{-14}$) and ^{36}Cl ($^{36}Cl/^{37}Cl \sim 10^{-15}$) make their measurement difficult in environmental materials.

Man-made (artificial) radionuclides originate from testing of nuclear weapons, controlled discharge of liquid effluent from nuclear facilities and as a consequence of nuclear accidents. The long-lived anthropogenic radionuclides:

^{137}Cs (Half-life: 30 y),

^{90}Sr (Half-life: 28.8 y),

^{238}Pu (Half-life: 87.7 y),

^{239}Pu (Half-life: 24100 y) and

^{241}Pu (Half-life: 14.4 y)

released into the stratosphere as a result of atmospheric nuclear weapons tests during 1950's and early 1960's have been distributed globally and deposited on the earth's surface as particulate fallout with a mean atmospheric residence time of about 1 year. The general global pattern of fallout horizontal distribution shows maxima at 45 °N and S, and minima at equator and the poles (Martell, 1970; Fukai and Yokoyama, 1982; Pentreath, 1984; Stanners and Aston, 1981 Holm, 1994). The vertical distribution of these nuclides in various sediments, soils and ice sheets can be correlated with the recorded fallout patterns to obtain time horizons for the period since the onset of weapons testing or accident e.g. $^{134}Cs/^{137}Cs$ activity ratio due to the previous nuclear weapons test is zero, 0.5 in the Chernobyl fallout in 1986 and 0.25 in releases from nuclear fuel reprocessing plants (Krishanswami et al., 1971; Pennington et al., 1973; Ritchie et al., 1973; Kiode et al., 1979; 1985; Cutter et al. 1979; Kiode and Goldberg, 1981; Aarkrog, 1994).

1.2 Geochemistry of ^{238}U, ^{232}Th and their decay products

Uranium and thorium occur naturally occur in association with varying amounts of their radioactive decay products (**Fig. 1.1-2**),viz. the isotopes of radium, radon, polonium, bismuth and lead (see **Table 1.1** for electronic structure). The

differences in chemical and physical properties of the parent and its daughters usually lead to separation (termed fractionation) of these radionuclides, thus giving rise to radioactive disequilibrium.

Uranium, thorium and radium ([Rn]$7s^2$) are electropositive elements and tend to form strong ionic bonds. Radon is a noble gas and is not ionized or reactive under environmental conditions. Polonium, lead and bismuth are amphoteric and in the natural environment may form ionic bonds with some covalent character, which leads to difficulties in predicting their behaviour in natural waters of high ionic concentrations (e.g. sea water) or in the presence of organic compounds.

In aqueous media Ra^{+2} and Th^{+4} generally form colourless solutions but due to the presence of one or more electrons in the outer shells the concentrated U^{+4} and U^{+6} solutions are often coloured (green and yellow, respectively). In aqueous solutions, they all hydrolyze to varying extents depending on the pH. Th^{4+} hydrolyzes when the pH is above 3, forming a variety of hydroxide species. The U^{6+} ions do not exist in solution simply as hydrated ions but instead as "oxo ions" of the form UO_2^{2+} (Gascoyne, 1992).

1.2.1 Geochemical associations

Uranium and thorium are mainly found associated with granites and pegmatites (Goldschmidt, 1954). Most radium salts are insoluble, particularly the sulphate and carbonate. Bismuth has only one stable isotope (^{209}Bi) and is generally found in apatides and sulphides. Little is known about the chemical properties of polonium, and ^{210}Po is intensively radioactive with a short half-life (138 days). Stable lead isotopes are usually occur in association with sulphides and apatite.

Fig 1.1: ^{238}U decay series

↗ β-decay

↓ α-decay

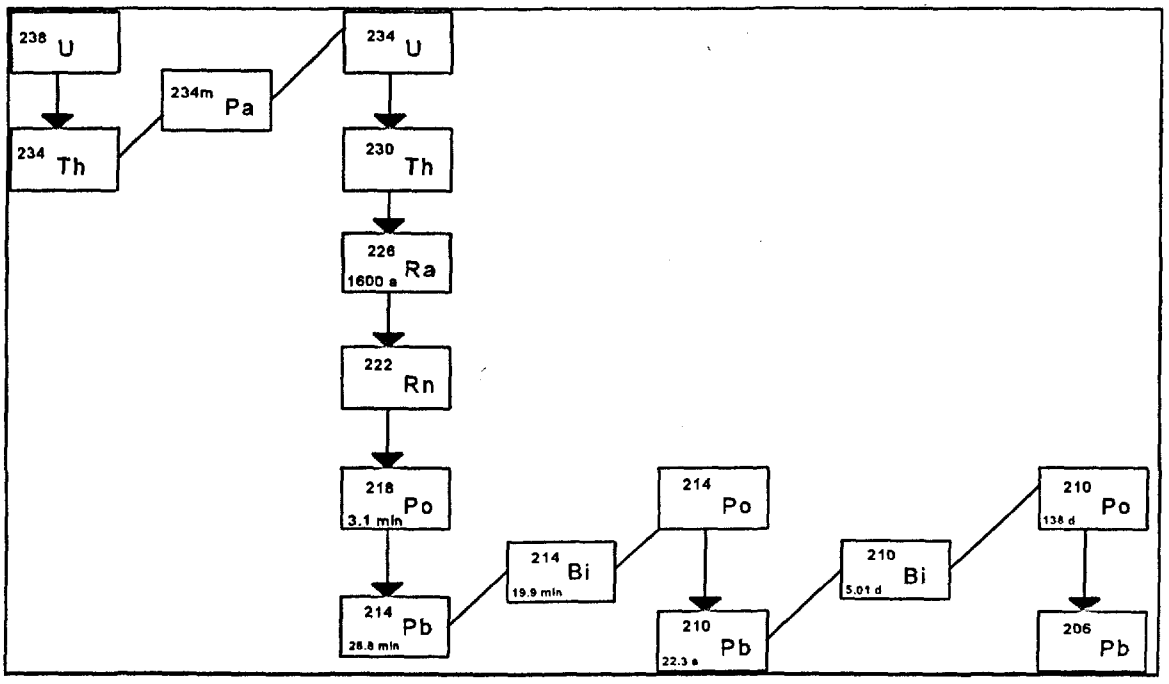

Fig 1.2: ^{232}Th decay series

↗ β-decay

↓ α-decay

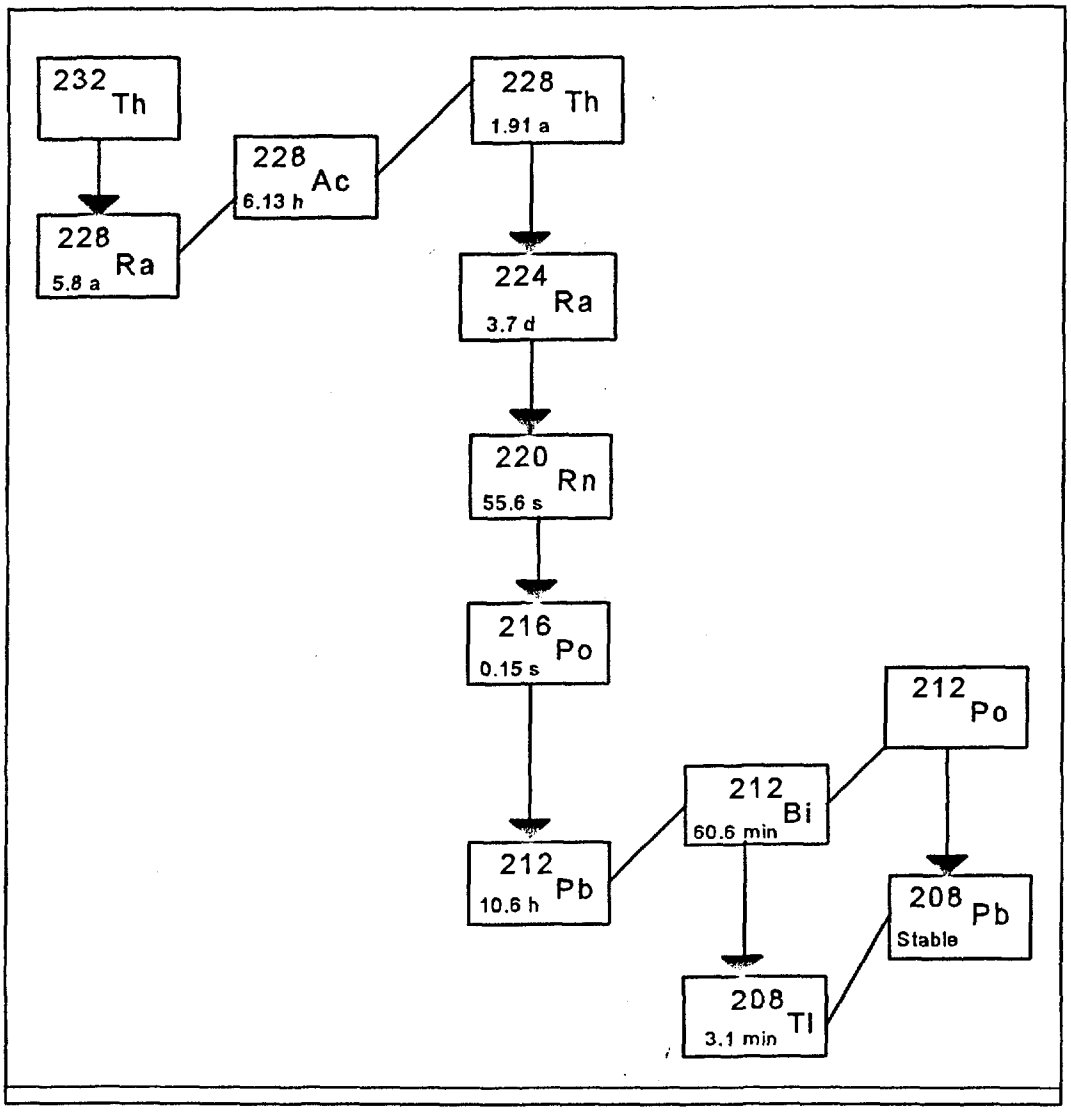

Table 1.1

Electronic structure of uranium, thorium and their decay products

Element	Z	Electronic structure
Pb	82	$[Xe]\ 4f^{14}\ 5d^{10}\ 6s^2\ 6p^2$
Bi	83	$[Xe]\ 4f^{14}\ 5d^{10}\ 6s^2\ 6p^3$
Po	84	$[Xe]\ 4f^{14}\ 5d^{10}\ 6s^2\ 6p^4$
Rn	86	$[Xe]\ 4f^{14}\ 5d^{10}\ 6s^2\ 6p^6$
Ra	88	$[Rn]\ 7s^2$
Th	90	$6d^2\ 7s^2$
U	92	$5f^3\ 6d^1\ 7s^2$

Source: Cotton and Wilkinson (1988).

1.2.2 Influence of weathering

Both Th and U are mobilized in the oxidized zone of the terrestrial near-surface environment, but in different ways. Thorium is transported either in insoluble resistate minerals (e.g. silicates, monozite) or is adsorbed on the surface of clay minerals whereas uranium either moves in solution as a complex ion, or like thorium in a sorbed phase. Both elements occur in the 4+ oxidation state in primary igneous rocks and minerals, but uranium can be oxidized to the 6+ state in the near-surface environment. The 6+ state is the most stable and forms soluble uranyl complex ions which play the most important role in uranium transport during weathering.

In a closed geological system the activity concentrations of the daughter nuclides should be equal to the activity of their respective parents, this state is

known as radioactive secular equilibrium. However, most surface and near-surface geological environments are subject to migration of radionuclides due to either physical or chemical processes. For instance, radon gas is an intermediate product in all three decay chains and may diffuse out of a deposit if the structure is slightly porous. Radioactive disequilibrium is, therefore, induced between the nuclides above and below radon in the decay series. Similarly, loss of an intermediate nuclide, e.g. radium may also be a cause of such disequilibrium due to its greater solubility. Many decay products of Th and U are too short-lived to become appreciably fractionated from their immediate parents. Longer-lived intermediate nuclides are often fractionated from the parents in the near-surface environments, and become concentrated in a geological or hydrological bodies. Since they are unsupported their activity decays away exponentially and its value at any time after formation can be used to determine the age of the body.

1.2.3 Geochemical cycles

Both Th and U in the 4+ oxidation state are chemically immobile in the near-surface environment at low temperatures. However, uranium can be mobilized by oxidation to the 6+ state (Langmuir, 1978):

$$U^{4+} + 2H_2O = UO_2^{2+} + 4H^+ + 2e^-$$

Further complexing of the uranyl ion may then occur depending on the pH and the presence of other ions. In pure solution, under reducing conditions, tetravalent uranium forms the hydroxy complexes

$$U^{4+} + nH_2O = U(OH)^{4-n} + nH^+$$

where $0 \leq n \leq 5$, and n is dependent on temperature and pH (Parks & Pohl,

1988). Under oxidizing conditions uranyl complexes are far more soluble than uranous species. The reduction of uranium from the soluble U^{6+} to the less soluble U^{4+} is believed to be the primary mechanism for its removal from solution. For this reason, the well-oxidized pelagic clays that represents 80% of the ocean floor is not a significant sink for uranium; the major sinks are the areas underlying highly productive waters where sedimentation rates are high and reducing conditions lead to the transformation of uranium to the more insoluble U^{4+} state (Huh and Kadko, 1992).

Unlike uranium isotopes, which are derived from the solution by the same removal processes, thorium isotopes in marine sediments come via various geochemical pathways. ^{232}Th is the only non-radiogenic isotope of thorium and is primarily deposited as detritus from the continents. ^{234}Th ($t_{1/2}$ = 24.1 d) and ^{230}Th ($t_{1/2}$ = 75200 y) are produced by the decay of ^{238}U and ^{234}U, respectively, ^{228}Th ($t_{1/2}$ = 1.91 y) is produced by the decay of ^{228}Ra. The solubility of Th in natural waters is extremely low owing to the low solubility of thorianite (ThO_2) and ability of Th ions to sorb on to particulate surfaces (Kaufman, 1969). Therefore, thorium is largely transported in particulate matter, even when it generated in solution by the radioactive decay of uranium it rapidly hydrolyzes and adsorbs on the nearest solid surface so that in the upper layers of marine sediments high activity concentrations of unsupported ^{230}Th are observed. Excess radium in sediments is mainly due to the excess of parent ^{230}Th, and its upward migration in the sediment column rather than adsorption on particulate.

1.2.4 Fractionation of uranium, thorium and their daughters

The isotope ^{238}U and its daughter ^{234}U are fractionated in natural processes because of the α- recoil effect. Radioactive decay of ^{238}U to ^{234}U usually involves one α- and two β- particle emissions (**Fig.1.1**). The ejection of an α- particle into

the body of a mineral by a ^{238}U atom situated near the mineral's surface, will recoil the daughter nuclide ^{234}Th into the medium surrounding the grain. Subsequent decay to ^{234}U will result in its enrichment relative to ^{238}U (Kigoshi, 1971 & Fleischer, 1988).

Fractionation of the thorium isotopes ^{232}Th and ^{228} Th is explained by the chemical properties and the long half-life of the intermediate ^{228}Ra ($t_{1/2}$ = 5.75 years) rather than the recoil mechanism. Most of the ^{228}Th in marine environment derives from the radium that diffuses upward from bottom sediments (Koide et al., 1973 & Ku, 1976) and the rapid leaching from surface weathered rocks (Dickson et al., 1983). In hydrological bodies the activity of ^{230}Th is negligible since most of the ^{230}Th is rapidly removed by adsorption on to sediments, being present as unsupported nuclide in surface layers of sea sediments in concentrations largely determined by the rate of sedimentation.

^{226}Ra (half-life = 1600 years), is generally found in excess of the parent ^{230}Th in most natural waters owing to its greater solubility and the resulting diffusion into the water column from sediments. In soils and sediments it is generally in excess of both ^{230}Th and ^{238}U due either to deposition by ion exchange on to clays and organic material from percolating soil solutions or to preferential leaching of ^{238}U from the soil or precursor rock (Titayeva et al., 1977). In weathered rocks ^{226}Ra is depleted with respect to ^{230}Th since it is more soluble than thorium (Gascoyne and Schwarcz, 1986).

^{210}Po (half-life = 138.5 days) is the only naturally occurring polonium isotope with a sufficiently long half-life to appreciably influence the state of equilibrium in the ^{238}U decay series. It decays with emission of a 5.3 MeV α-particles to stable ^{206}Pb. In the hydrological cycle polonium generally follows its parent ^{210}Pb but is often found out of radioactive equilibrium in marine environment. ^{210}Po is more readily adsorbed than its parent on to particulate matter, mainly

marine algae (Fisher et al., 1983). In fresh water ^{210}Po is depleted with respect to ^{210}Pb (Harada et al., 1989). Together they contribute the highest radiation dose to the human body of all bone seeking radionuclides (Jaworowski, 1969) and ^{210}Po provides the major natural radiation dose for many marine organisms (Heyraud and Cherry, 1979). ^{210}Pb is used in dating of sediments, and its activity is usually inferred from the ingrowth of the ^{210}Po daughter (Robbins, 1978). Uranium mining and processing operations release ^{210}Pb and ^{210}Po to the environment, and these must be monitored.

Chapter 2

MEASUREMENT OF ENVIRONMENTAL RADIOACTIVITY

2.1 Introduction

There are several radioanalytical and instrumental techniques developed for the measurement of environmental radioactivity. This chapter contains a brief review of instrumentation and principle of nuclear radiation detection, α-particle spectrometry, γ-spectrometry, liquid scintillation counting and their application in the study of environmental radioactivity with emphasis on the subject of radiochemical separations.

2.2 *Interaction of nuclear radiation with matter*

The study of the interaction of nuclear radiation with matter contains the clues to the methods of detection of alpha-, beta- and gamma- radiation.

The main process by which a charged particle from a radioactive decay lose energy in passing through matter is interaction with atomic electrons through the coulomb force. Alpha particles (He^{2+}) lose most of their energy through ionization and excitation of the atoms in the absorber. Because of their charge (2+) and their slowness they give up all their energy in short, dense and straight tracks. When the incident particle is no longer able to ionize, the exhausted particle attracts two electrons to itself and becomes a neutral helium atom (Knoll 1989 & Coggle, 1983).

The interaction of gamma- radiation with matter occurs differently from the interaction of alpha and beta radiations. Whereas charged particles transfer energy to electrons in atomic orbitals by many single processes, γ-quanta is uncharged and creates no direct ionization or excitation of the material through

which it passes. The detection of gamma- rays is therefore ceritically dependent on causing the gamma-ray photon to undergo an interaction that transfers all or most of its energy to an electron in the absorbing materials. Because the primary gamma-ray photons are invisible to the detector, it is only the fast electrons created in gamma-ray interactions that provide any clue to the nature of the incident gamma-ray. These electrons have a maximum energy equal to the energy of the incident gamma-ray photons and will slow down and lose their energy in the same manner as any other fast electrons, such as a β- particle. Energy loss is therefore through ionization and excitation of atoms within the absorber material and through bremsstrahlung emission (Knoll, 1989). Absorption of gamma- radiation varies exponentially with absorber thickness:

$$I = I_0 e^{-\mu d}$$

Where, I_0 is the intensity of incident radiation, I is the intensity of transmitted radiation, d is the absorber thickness and μ is the absorption coefficient.

The absorption of gamma photons is caused by three independent physical processes : the photoelectric effect, the Compton effect and the creation of electron - positron pairs. Each process has its own absorption coefficient.

$$\mu T = \mu e + \mu c + \mu p$$

In the photoelectric effect the γ-quantum transfers its total energy to an orbital electron by collision. The energy of the emitted photoelectron is equal to the energy of the γ-quantum minus the binding energy of the electron. In the Compton effect the γ-quantum transfers only part of its energy to an orbital electron and the degraded γ-qantum is scattered. The process is described by collision law. The scattering angle is variable as is the energy of the emitted electron. Therefore, Compton electron exhibit a continuous energy spectrum.

Pair production results from the behaviour of a γ-quantum in the electric field of an atomic nucleus to produce a negatron-positron pair. The process can happen only if the energy of the quantum is greater than 1.02 MeV (the rest mass of the two particles). The contributions of the three effects to the total absorption depends on the energy of γ-quantum and upon the atomic number of the absorber (Keller, 1988).

2.3 Instrumentation

The essential parts of any simple electronic counting system used with a nuclear radiation detection are shown in block schematic form in **Fig.2.1.**

The general principle behind detection of nuclear radiation is that whatever the form of radiation, it gives up some or all of its energy to the medium of the detector, either by ionizing it directly, or by causing the emission in it of a charged particle which in its turn produces ionization in the medium. The ionization produced is then detected by one of several methods: the charge may be collected directly by electrical means as it is in semiconductor detectors or it may cause the emission of photons as in scintillation detectors. The output of the radiation detector or the pulses whose amplitudes will be proportional to the detected particle energies are fed to a pulse height analyzer after amplification and shaping by the amplification system (i.e pre-amplifier and amplifier units). The pulse height analyzer sorts the pulses according to their amplitudes thus forming the required spectrum. The pulse enters an analog-to-digital convertor (ADC) which gives out digital signal proportional to the pulse height. This signal is then used to add one unit into the memory word or channel corresponding to the size of the digital signal. The rest of the pulse height analyzer consists of units performing such functions as automatic timing, spectrum manipulation and analysis and output of the spectral data. These

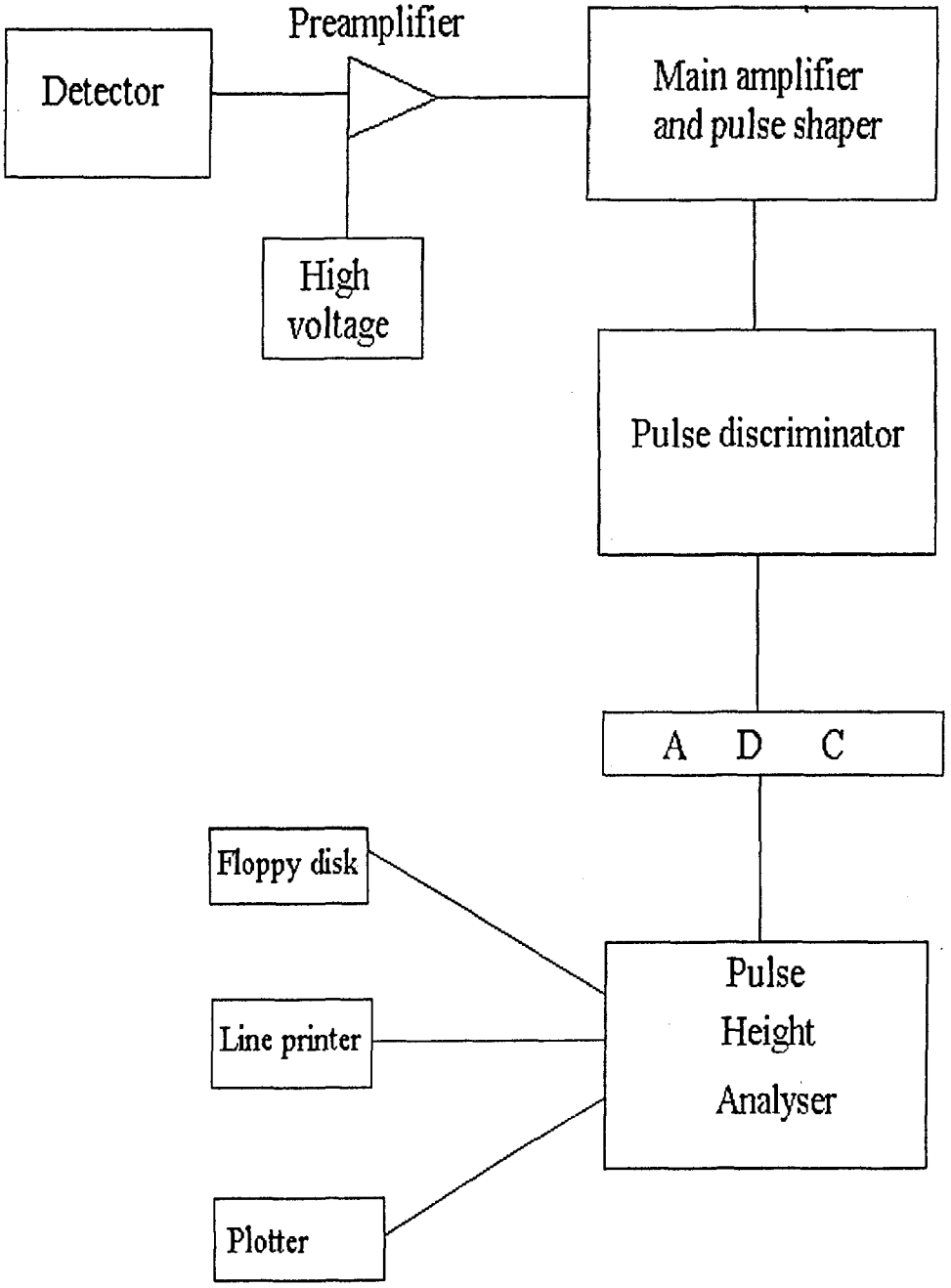

Fig. 2.1: Block diagram of a typical electronic system used with nuclear radiation detection

devices usually record data on computer disc as well as control plotters and printers for hard copy. Thus, the spectroscopic data can be analysed, evaluated by a computer (Ivanovich and Murray, 1992).

2.4 Alpha-particle spectrometry

High resolution α-spectrometry is a very precise and sensitive method. The technique is widely used in studies of uranium and thorium series disequilibria (Ivanovich, 1992) and in process control and environmental monitoring in nuclear fuel cycle (Sill, 1977; Hirayama et al., 1984). Most elements of interest emit α-particles in the energy region of 3.95 (^{232}Th) to 8.8 MeV (^{212}Po). In a sample containing several α-emitters, it is difficult to perform quantitative spectrometry of all of them at once because of spectral interference with each other. Therefore, the success or failure in α-spectrometry is largely dependent on the preparation of a thin, uniform activity deposit from chemically pure solutions of the element being determined. The mass of material used must contain sufficient activity for counting and be reduced to less than a few micrograms on the final source plate. Alpha-particles have a short range in solids and failure to produce a source of negligible thickness will cause excessive energy straggling and loss of α-energy resolution. Accuracy and precision also depend on clean separation from interfering radioelements, and on overall chemical recovery. α-spectrometric measurement of radionuclides in environmental samples can be subdivided into five basic operations (a) sample preparation, (b) preconcentration, (c) chemical separation,(d) source preparation, and (e) α-counting. Fuller details on these operations will be given below under radiochemical separations.

Silicon surface-barrier detectors are most commonly used for α-particle detection, with advantages of low background, excellent energy resolution, good

stability, high detection efficiency, low cost and compact size. Spectral resolution is largely dependent on the quality of source preparation, system electronics and on the manufacturer's detector specifications. In general, α-energy resolution improves with smaller detector size, decreasing air pressure, and with increase in source-detector distance and detector bias.

In set-up of modern α-spectrometers, several detectors are often connected via routing systems to one multi-channel analyzer. The detector system is calibrated with respect to the energy, resolution and efficiency with sources of known energy. Sources of ^{233}U (4.82 MeV) and ^{241}Am (5.28 MeV) are used usually as reference. Alpha-spectrometry is performed under vacuum, the air pressure is typically about 5-6 Pa (40-45 μm Hg). Contamination of the detector may occur either by evaporation/diffusion of a volatile polonium isotopes or by recoil nuclei such as ^{224}Ra from ^{228}Th. Contamination by recoil nuclei can be avoided by applying a negative potential of a few volts to the source plate to impede the number of positive recoil ions striking the detector (Sill and Olson, 1970) and therefore helps reduce recoil contamination.

2.4.1 Optimization of source-detector separation

In low-level α-spectrometric measurements of α-emitters in environmental materials there must be some compromise between the optimum count rate obtained with a minimum source-detector separation, and the optimum α-energy resolution and best conditions for prevention of recoil contamination obtained with a large separation. Careful consideration must also be given to the source diameter. Spot sources provide an optimum geometrical configuration but self-adsorption in a thick source may lower α-energy resolution relative to an extended source. The best count rate would be achieved with the source diameter equal to, or smaller than that of the detector, and with the source in

contact with the detector surface. In practice, some distance is necessary to avoid contamination of the detector (Sill and Olson, 1970).

The geometry (G) of the source-detector arrangement is the fractional solid angle Ω subtended by the detector, averaged over the detector volume, G = Ω/4π. Wilson (1980) has calculated the geometrical factors, G_s as a function of source diameter and source-detector separation for a coaxial planar source-detector arrangement, e.g. a source of 17.5 mm in diameter and 4 mm from the detector gives a theoretical geometric counting efficiency of 25.52% and is not sensitive to small change in geometry. A 1% change in geometric efficiency would be caused by variations of ±1.3 mm in the source diameter or ±0.25 mm in the source distance.

2.4.2 Data processing and analysis

Radiation measurements are subjected to random fluctuations in the process of radioactive decay. The frequency of decay can be expected to follow the Poisson distribution

$$P_r = \frac{m^r}{r!} \exp^{-m}$$

where the variance about the mean (m) for a large number of observations is given by: $\sigma^2 = (r-m)^2\ P_{(r)}$, and substitution for $P_{(m)}$ yields $\sigma^2 = r$ or $\sigma = \sqrt{r}$. Thus, for a Poisson distribution the single parameter (r) is both the mean and variance of the distribution. The standard deviation (σ) is equal to $\mp \sqrt{r}$. This approximation requires that a large number of atoms to be observed over a short time relative to the half-life of the nuclide (Friedlander et al., 1981). About 1000 counts are necessary for a standard deviation in the total counts of about 3% and

over 10000 counts for a standard deviation of 1% (**Table 2.1**). Approximately 68% of the observations should lie within this deviation and about 95% within two deviations. The precision of radioactivity measurements is therefore largely dependent on the counting time and on the activity of the source. Counting times of up to 10 days are used for low-level α-spectrometric measurements of environmental samples so as to accumulate 1000 counts.

Table 2.1 Statistical uncertainty in total accumulated counts

Total count	50	100	300	500	1000	2000	10000
$\mp 1\sigma$	7.1	10	17.3	22.4	31.6	44.7	100
C.V %	14.1	10	5.8	4.5	3.2	2.2	1.0

Source: Friedlander et al., 1981.

2.5 Gamma-spectrometry

Gamma-spectrometric measurements of environmental radioactivity has a number of practical advantages: tedious chemical operations are avoided, the method is simple, non-destructive, allows simultaneous identification and determination of radionuclides in a γ-emitting sample, and is capable of high sensitivity. The utilization of γ-spectrometry in low-level environmental studies has increased over recent years. This is mainly due to the development of low-background high-purity Ge detectors of high efficiency and excellent energy resolution (<2 keV) and to on-line microcomputers for peak search, data reduction and error analysis. Quantitative γ-spectrometry depends on careful calibration of detector efficiency over the energy range of interest and in the same geometry as the sample. Precision and accuracy is limited by the

availability of material (up to 100 g) and counting time (12-48 hours), and by uncertainties in the calibration standards and detector background. Counting efficiency increases with detector size and with use of well-type detector crystals (Hine, 1967) or Marinelli beakers (May and Marinelli, 1960). Variations in self-absorption between samples and calibration standards arises from both variations in bulk density and in mass attenuation coefficients, and is usually a problem below 100 keV. Bulk density variations can be minimized by mixing with resin and casting in one of several geometries.

2.5.1 Minimum detectable concentration (MDC)

Detection limits is a term used to express the detection capability of a measurement system under certain conditions. An estimate for the lowest amount of activity of a specific gamma-emitting radionuclide that can be detected at the time of measurement can be calculated from different expressions (Head, 1972 ; Pasternack and Harley, 1971).

When a sample is introduced into the gamma measurements, the term usually associated with detection is the minimum detectable concentration (MDC) which can be expressed by:

$$MDC = \frac{4.66\ S_b}{\varepsilon\ P_\gamma\ W}$$

Where, S_b is the estimated standard error of the net count rate;

ϵ is the counting efficiency of the specific nuclide's energy;

P_γ is the absolute transition probability by γ-decay through selected energy (branching ratio);

W is the mass of the sample.

As can be seen from the above equation, the factors that tends to influence the detection limits are the counting efficiency, the quantity of sample (mass or volume), the counting time associated with S_b, and the background. In order to obtain low detection limits the efficiency should be high, the sample should be as large as practicable, the counting time should be as long as practicable, and the background should be as low as attainable. The efficiency is strongly influenced by the sample geometry and tends to decrease as the sample height (distance away from the detector) increases. Therefore, an optimum sample size and geometry must be used to obtain low detection limits.

The background of a measurement system is usually kept as low as possible. However, the number and type of radionuclides in a gamma spectrum can influence the level of background in the Compton continuum region. Consequently, the detection limits for radionuclides with lower energies (i.e. energies in the Compton continuum region) will be higher. The concentration of potassium in samples has a direct influence on the detection limits for many radionuclides because of the Compton scattering caused by ^{40}K (IAEA, 1989). Because of this dependence of both the continuum and interfering photopeaks on other radionuclide activities present in the sample, minimum detection limits for particular radionuclides are difficult to define from first principles in natural series gamma spectrometry.

2.5.2 Accuracy

The total error in a determination of radionuclides (exclusive of sampling error) depends on the error in the determination of the nuclide specific counting efficiency (3-5%) and the statistical counting errors (1-5%). Therefore, the concentrations of activities of the various radionuclides in the standards used for calibration of the gamma spectrometer system should be known to at least 3%.

The counting time should be optimized to accommodate the operating conditions and should be for a period long enough to minimize the statistical counting error.

An increase of the counting time affects the statistical counting error of a radioactivity measurement. The relative counting error will vary inversely as the square root of the counting time; e.g. by doubling the counting time the relative error will be reduced by $\sqrt{2}$.

The statistical counting error decreases in direct proportion to increasing sample activity if the counting time is constant when the background (B) is much larger than the sample counts (n). This is typical for low level counting. The relative counting error is then given by the approximation ($\sqrt{B}/n$). In cases where the background is much smaller than the sample counts, the estimate of the relative error is given by the approximation ($\sqrt{n}/n$).

An average error of 10% for the determination of gamma emitters in environmental samples should be assumed, but if the activity levels are very low then larger errors can be expected (IAEA, 1989).

2.6 Liquid scintillation counting

Liquid scintillation counting (LSC) has become of widespread interest during the last 15 years. This is due to the fact that more attention is paid to α- and β-emitters than before and because the performance and the features of liquid scintillation spectrometers have improved considerably. From the point of view of low-level LSC one may briefly outline the development as follows:

In the early days of LSC the determination of soft beta-emitters like ^{3}H and ^{14}C were the most important applications. From the standpoint of environmental radioactivity monitoring there was no need for low-level liquid scintillation spectrometry in the 1960's. Environmental contamination from atmospheric nuclear tests was very high. Towards the end of the 1970's interest grew in the

determination of other beta- and also alpha-emitters.

One important advantage of LSC is the high counting efficiency, which for beta-emitters is between 80 and 90%, and for alpha-emitters is ~ 100%. Another important advantage is homogeneous distribution of the sample in the scintillation cocktail, therefore no self-absorption occurs. Sample preparation is often simple and extraction methods usually yield solutions of the desired radionuclides which can be mixed directly with a scintillation cocktail and counted without further sample preparation. Use of an internal standard is a very convenient and simple method for accurate efficiency determination especially in low-level counting (Noakes et al., 1992).

There are also disadvantages associated with low-level applications of LSC. Compared with spectra of beta-emitters, relatively sharp peaks are obtained for alpha-emitters, but the resolution in alpha-spectrometry with surface barrier detectors is far better. The full width half maximum (FWHM) depends very much on the type of cocktail. If the radionuclide is present as an organophilic compound in an organic scintillation cocktail the FWHM is ~ 200 - 300 keV. The position of the alpha-peak is relatively insensitive to quenching and the efficiency is not affected (Schönholer, 1995).

The poor energy resolution in many applications is of little concern when it is possible to isolate the radionuclide radiochemically. In the case of ^{222}Rn and ^{226}Ra, the enhanced efficiency provided by the daughter products is an advantage. Another alternative is to use mathematical means to resolve overlapping alpha-peaks.

2.7 Radiochemical separations

The analysis of environmental and biological materials for low concentrations of artificial or natural radionuclides presents a number of problems to the

analytical radiochemist. It is of course possible to determine some radionuclides direct, or by methods requiring the minimum of sample separation as for example the determination of γ-emitting nuclides by high resolution γ-spectrometry. However, where a radionuclide of interest is present at a low concentration or emits no penetrating radiation, radiochemical separation is usually required.

In many cases radiochemical separation is often based on procedures used in non-radiochemical work though there is some change of emphasis. In precipitation reactions the need to achieve complete recovery necessary in gravimetric analysis disappears in radiochemical separations since correction for incomplete yield can be applied. However, traces of impurities which would be of no importance in gravimetric analysis will contribute considerable undesired activity to the counting source and repeated re-precipitation in the presence of hold-back carriers is needed (Coomber, 1975). Ion exchange and extraction chromotography can be carried under near ideal conditions for separation since the amount of material involved is small. The co-precipitation method is more widely used in radiochemical separations, while others such as those based on recoil or isotopic exchange have no counterpart in non-radiochemical work.

Apart from the specific properties of the elements themselves a number of factors determine the choice of separation method. These include the nature of the matrix, the level of activity of the nuclide being determined and of the other radionuclides present, their half-lives and other nuclear properties which determine the method of measurement and the degree of accuracy required.

Problems commonly encountered in radiochemical separation procedures range from the difficulty in separating a component from highly active material where the initial separation stages will require remote handling behind shielding to the problem of separating low levels of activity sequentially from a limited amount

of sample prior to low level counting.

This section gives an account of the basis of and special features of radiochemical analysis as well as the principal methods used in separating radioactive elements, followed by a review of the literature dealing with the separation chemistry of uranium, thorium and polonium.

2.7.1 Basis of radiochemical separation procedure

The majority of radiochemical separation procedures can be subdivided into five basic stages:

2.7.1.1 Sample preparation

As the name implies, sample preparation includes all treatments or additions to the sample before the preconcentration stage begins. It may consist of drying, grinding and homogenizing a solid sample, the filtration and acidification of an aqueous sample in order to ensure isotopic exchange, dissolve colloidal particles and remove any carbonates from the samples, the addition of radiotracers and/or stable element carriers or other similar steps.

2.7.1.2 Preconcentration

Preconcentration is a common preliminary to chemical separation, the aim being to reduce the bulk of a sample before separative steps begin, although a certain degree of chemical separation may be achieved. The commonest preconcentration steps are the evaporation of aqueous samples to reduce their volume and the ashing of solid samples to remove organic material. Other procedures frequently used are the acid leaching of solid samples followed by the evaporation of the leachate and bulk coprecipitation steps. Preconcentration procedures for water samples with calcium and magnesium carbonates or iron

hydroxide have been reported (Holm et al, 1979) and (Holm and Fukai, 1977).

2.7.1.3 Separation

This involves the removal of the radionuclide of interest from both the stable elements and interfering natural or artificial radioelements in the matrix. At this stage the sample is usually in solution and in a suitable volume for processing by a wide variety of chemical procedures the most commonly used being ion exchange (Knab, 1979; Yamato, 1982), solvent extraction (Butler and Hall, 1970), coprecipitation (Sill and Williams, 1981), extraction chromatography (Martin and Pope, 1982) and distillation (Eakins and Morrison, 1978). These steps may be used singly or in various combinations to obtain the required degree of decontamination.

2.7.1.4 Source preparation

Once chemical separation has been completed, consideration must be paid to source preparation and this depends on the counting procedure to be adapted. In the case of α-emitters an infinitely thin and weightless source on a perfectly flat substance is required to achieve the highest resolution possible in α-spectrometric measurements. Failure to achieve this results in deterioration of the spectra due to scattering of the α-particles in the source which in turn leads to excessive tailing and loss of resolution. Source may be prepared by direct evaporation, vacuum sublimation, electrospraying, coprecipitation or electrodeposition (Lally and Glover, 1984). Electrodeposition is the preferred method for routine laboratory work. The technique is simple and gives a very thin deposit which is essential for a high resolution of peaks (undegraded spectra). The method is based on cathode deposition of the hydrated oxides either from an alkaline medium or from acidic media (Talvitie, 1972 and

Hallstadius, 1984). However, the chemistry of electrodeposition is not yet well understood due to the negligible mass at deposition stage.

2.7.1.5 Counting stage

In many cases spectrometric counting techniques, such as α-spectrometry, enable the radionuclide of interest to be detected in the presence of other radionuclides so that complete decontamination is not always necessary. Because of low background the lowest limits of detection are generally obtained by α-spectrometry, followed by β-counting and γ- spectrometry (Eakins, 1984).

2.7.2 Special features of radiochemical analysis

2.7.2.1 Handling extremely small quantities of material

The most characteristic feature of work with radioactive material apart from the radioactivity involved is that it has to be prepared and applied in amounts and concentrations lie far below the limits measurable by standard physical and chemical means, as the weight of radioisotope necessary to give a measurable activity is 10^{-15} g (Cook and Duncan, 1952) . The mass equivalent (m) for a radionuclide of a given activity (A) can be calculated by the following equation:

$$A = \lambda N = \frac{ln2}{T_{1/2}} x \frac{m N_L H}{M} \qquad (1)$$

where λ is a decay constant, N the number of radioactive atoms, $T_{1/2}$ the half-life, N_L Avogadro's (Loschmidt's) number, H isotopic abundance and M is the atomic weight.

2.7.2.2 The use of carriers

In many cases the mass of a radionuclide is often extremely small, and chemical operations with such exceedingly small amounts of material are therefore greatly facilitated by diluting the radionuclide with isotopic or at least chemically similar element referred to as a carrier which serves two main purposes: In the first place it provides sufficient material to allow manipulations, e.g. it makes possible to form a precipitate from aqueous solutions. The second function of the carrier is to gurad against loss of the radioactive material since minute traces of the material are highly susceptible to accidental losses. A frequent causes are the adsorption on vessel walls and reaction with trace impurities (Mackay, 1971). The amount of added carrier should not be unduly large because it reduces the specific activity.

When the radionuclide of interest is transferred to a new phase by precipitation or solvent extraction, carriers may sometimes be added to prevent the coprecipitation of impurities, i.e, to hold-back unwnated species. This later category is known as *hold-back carriers*. Another feature of carrier addition is the formation of gelatinous precipitates such as $Fe(OH)_3$, $Al(OH)_3$ and manganese dioxide (MnO_2) which are liable to adsorb and occlude other substances from the solution. They are known as *scavengers* and serve to remove traces of radioactivity from the solution leaving behind the more electropositive cations. Other substances such as charcoal, silica gel, alumina, etc., are quite efficient scavenging agents, but their use in radiochemical separations has not been extensively reported (Cook and Duncan, 1952).

2.7.2.3 Holding oxidants and reductants

Reaction with trace impurities can sometimes be prevented by adding a reagent which destroys the impurities rather than by adding carriers. So-called holding

oxidants and reductants belong to this category. They are used when a radiotracer exists in several valency states, and needs to be kept in one particular state. Thus, to maintain a trace of uranium in the readily oxidized tetra-valent state a small amount of iron (II) or hydrazine (N_2H_4) is added as a holding reductant. Similarly, to maintain neptunium in the 6-state, bromate or persulphate is used as a holding oxidant.

2.7.2.4 The use of yield tracers

The direct measurement of trace constituents in a sample is frequently rendered impossible because of interferences from other components in the matrix. The success of classical chemist determining the elemental composition of a sample relies on the quantitative recovery of the element of interest in a form that can be determined by gravimetry, spectrometry or other means. If the element is present in reasonable abundance, the number of separation steps are few and quantitative recovery is attainable. However, when determining very low concentrations of radionuclides in environmental and biological materials the matrices are often complex, numerous and seldom quantitative. It is necessary, therefore, to establish a relationship between the amount of radioactivity detected at the counting stage and that is initially present in the sample. This can be achieved by the use of a yield tracer, which may be either radioactive or stable. To be effective the tracer, which is usually added in a known amount at the commencement of the analysis, must behave chemically in the same way as the radioelement being determined. Preferably, therefore, it should be an isotope of the element and, if radioactive, its emissions should be capable of differentiation from those of the radionuclide being determined. A stable nuclide can be used as a yield tracer if it is not present in significant quantity in the matrix, otherwise its yield at the end of the analysis can be determined by

gravimetric or other means (Eakins, 1984; Harvey and Lovett, 1984). If the added tracer is radioactive it should not be present in the matrix i.e, artificial radionuclides are used for the determining low activities of natural analogues in the environmental and biological samples.

Non-isotopic tracers are used where there is no convenient or available isotopic form, close analogues of the given element with similar chemical properties being used, as for example in the use of ^{244}Cm as a tracer for ^{241}Am (Yamato, 1982), and ^{133}Ba has similarly been much used as a non-isotopic tracer for radium; this is possible because very little separation of the two elements occurs under most conditions (Pennington et al., 1976).

2.7.2.5 Adsorption of radioelements

Adsorption phenomena have a significant role in radiochemical analysis, the adsorption capacity of the radioelements is determined mainly by their chemical properties, their state in solution, the type of adsorbent and the nature of its surface. As a general rule, all forms of adsorption from solution increases with ionic charge in the following order:

$$M^{+} < M^{2+} < M^{3+} < M^{4+}$$

The addition of an isotopic carrier dilutes the radiotracer and a smaller fraction of tracer is adsorbed. In addition to adsorption on the walls of the container, radioactive species frequently adsorb on precipitates present in the system. The nature of the precipitate as well as its mode of precipitation are major factors in the amount of adsorption. The Fajans-Paneth rule for tracer precipitation-adsorption states that: "*when a precipitate is formed in a solution containing micro-concentrations of a radioactive element, the lower the solubility of the compound between the anion of the precipitate and the radioactive element (cationic), the greater is the amount of radioactive element carried down with*

the precipitate" (Cook and Duncan, 1952). Valency of the ions has a pronounced effect in all forms of adsorption from solution, but for ions of the same valency, those of the smallest ionic size when hydrated are most strongly adsorbed, e.g. Li < Na < K < Rb < Cs.

According to the Fajans-Paneth precipitation and adsorption rule, low solubility is considered to be the sole criterion of co-precipitation. This rule is originated from observations such as the co-precipitation of small amounts of radium and lead with barium sulphate, and of radium, lead, and bismuth with barium carbonate. As more data were accumulated, several examples which could not be reconciled with the Fajans-Paneth rule were observed. Perhaps the more remarkable example is the failure of gypsum ($CaSO_4.2H_2O$) to carry down traces of radium, although radium sulphate is one of the least soluble compounds known. These discrepancies showed that low solubility is not the sole criterion of co-precipitation. In a number of precipitation reactions, it was observed that the separation of the micro-component depends on the precipitate and the manner in which it is produced and such reactions are considered to be due to surface adsorption. In these cases the conditions for separation are given by Hahn's adsorption rule, which states that "*anion at any desired dilution will be adsorbed by a precipitate if that precipitation has acquired a surface charge opposite in sign to the charge of the ion to be adsorbed and if the adsorbed compound is slightly soluble in the solvent involved*"

In general, the adsorption properties have been used for the separation of different trace elements with different adsorption properties. However, the adsorption phenomenon is detrimental in radiochemical analysis, and some means are often used to prevent and decrease the losses due to adsorption, these include:

a. Maintaning high acid concentration (low pH),

b. the use of complexing agents e.g citrate, EDTA, fluoride ion, oxalate,

c. the avoidance of finely-divided precipitates with large surface areas,

d. to avoid the storage of dilute solutions,

e. the addition of carriers.

2.7.2.6 Isotopic exchange

The main requirement for correct results in radiochemical analysis is the achievement of an exchange equilibrium between the added isotopic carrier and the radioactive isotope. Since the carrier is added to the solution in the form of a known compound, whilst the radioactive isotope may be present in the form of a compound of a different valency state which cannot always be predicted beforehand, it is necessary to be convinced that complete isotopic exchange has taken place between the carrier and the compounds of the radioisotope within a relatively short time. The question of the rates of isotopic exchange between compounds of one element in different valency states has been studied by a number of people (see Lavrukhina et al. 1967). A convenient magnitude for expressing the rate of exchange is $t_{1/2}$, the time necessary for the achievement of half the equilibrium distribution, in other words, the half-exchange time. It is expressed by the formula:

$$t_{1/2} = \frac{a\ b}{(a\ +\ b)\ R}\ X\ ln2 \qquad (2)$$

where a and b are the numbers of molecules in unit volume between which the exchange of isotopes takes place, and R is the exchange velocity constant, which varies according to the order of the reaction, the concentration of the components, and the presence of other substances in the solution.

In order to exclude errors due to incomplete isotopic exchange, it is always necessary to create conditions under which the radioisotopes and their stable carriers will have the same valency states before they are to be separated from the solution. One method is to introduce the carrier in one valency state and to carry out a cycle of oxidation-reduction reactions to bring all the possible valency states of the element concerned to one form or state necessary for separation.

2.7.3 Separation methods

2.7.3.1 Precipitation and co-precipitation

These techniques are the earliest used in radiochemical separations. The amount of added carrier used in precipitation steps may be a disadvantage when the subsequent procedures, e.g ion exchange, are most satisfactory with small amounts of material (ultramicro-concentrations).

^{140}Ba (tracer) + $BaCl_2$ (carrier) + $SO_4^{-2} \rightarrow BaSO_4$ (precipitation)

^{226}Ra (tracer) + Ba^{+2} (carrier) + $SO_4^{-2} \rightarrow Ra\,Ba\,(SO_4)$ (co-precipitation)

In the precipitation reaction cited, the isotopic ions are equivalent and are homogeneously incorporated in the barium sulphate crystals. The percent of ^{140}Ba carried would be the same as the percent of a total barium carrier precipitated. ^{140}La, the 40 hour daughter of ^{140}Ba, would be present in solution with its parent and would also be present in $BaSO_4$, which acts as a nonisotopic carrier for the ^{140}La. The percent of ^{140}La carried would be less than that for ^{140}Ba and could be further decreased by addition of lanthanum "hold-back" carrier.

Co-precipitation is a process in which a tracer ion is carried by another precipitate, though the tracer concentration is too low for it to be precipitated

on its own by exceeding the solubility of a compound considered to be insoluble. Several mechanisms are involved, viz. compound formation, mechanical inclusion and surface adsorption. When the distribution of the tracer (micro-component) is found to be uniform throughout the precipitate, the system is said to be homogeneous and follows the Berthelot - Nernst distribution law which has the form:

$$\frac{x}{y} = D' \frac{a - x}{b - y} \qquad (3)$$

where x and y are the amounts of tracer ion (A^+) and carrier ion (B^+) in the precipitate, a and b are the initial concentrations of these ions in solution respectively, (a-x) and (b-y) are the concentrations after separation of the crystals, and D' is the distribution coefficient. A truer distribution constant (D = concentration of tracer in solid / concentration of tracer in solution) can be obtained by using a conversion factor, e.g. C = gram solute per ml of saturated carrier solution divided by density of the solid; thus:

$$D' = D\,C \qquad (4)$$

In this system the entire precipitate is in equilibrium with the solution. If only the freshly forming surface of the growing crystal is in equilibrium with the solution phase, a nonuniform distribution is observed and the system being described according to Doerner and Hoskins logarithmic distribution law, which has the form:

$$\log \frac{a}{a - x} = \lambda' \log n \frac{b}{b - y} \qquad (5)$$

where λ' is the logarithmic distribution coefficient, which is a constant characteristic of the system (Cook and Duncan, 1952).

2.7.3.2 Solvent extraction

(I) Chelate extraction

When metals form uncharged inner complexes with large organic molecules and the complexes are not appreciably hydrated, these can be extracted into immiscible organic solvents. The extraction can be represented by:

$$M^{n+}_{aq} + nHL_{org} = (ML_n)_{org} + nH^{+}_{aq}$$

The suffixes, aq and org, refer to the aqueous and organic phases. The extraction constant is given by:

$$K_{ex} = \frac{[M\ L_n]_{org}\ [H]^n_{aq}}{[M^{n+}]_{aq}\ [H\ L]^n_{org}} \qquad (6)$$

Solvent extraction holds a privileged position among radiochemical separation methods with high separation factors, sufficient material throughout and the possibility of on-line process flow. It is applied in industry for the chemical reprocessing of spent nuclear fuel. Separation by solvent extraction is based on the difference in affinity of the ions between two immiscible liquid phases. The distribution of the element (X) is described as:

$$(X)_{aq} \leftrightarrows (X)_{org}$$

$$D_x = \frac{[X]_{org}}{[X]_{aq}} \qquad (7)$$

Where $(X)_{aq}$ and $(X)_{org}$ are the total equilibrium concentrations of the element X (solute) in aqueous and organic phase, respectively. For an ideal system in which the solute does not dissociate or associate and the miscibility of the solvents is not altered by the dissolved substances, the distribution ratio is essentially independent of the total amount of extractable solute present. In fact there are relatively few systems which are almost ideal in this sense over even a limited range of initial solute concentrations (Overman and Clark, 1960).

The distribution coefficient D_x is a property of matter and has a constant value for a given organic phase and aqueous acidity. When two species x and y are present the ratio of their distribution coefficients gives the separation factor (α); thus:

$$\alpha = \frac{D_x}{D_y} \qquad (8)$$

Difficulties will arise for ions with similar chemical properties, ($D_x = D_y$). Such ions are mostly highly hydrated positively charged metal ions. They are usually separated after previous chemical reaction steps such as coordination, association, or chelate complexation.

For the extraction into the organic phase, the recovery factor or the fraction of a substance extracted (%E) is calculated as:

$$\%E = \frac{100\ D_x}{D_x + \frac{V_{aq}}{V_{org}}} \qquad (9)$$

where V_{aq} and V_{org} are the volumes of the aqueous and organic phases, respectively. Examples of chelating agents widely used in radiochemical analyses are acetylacetone, thenoyltriflouroacetone, 8-hydroxyquinoline,

cupferron and dithizone.

If the recovery is not adequate in a single contact, the aqueous phase may be contacted successively with fresh solvent. Repeated extractions with small portions of solvent is preferable to one extraction with a large volume. If the combined extract does not meet purity requirements, the solute can be back-extracted into water (or the solvent removed by evaporation) and re-extracted after adjustment of reagent concentrations.

Solvent extraction is generally used to separate a given solute from substances which interfere in the ultimate quantitative analysis of the material. The choice of solvent is governed by the following:

1. A high distribution ratio for the solute and a low distribution ratio for unwanted impurities,
2. low solubility in the aqueous phase,
3. sufficiently low viscosity and sufficiently high difference in density from the aqueous phase to avoid emulsification,
4. low toxicity and inflammability,
5. ease of recovery of the solute from the solvent for subsequent analytical processing.

Mixed solvents may sometimes be used to improve on these properties, salting-out agents may also improve extractability (Vogel, 1979). The tendency to form emulsions is an inherent characteristic of the mixtures of solvents and reagents used in an extraction system, or it may be attributed to the sample of material to be separated. The relative densities and viscosities of the organic and aqueous phases are factors which related to the formation of emulsions. The rate of separation of the phases after equilibration is generally greater, the greater the difference in density between the organic and the aqueous layer. A low viscosity favours rapid separation of phases. Among the techniques used to break

emulsions is the addition of an inert dilution such as CCl_4 to increase the density of the organic layer and lower the viscosity (Overman and Clark, 1960). The hydrogen ion concentration must be carefully adjusted in systems involving chelates, since their stability is pH dependent.

(II) Ion association extraction

Extractable ion association complexes consist of ionic species, which are mostly individual ions in the aqueous phase that may enter the organic phase by virtue of their formation of electrically neutral aggregates. The mechanism of these extractions is more complicated than that of chelate extraction (chelates are large, neutral complexes which have solubilities in non-polar solvents characteristic of the chelating agent).The extraction of 4- and 6-valent metal nitrates by tri-n-butylphosphate (TBP) from slightly acid medium can be described as:

$$(Me^{4+})_{aq} + (4NO_3^-)_{aq} + (2TBP)_{org} \leftrightarrows Me(NO_3)_4(TBP)_{2\,org} \quad (10)$$

$$(MeO_2^{2+})_{aq} + (2NO_3^-)_{aq} + (2TBP)_{org} \leftrightarrows MeO_2(NO_3)_2(TBP)_{2\,org} \quad (11)$$

Due to the large alkyl groups of TBP ($C_{12}H_{27}O_4P$) the complex compounds are readily soluble in organic solvents (e.g kerosine). As it has been previously stated, the distribution coefficient (D) as characteristic size for the extent of extraction is defined as:

$$D = \frac{[Me]_{org}}{[Me]_{aq}}$$

where [Me] is the total metal ion concentration in the corresponding phase. The distribution coefficient for the TBP-extraction is given as:

$$D = \frac{[complex]_{org}}{[Me]_{aq}} \qquad (12)$$

The application of the law of mass action to equation (10) gives:

$$K = \frac{[complex]}{[Me^{4+}]\ [NO_3^-]^4\ [TBP]^2} \qquad (13)$$

where K is the equilibrium constant. Thus, the distribution coefficient finally becomes:

$$D = K \times [NO_3^-]^4_{aq} \times [TBP]^2_{org} \qquad (14)$$

From equation (14) it can be seen that the distribution coefficient increases with increasing nitrate content (Möbius, 1988).

The extraction power of other neutral phosphorus compounds increases in the following order:

$$(RO)_3.PO < (RO)_2R.PO < (RO)R_2.PO < R_3.PO$$

one representative of the last group, n-octylphosphine oxide (TOPO), being an extractant of considerable importance reviewed by White and Ross (1961).

2.7.3.3 Ion exchange

Many substances, both natural (clay minerals) and artificial have ion exchange properties, but for analytical work synthetic organic ion exchangers are of chief interest, although some inorganic materials, e.g Zirconyl phosphate and ammonium 12-molybdo-phosphate, are useful and have specific applications (Vogel, 1979).

All ion exchangers of value in analysis have certain properties in common: they are almost insoluble in water and in organic solvents, and they contain active ions or counter ions that will exchange reversibly with other ions in the surrounding solution without any physical change occurring in the material. In fact ion exchangers consist of organic polymeric networks containing basic or acidic groups attached to the organic framework.The polymer carries an electric charge that is neutralized by the charges on the counter ions which are cations in an cation exchanger and anions in an anion exchanger. Thus, a cation exchanger consists of a polymeric anion and active cations and an anion exchanger of a polymeric cation and active anions.

Ion exchange on synthetic resin exchangers is widely used in radiochemical analysis. The scope of these exchangers has been greatly extended with the use of complexing agents in cation exchange, eluent of high ionic strength in anion exchange and the use of mixed solvent systems (Coomber, 1975).

In the acidic cation exchangers the exchange process take place according to the equation:

$$M^{n+}\,(aq) + n\,R\,H\,(resin) \rightleftharpoons M\,R_n\,(resin) + nH^{+}\,(aq)$$

(e.g. RH = sulphonic acid group- RSO_3H, carboxylic groups-RCOOH, or phenolic-ROH)

$$K = \frac{[M\,R_n]\,[H^{+}]^n}{[M^{n+}]\,[R\,H]^n} \qquad (15)$$

the equilibrium constant for such reaction depends on the specific properties of the ion exchange material, such as the amount of cross-linking of the polymer network as well as on such solution parameters as the nature of the metal ion, the ionic strength of the solution and the temperature.

An anionic exchanger may be weakly basic, in which case anions may be removed only from acid solution, e.g. $n RNH_2OH + nH^+ + X^{n-} = (RNH_3)_n X + n H_2O$, or it may be strongly basic, when it is possible to remove the chloride ion from a neutral solution of sodium chloride to give caustic soda e.g., $nR_3NOH + X^{n-} = (R_3N)_nX + n\ OH^-$ (Cook and Duncan, 1952).

The choice between a cation and an anion exchanger is governed by the particular separation. A few elements may be adsorbed in either cationic or complex anionic form. In selecting a particular resin within each of the two classes, consideration must be given to selectivity, exchange capacity, solubility, chemical stability, swelling, mechanical strength, particle size and particle shape. For a given type of exchanger usually a choice is to be made with respect to the degree of cross linkage and the particle size. The greater the cross linkage, the tighter the resin structure. The extent of cross linkage is usually expressed as the percent content of one of the materials copolymerized, e.g. 8% divinylbenzene. In general, the lower the percent cross linkage, (1) the greater the swelling (or shrinking) resulting from the adsorption of water, (2) the lower the mechanical strength, (3) the higher the capacity for exchanging ions of high molecular weights, (4) the faster the internal diffusion rates, (5) the lower the selectivity, (6) the lower the exchange capacity on a volume basis, (7) the higher the solubility, and (8) the greater the influence of flow rate on the exchange process. The overall rate of separation by ion exchange is determined by the rate of diffusion of ions through the resin particles rather than by the rapid exchange of ions at the functional groups. The resin is more effectively used when in the form of small particles. For example, the overall exchange rate is more rapid, separations are sharper, and less elutriant is required. Since flow rates decrease with decreasing particle size, the improved separation is at the expense of time.

Ion exchange material can be used either under column operation or with a batch technique depending on the experiment. The batch process of ion exchange separation is a process in which an adequate amount of resin in the appropriate form is mixed with a known volume of solution, and adsorption occurs. The resin is then separated and treated to remove the adsorbed elements. In column ion exchange separation a vertical cylinder is filled with the resin and the solution of ionic species is passed through the column. The batch process is useful for equilibrium distribution studies, but the non-equilibrium column technique is generally used for actual separations. The column system can be considered as a large number of consecutive batch equilibria where fresh resin is brought into contact with the ion-depleted solution in each equilibrium step. The adsorbability of ion is given by a distribution coefficient K_d, defined as:

$$K_d = \frac{C_1}{C_2} \qquad (16)$$

where C_1 is the amount of metal ion adsorbed per gram of dry resin, and C_2 is the amount per millilitre of solution that remains after equilibrium has been reached. When K_d is greater than 10 the batch system can be applied. However, when K_d values of less than 10 are found or where elements with similar K_d values are to be separated column ion exchange is to be preferred (Lally, 1992). The adsorbability of ion can also be described by a volume distribution coefficient D_v, defined as:

$$D_v = \frac{amount\ of\ ion\ per\ gram\ of\ resin\ bed}{amount\ of\ ion\ per\ milllitre\ of\ solution} \qquad (17)$$

D and D_v are related by: $D_v = D\ r$, where r is the resin bed density.

When two ions, a and b are to be separated by ion exchange column, the ratio of their distribution coefficients (D_a/D_b)) gives the separation factor, α, i.e, the ability of the ion exchange system used to separate these two ions, and it must be considered the most important parameter in ion exchange chromatography.

In elution chromatography the ions to be separated are adsorbed as a thin band on the top of the column containing the ion exchange resin in either cationic or anionic form.The sorption in the resin phase increases with the valency of the cation so that multivalent ions are adsorbed more strongly than divalent or monovalent ions (i.e. the higher the electrochemical valency and the lower the radius of the solvated ions, the higher will the strength of adsorption be so that: $M^{3+} > M^{2+} > M^{+}$), after which an eluent is passed through the column to effect the stripping from the resin bed. The volume of eluent required depends upon the nature of the cation to be eluted, the more strongly adsorbed higher valent cations requiring more eluent. Elution flow rates are usually about the same as adsorption rates (Overman and Clark, 1960). If the zone in the resin column where the ions are adsorbed is only a few percent of the column capacity and the flow rate is slow, the shape of the elution curve (concentration of ion versus volume of eluent) resembles a Gaussian curve (Jaakkola, 1994). The peak elution volume v (v = the elution volume with which the maximam concentration of ions in eluate is attained) is related to the total volume V as:

$$D_v = \frac{v - iV}{V} \qquad (18)$$

where i is the void fraction of the column. In the case of poor separation, the elution curves will overlap.

Elution may be accomplished by using another metal ion (e.g. trivalent) which

shifts the equilibrium of the exchange reaction through competing with M^+ for positions in the resin (Choppin et al., 1980). The adsorbed ions are eluted in succession, those with the lowest distribution coefficients eluted first (Coomber, 1975).

One of the basic concepts of ion exchange is the affinity of ions for the adsorbent. An affinity scale of cations according to the numerical value of the K_d (equation 16) are of limited use for the prediction of the column exchange behaviour of a cation beacuse they do not take account of the influence of the aqueous phase (Strehlow, 1960). More specific information about the behaviour to be expected from a cation in a column elution experiment is given by the equilibrium distribution coefficient:

$$K_d = \frac{C_1 \; x \; V_{aq}}{C_2 \; x \; m} \qquad (19)$$

where C_1 is the amount of ion on resin, C_2 is the amount of ion in aqueous phase, V_{aq} is the volume of aqueous phase (ml), and m is gram dry resin. Mayer and Tompkins (1947) developed the equation: $\upsilon = K_d$ x mass of dry resin in the column, where υ stands for the volume of the eluting agent, in milliliters, which has to be passed through the column to elute the maximum of the elution peak.

Trivalent actinides show weak retention on anion exchangers although they form negatively charged complexes with nitrate or chloride ions (De Regge and Boden, 1984). So as to increase their retention and separate them from mono- and divalent ions, alcohols are added to the aqueous phase. The method has been used to achieve group separation of thorium, uranium, neptunium, plutonium, americium and curium from other elements in marine environmental samples (Holm and Fukai, 1977).

The separation factor (α) can be increased by using complexing agents. A great

number of ions form anionic complexes with strong acid residues such as chloride; thus:

$$M^{m+} + n\,Cl^{-} \rightleftharpoons M\,Cl_n^{-(n-m)}$$

The function of complexing agent is not only to reduce the ionic concentration of different ions in solution but also to introduce a secondary equilibrium between ionized and complexed species. The differences in the stability constants of the complexes of the several ionic species results in different concentrations of the free ions and enables a separation to be affected (Cook and Duncan, 1952).

Kraus and Nelson (1956), have demonstrated the applicability of anion exchange resins in metal ion separation in the system of DOWEX-1 and hydrochloric acid. They measured the values of volume distribution coefficient (D_v) for most elements in a large range of HCl concentrations.

Inorganic ion exchangers are much more resistant to high temperature and to radiation than organic exchangers and are not subject to swelling and shrinking with change in the ionic strength of the medium. They show high selectivity for certain ions. In particular the high affinity of ammonium molydophosphate (AMP) for caesium has been of great importance in the nuclear energy field (Fuller, 1971), and K_2 $[CoFe(CN)_6]$ has also been used to separate the radiocaesium from large volumes of sea water (Folsom et al., 1960). Other transition metal ferrocyanides have been used by Roos et al. (1994). High pressure ion exchange chromatography offers the advantage of high flow rates and a reduction in radiation damage to the resin, while gases formed by radiolysis remain in solution.

2.7.3.4 Electrodeposition

In electrolysis the desired material is removed from aqueous solution by cathodic electrodeposition as a elemental form or hydrous oxides (e.g. Th and U). Internal electrolysis (spontaneous) is a means for separating elements without an external source of potential. The technique has been used less for separating ions than as a means of producing thin sources for counting α-emitters, or low energy β-emitters. Spontaneous electrolysis has been used as a final step in the separation of polonium, which is usually deposited on nickel or silver discs (Blanchard,1966 and Flynn,1968). Electrodeposition of metals is sensitive to the presence of other substances. The deposition of polonium is inhibited by the presence of Fe^{+3} and Cr^{+6} and other oxidants unless a reducing agent is present.

2.8 Review of separation chemistry of U, Th and Po

There is an extensive literature dealing with the separation chemistry that applied to these elements irrespective of the host matrix. They can be divided into the following: coprecipitation characteristics, ion exchange behaviour and solvent extraction.

The separation chemistry of the early actinide elements is largely controlled by redox reactions. The 5f shell electrons have a lower binding energy and greater spatial bonding capacity than the inner 4f orbitals of the lanthanide series. This is indicated in the comparative chemistries, the actinides form higher oxidation states and show a stronger tendency towards complexation than the lanthanide elements (Cotton and Wilkinson, 1988).

2.8.1 Uranium

Coprecipitation: When traces of uranium are being assayed in a complex

mixture preliminary separation is often carried out using a coprecipitation procedure. Iron or aluminium hydroxide can be used for isolating uranium from acid aqueous solutions by the addition of carbonate-free ammonium hydroxide. It is essential that the ammonia solution is free from carbonate since the uranium will otherwise form a carbonate complex which will remain in solution (Urry,1941). Uranium also can be coprecipitated from acid solution as the fluoride or phosphate. The host coprecipitant can be aluminium, titanium, zirconium or lanthanum (Korkisch, 1969).

Ion exchange: Cation exchange resins have frequently been used for separating uranium from other elements including the actinides. The sulphuric acid type cation resin shows little selectivity for the divalent uranyl ion (UO_2^{2+}) compared with other divalent metal ions. However, in sulphuric acid solution uranium can be separated more easily than in nitric acid or hydrochloric acid media. Since uranium is one of the few elements that form stable anionic sulphate complexes that allow it to be preferentially eluted from a column containing other elements. Many elements in the 2+ and 3+ oxidation states form strong chloride complexes in the same way as uranium and it is difficult to separate them out because of non-adsorption on the cation resin. The use of a cation resin in a nitric acid medium is also of little use since most of transition elements and uranium form no complexes with nitric acid or else very unstable complexes particularly at low concentrations of acid. Distribution coefficients of uranium, thorium and some other elements between a cation resin, Dowex AG50-WX8, and pure acid media are shown in **Table 2.2** (Strehlow,1960 and Strehlow et al., 1965).

Organic compounds have been used for complexing uranium and separation on cation resins. These include oxalic acid (Ishimori and Okimo, 1956) and ethylenediamine tetra-acetic acid (Kennedy et al., 1956), but they are of little value in the analysis of environmental samples.

With many common anions uranium forms anionic or neutral complexes that are useful in anion exchange separation. The anions used include acetate, chloride, fluoride, nitrate, phosphate and sulphate (Kraus and Nelson, 1956). Uranium can be separated from iron on a chloride column if it is first reduced to the divalent state with ascorbic acid, hydrogen iodide or ammonium iodide, when it will not be retained on the resin.

Uranium is weakly adsorbed on to strongly basic anion resins in the nitrate form. The distribution coefficient (K_d) rises to about 20 at 8 M nitric acid and then falls with increasing acid concentrations. This can be compared with a distribution coefficient of 10^3 in 8-10 M hydrochloric acid. Uranium can be separated from thorium in the nitrate form, but iron is only separated out with difficulty.

In dilute aqueous sulphuric acid solutions uranium forms anionic sulphate complexes that are strongly adsorbed on to strongly basic anion resins. A K_d value of c.10^4 in 0.05 M sulphuric acid rapidly decreases with increasing concentration (Korkisch, 1969).

Solvent extraction: This technique has been commonly applied for separating uranium from a considerable range of accompanying elements, e.g. organic acids, ketones, ethers, esters, alcohols and organic derivatives of phosphoric acid. In the early days of uranium chemistry diethyl ether was used for extracting uranyl nitrate but more recently its place has been taken by less volatile and less flammable ketones and phosphate derivatives. Methyl isobutyl ketone (MIBK) has been used extensively in the nuclear industry for the large-scale separation of uranium (Culler, 1956) and ethyl acetate in a nitric acid

Table 2.2

K_d values of uranium, thorium and iron between a cation exchange resin, AG50-WX8, and different normalities of HCL, HNO_3 and H_2SO_4

Cation	Acid	0.1 N	0.2 N	0.5 N	1.0 N	2.0 N	3.0 N	4.0 N
Th^{+4}	HCl	$> 10^5$	$> 10^5$	$\sim 10^5$	2049	239	114	67
UO_2^{+2}		5460	860	102	19.2	7.3	4.9	3.3
Fe^{+2}		1820	370	66	19.77	4.1	2.7	1.8
Th^{+4}	HNO_3	$> 10^4$	$> 10^4$	$> 10^4$	1180	123	43	24.8
U^{+4}		659	262	69	24.4	10.7	7.4	6.6
Th^{+4}	H_2SO_4	$> 10^4$	3900	263	52	9.0	3.0	1.8
U^{+4}		596	118	29.2	9.6	3.2	2.3	1.8
Fe^{+2}		1600	560	139	46	15.3	9.8	6.6

Source: Strehlow (1960) and Strehlow et al., 1965.

medium to extract uranium from solutions containing large amounts of salting-out agents, e.g. aluminium nitrate (Callahan, 1961). Uranium can be recovered by back-extraction of the organic phase with water or by evaporation of the solvent. A common organic phosphate, tri-butyl-phosphate (TBP), is widely used for separating uranium from many co-existing elements in a nitric acid medium. The distribution coefficient is considerably large over an acid range from pH3 to 6 M nitric acid. The advantages of TBP are its non-volatility (boiling point 289 °C) and its stability with concentrated nitric acid. Iron, thorium and protactinium are all co-extracted with uranium in nitric acid. A number of methods have been published for recovering uranium from the TBP complex including those using ammonium carbonate (Nemodruck and

Varotimtskaya, 1962), sodium carbonate (Bril and Holzer, 1961), oxalic acid (Pfeifer and Hecht, 1960) and water (Wood and Mckenna, 1962).

Tri-octylphosphine oxide (TOPO) in both cyclohexane and carbon tetrachloride has been used for the complete extraction of uranium from 1-7 M nitric acid solutions where separation from iron and chromium is readily achieved (White and Ross, 1961).

Thenoyltrifluoroacetone (TTA) is one of the most widely used extractants. Uranium forms a complex with TTA that can be extracted from aqueous solutions with a pH of 3 or higher using 0.15-0.5 M TTA in benzene. Thorium and iron are also co-extracted but the addition of EDTA and a solution with a pH of 6 increases the selective extraction of uranium (Khopar and De, 1960).

2.8.2 Thorium

Coprecipitation: Thorium forms hydroxide, fluoride, iodate, oxalate and phosphate precipitates. Of these the hydroxide and fluoride precipitates have been used to remove trace amounts of thorium from solution. Thorium can be coprecipitated quantitatively as the hydroxide with iron, lanthanum and zirconium by the addition of ammonium or alkaline hydroxide to an aqueous solution. If lanthanum fluoride is used to coprecipitate thorium, the insoluble fluoride is converted after separation to the hydroxide by metathesis (fusion) with alkaline hydroxide (Ko and Weiller, 1962).

Ion exchange: Thorium is adsorbed well on to acidic cation resins in all three mineral acid media, hydrochloric, nitric and sulphuric. The distribution coefficients for thorium in these acids and Dowex-50 resin are given in **Table 2.2**. The strongest affinity is in the hydrochloric acid medium since thorium does not form an anionic complex in aqueous hydrochloric acid. Thorium and trivalent transuranium elements are not retained on basic anion resins in aqueous

hydrochloric acid solutions, this property being widely used to effect separation of thorium from uranium, iron and protactinium. Thorium forms a stable nitrate complex, the best k_d value

being obtained with 5-10 M nitric acid solutions (Chow and Carswell, 1963).

Solvent extraction: Thorium can be extracted from nitric acid solutions with diethyl ether, the use of salting-out agents such as zinc nitrate increasing extraction (Bock & Bock, 1950). Thorium neither forms a stable chloride complex nor is extracted from hydrochloric acid solutions with diethyl ether (Jenkins & Mckay, 1954) which is put to practical account in separating iron from thorium in 6 M hydrochloric acid solutions. Thorium, like uranium, can be extracted with many organic ethers, ketones and etc.

Organic phosphorus compounds are useful for extracting thorium from a variety of solutions. In a range of organic solvents TBP will extract thorium together with uranium from nitrate solutions. Thorium is separated from uranium by extraction with TBP in hydrochloric acid solutions. Of the chelating agents used for the extraction of thorium, the β-diketone TTA in benzene or toluene (Ko & Weiller, 1962).

2.8.3 Polonium

Polonium [Xe] $4f^{14}5d^{10}6s^{2}6p^{4}$ is a group VI element and was first isolated from pitchblende (0.1 mg per ton). The halides are analogous to the Te salts but show increased stability in the Po^{+2} oxidation state (Bagnall, 1957). The chloride salts are volatile at temperatures greater than 150°C. The aqueous chemistry of polonium is complex; the common oxidation states are Po^{+2} and Po^{+4}. Polonium shows a strong tendency for colloid formation and complexation (Figgins, 1961). These properties influence environmental behaviour and separation chemistry (Sedlet, 1964). Spontaneous deposition of polonium on some metals

(eg. Ag, Cu and Ni) greatly simplifies source preparation for α-spectrometric measurements.

Coprecipitation: Polonium is isolated from solution with metallic tellurium as the carrier. Coprecipitation from a strong hydrochloric acid is carried out by the addition of sodium hypophosphite which reduces both tellurium and polonium to the metallic state. After tellurium has been filtered off, polonium can be dissolved in a HBr-HCl acid mixture and the tellurium selectively reduced with hydrazine hydrochloride (N_2H_4.HCl), leaving the polonium in solution. Polonium can also be coprecipitated on to manganese dioxide (Eakins & Morrison, 1978). The addition of potassium permanganate solution to a nitric acid solution containing polonium will scavenge it with the manganese dioxide precipitate.

Ion exchange: Polonium is strongly adsorbed on basic anion exchange resins from hydrochloric acid solutions. Ishimori (1955) has used this method for separating polonium from lead and bismuth.

Solvent extraction: Polonium is quantitatively extracted from nitric acid solutions with 0.25 M TTA in benzene. Separation of polonium from lead and bismuth can be effected by extraction of polonium from 6 M HCl acid solution with 20% TBP in dibutyl ether (Meinke, 1964).

Chapter 3

MATERIAL AND METHODS

3.1 Sample collection

3.1.1 Soil samples

Sampling areas were chosen on the basis of a geological map showing localities where granite was prevalent since radioactivity is highest in soils derived from granites (**Fig.3.1**). At each locality the background radiation levels were measured with a hand scintillometer (Scintrex Model BGS-15L) held 1 m above ground level. Readings ranging from 40 - 80 cps were observed. With this scintillometer readings above 50 cps are considered abnormal. A total of 60 soil samples c.2 kg each were collected from 20 districts as close as possible to habitation, the only stipulation being that the site should be on open reasonably level ground not prone to flooding or to erosion. At each site the soil was sampled by hand down to a depth of 30 cm. Several sites were sampled in each district. In the laboratory the samples from each of the 20 districts were hand-mixed to obtain a representative samples (20 in all). Samples were air-dried, pounded in a mortar and passed through a 2-mm sieve, the remaining gravel was discarded. The material was then oven-dried at 40 °C and again pounded in a mortar after which it was thoroughly mixed and analysed.

3.1.2 Rock phosphate samples

A total of 29 composite surface rock phosphate samples were collected from the Uro and Kurun rock phosphate deposits in the eastern part of the Nuba Mountains, western Sudan, according to the lithological differences within the ore deposit. A chisel and hammer were used to break off the phosphate chips,

which were then collected in cloth bags. Weathered edges and surfaces were avoided. Samples were crushed in a jaw crusher and then ground to very fine powder.

3.1.3 Marine sediments and organisms

Samples of marine surface sediments, seagrass and the green algae *Cystoseria* and *Halimedia*, the brown algae *Sargassum* and *Padina pavonia* (classified according to Alan, 1977) were collected from various areas along the Sudanese coast of the Red Sea as shown in **Fig.3.2**. Most of the samples were collected from the area of the fringing reefs at Port Sudan, in effect from the reef north to the harbour entrance which is the most affected and seriously endangered by human activities, and at the same time, this area being the most accessible to the people of Port Sudan. Samples were taken along transect at c.50 m intervals across the fringing reefs area into the open sea at depths ranging from 0.5 to 100 m. In shallow water the sampling was done by hand with the aid of hollow polystyrene cylindrical tube; in deep water bottom sediments were collected using 5 kg grab sampler. Detailed map of Port Sudan harbour and the fringing reefs showing sampling locations is given in **Fig. 3.3.** Sediments were also collected from other areas as follows:

1. The entrance of the main harbour, the south harbour (Khour Kilab), and the north harbour at depths ranging from 13-32 m.
2. The tidal flat of the Sanganeb atoll, 30 km northeast of Port Sudan at a depth of 3 m, as well as offshore south of the atoll at a depth of 750 m (this sample is taken from the board of German cruise in 1992 during field trip jointly conducted with researchers from the Institute of Oceanography, Port Sudan). **Fig. 3.4** shows the sampling locations in Sanganeb atoll.
3. Coastal black sand samples from Trinkitat Mersa, 180 km south of Port

Sudan.

4. Coastal black sand samples from Dungunab Bay, 65 km north of Port Sudan. Samples were placed in plastic bags and immediately transported to the laboratory. Samples of seagrass and algae were thoroughly washed with tap-water, freed of adhering soil particles and then oven-dried at 60°C. Sediment were air-dried on porcelain dishes and screened through a 2 mm sieve to get rid of fairly large grains as well as coral, crustacean and sponge debris. Those from shallow water regime in particular were largely associated with biogenic components.

During the last week of April, 1997 a second field trip was conducted in the Sudanese coastal waters of the Red Sea and a total of 27 samples of surface marine sediments were collected from the harbours at Port Sudan and Sawakin which are about 60 km apart (**Fig. 3.2**). Samples were taken at different depths using a 5-kg grab sampler, the sites being chosen to provide good spatial coverage of each harbour as in **Figs 3.5** and **3.6**. Samples were collected in polyethylene bottles with screw caps and transported to the laboratory in Khartoum, where they were thoroughly dried at room temperature on aluminium trays and ground with a large mortar and pestle. The material was then sieved through a 2-mm mesh sieve after which the remaining residue was discarded. The time delay between collection and the start of analysis for alpha-spectrometry was 8 weeks during which the samples were stored dry and homogenized.

3.2 Location and the geology of the Uro and Kurun phosphate deposits

The location of Uro and Kurun phosphate deposits is shown in **Fig. 3.1.** Kurun phosphate deposit was discovered by Brinkman (1986) in the neighbourhood of Jebel Kurun which is situated on the east border of the Nuba Mountains about

44 km southeast of Rashad town. The hill consists of graphite schist breccia, quartzite breccia and apatite breccia. The breccia fragments consist of graphite bearing schist components cemented by phosphate. The breccia is presumably of tectonic origin.

Uro phosphate deposit is also located on the east border of the Nuba Mountains about 10 km northwest of Abu Giubiha town. It is a volcano sedimentary rock, omphiolyte assemblage and quaternary sediments include rocks that belong to green schist facies consisting of a variety of schists e.g chlorite phyllite, chlorite schist, mica schist, graphite schist, marbles and quartz (Gamal, 1987).

3.3 Geography and the hydrology of the Red Sea

The Red Sea belongs to the category of land-locked seas, as it is in a semi-enclosed basin in an arid zone in which evaporation far exceeds precipitation and runoff. Like the other enclosed seas, its chemistry is intimately linked with physical and biological processes, in particular with topographical features (Morcos, 1970). It extends as a rift valley from the narrow land bridge between Africa and Arabia in the north to the straits of Bab el Mandeb. It has a total length of 2200 km and on the average is about 280 km broad and 491 m deep. It was formed by the separation of the two crustal blocks of Africa and Arabia (Swartz and Arden, 1960). The central rift valley is an oceanic crust, and the shallower parts on either side of the trough are down-faulted continental blocks that were covered by carbonate sediments (Girdler, 1966). The Red Sea is connected with the Mediterranean by the Suez Canal which has no locks; however, this connection is of no practical importance for the exchange of water. In the south, the straits of Bab el Mandeb limit water exchange between the Red Sea and the Gulf of Aden. The rainfall over the Red Sea and its coasts

is extremely low. Evaporation exceeds precipitation, and this combined with the very restricted exchange of water with the open sea leads to the production of the dense, highly saline water. The temperature of the surface water ranges between 15 to 20 °C in January and 27 to 34 °C in July, the pH ranging from 7.9 to 8.7 (Khalil, 1994). The absolute concentrations of oxygen are comparatively low because of the high salinity and high temperature of the surface water.

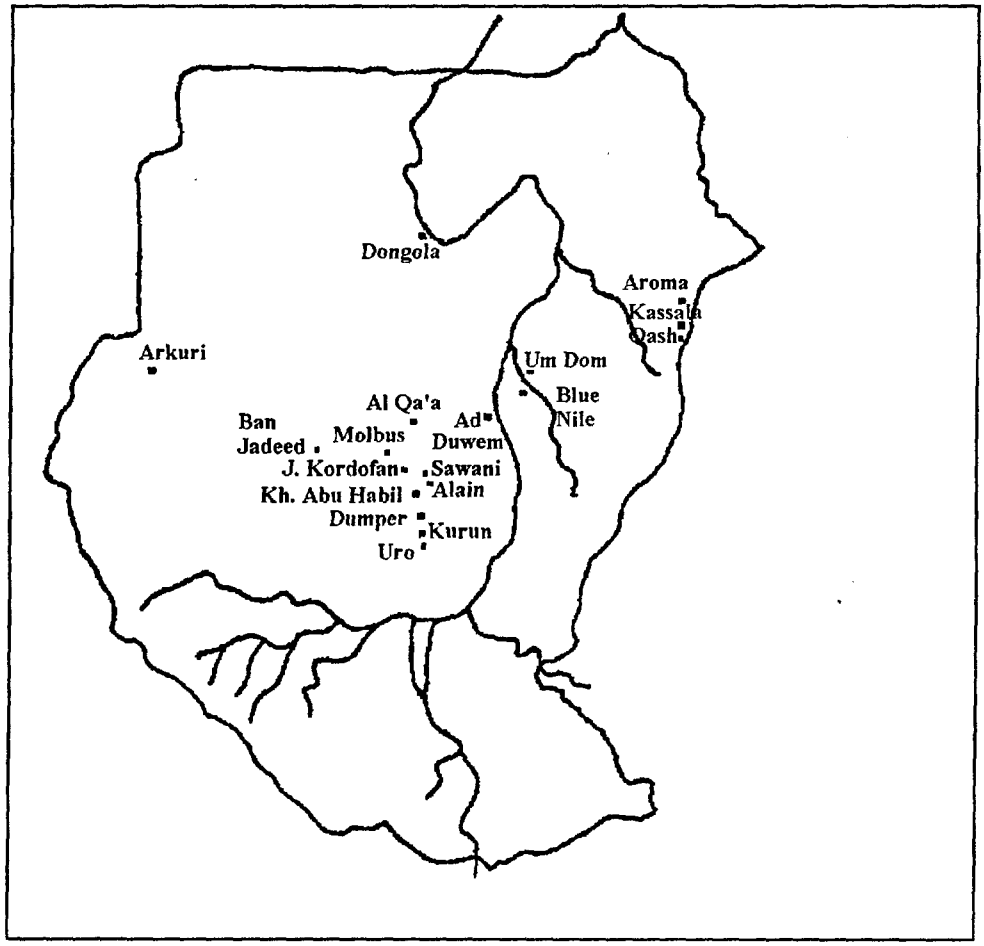

Fig. 3.1: Map of Sudan showing soil sampling areas

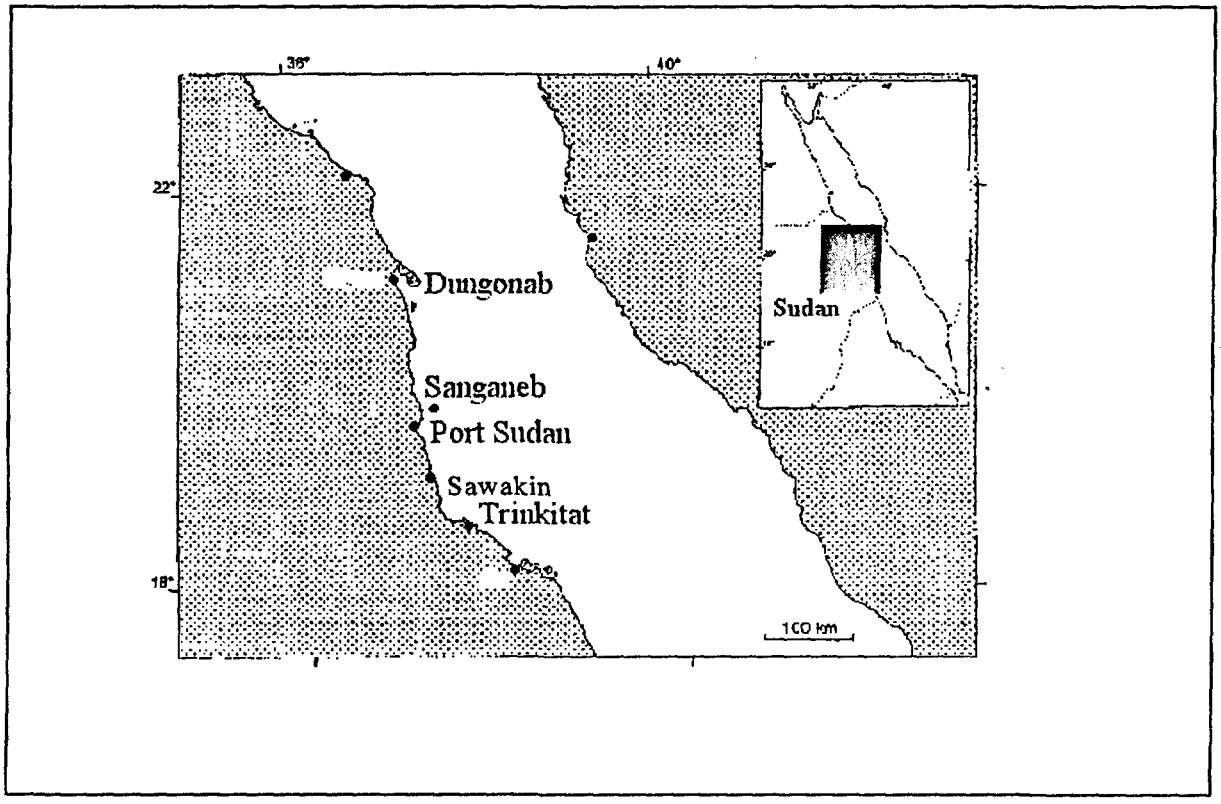

Fig. 3.2: Map showing sampling areas along the Sudanese Red Sea coast

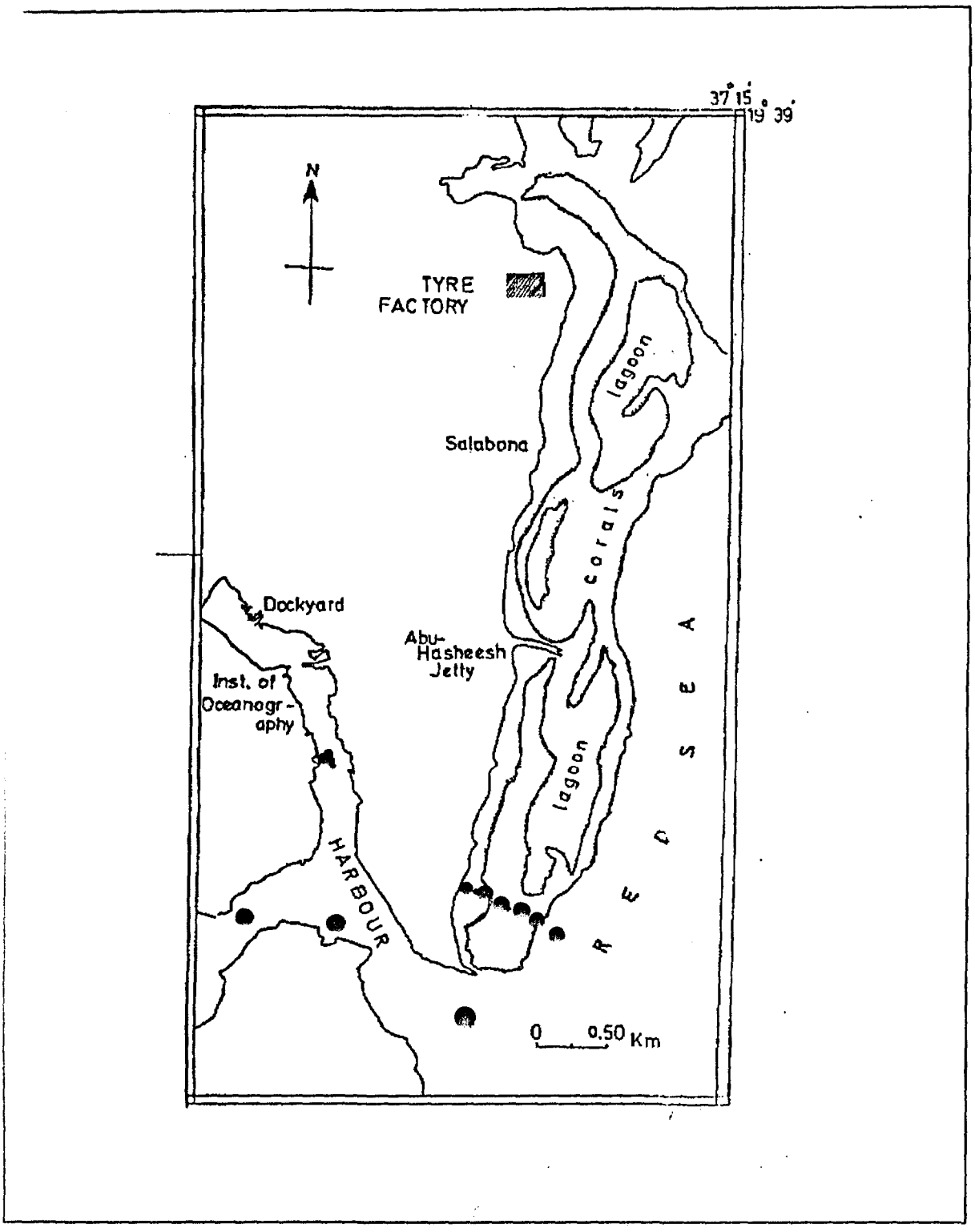

Fig. 3.3: Map of Port Sudan harbour and the fringing reefs north to the harbour showing sampling locations

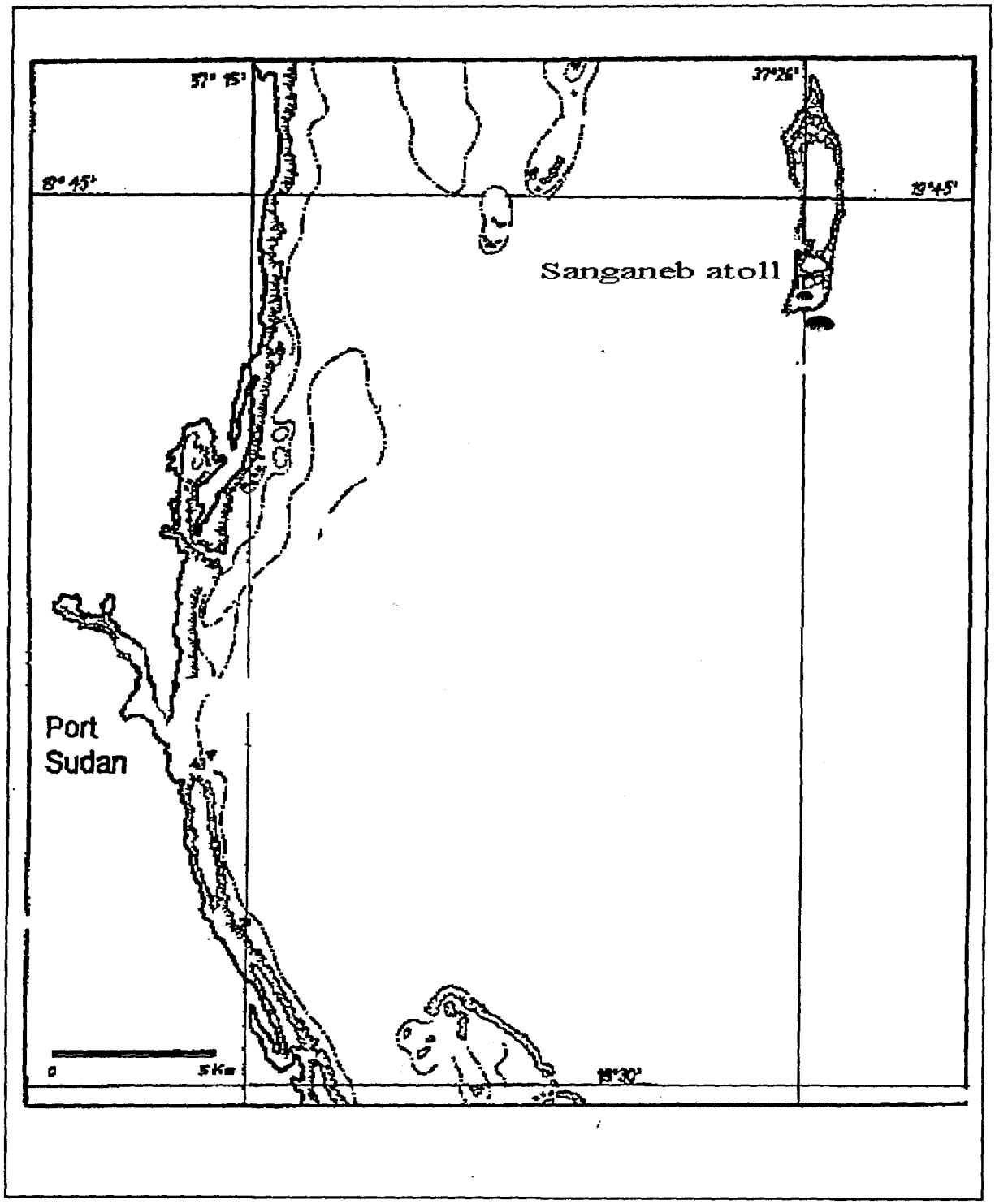

Fig. 3.4: Map showing sampling locations in Sanganeb atoll

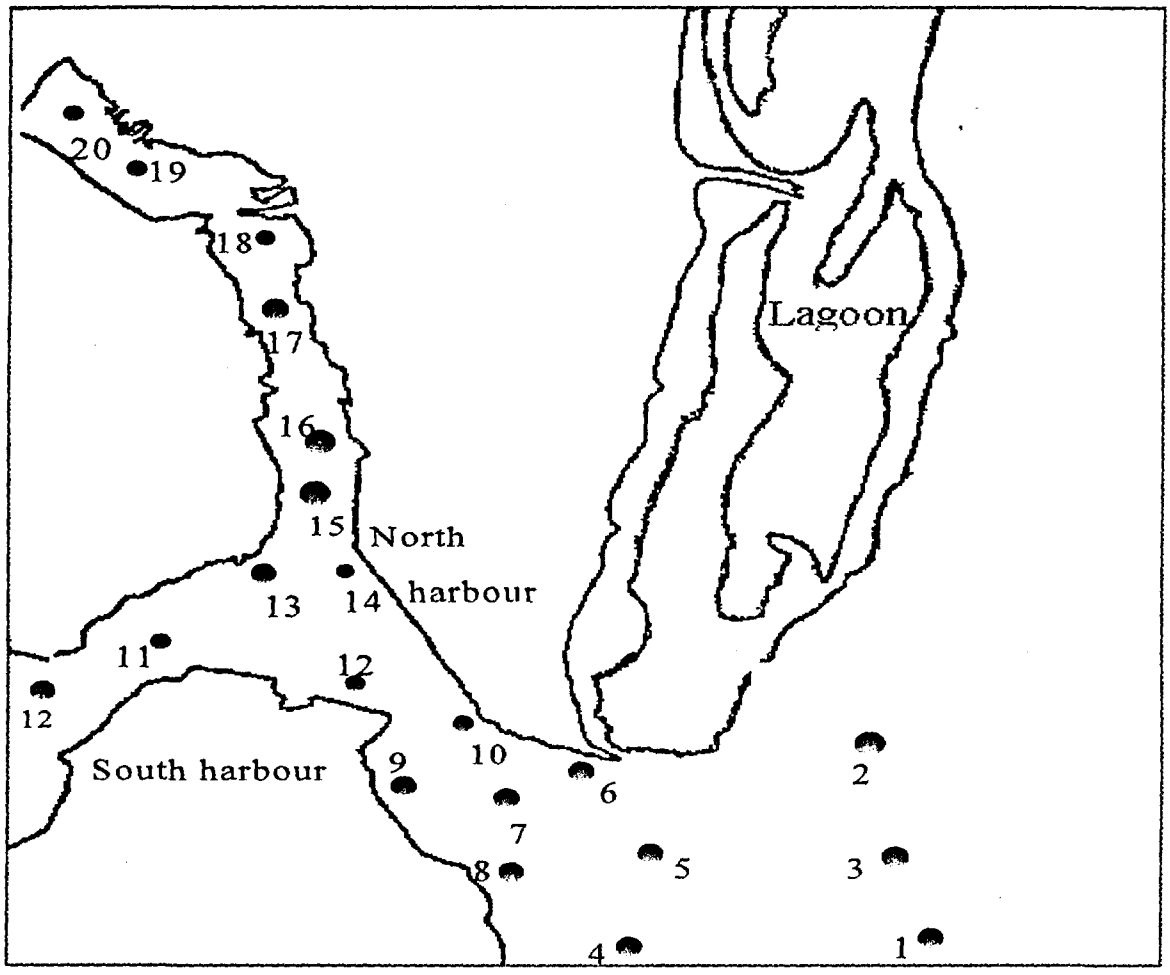

Fig. 3.5: Sampling sites in Port Sudan harbour (second field trip, 1997)

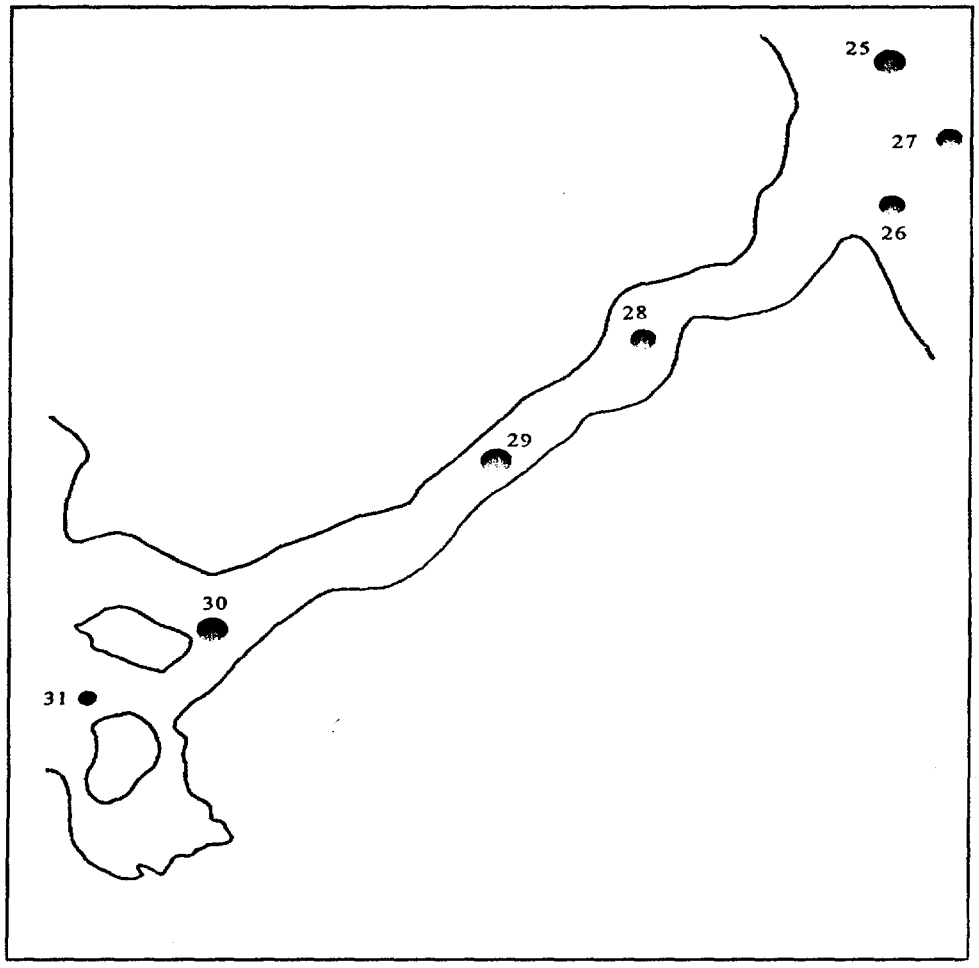

Fig. 3.6: Sampling sites in Sawakin harbour (second field trip, 1997)

3.4 Physical analysis of soil samples

Apparatus:

1. Standard hydrometer, ASTM No. 152H, with Bouyoucos scale in g/l,
2. Electrically driven mixer with replaceable paddle
3. Graduated cylinder, one litre
4. Brass plunger

Reagents:

1. Hydrogen peroxide, 35%
2. Hydrochloric acid
3. Sodium hexametaphosphate (Galgon), $(NaPO_3)_6$

Procedure: 50 g of 2 mm sieved soil sample was placed in 800 ml glass beaker. 1 M HCl was added dropwise until all carbonates in the sample have decomposed and the reaction ceases. 200 ml of deionized water was added, the beaker was covered with a glass dish and reflexed on water bath at 100 °C. 10 ml of 35% H_2O_2 was added at intervals of 20 min and the suspension was stirred frequently with a glass rod until the reaction ceased (i.e, complete oxidation of organic matter), after which the pH of the suspension was adjusted to 9.0 using 1 M NaOH solution. 25 ml of 10% $(NaPO_3)_6$ was added as a dispersing agent and the volume of the suspension was made up to 400 ml with deionized water. The suspension was then transferred to the dispersing cup and mixed at high speed for 15 min so as to complete dispersion. This dispersed slurry was passed through a 2 mm sieve into 1000 ml sedimentation cylinder and filled up to the mark with deionized water. The coarse sand fraction was ashed overnight in a muffle furnace at 600 °C and the weight was recorded.

The hydrometer was inserted into the blank solution (25 ml of 10% Galgon diluted to 1000 ml) and pushed slightly below the floating position to wet the stem so that meniscus would be fully formed. The scale reading RL (g/l) at the

upper edge of the meniscus surrounding the stem was recorded. The suspension was thoroughly mixed with the plunger and the hydrometer was slowly inserted and the scale reading (R) at 0.5 min, 1 min, 2 min, 5 min, 15 min, 45 min, 2 hrs, 5 hrs and 24 hrs from the start of sedimentation and the elapsed time were recorded. Immediately after the 15 min reading, the hydrometer was withdrawn very slowly from the suspension and wiped with a dry, clean cloth and left until the next reading period (do not hold the hydrometer by the stem). It is not essential that the reading be taken at the exact intervals stated above, but the exact time at which the readings were taken should be recorded. This procedure is a slight modification of that described by Day (1965).

Calculations:

The concentration of suspension for each reading (C) is given by the formula:

$$C = R - RL \quad (g/l)$$

The summation percentage (P) = 100 (C/C°), where C° is the dry weight of soil in grams per litre suspension.The particle size (X) in μm is given by

$$X\ (microns) = \frac{q}{\sqrt{t}}$$

where t is the sedimentation time in minutes and q is a sedimentation constant corresponding to each value of R obtained from the Standard Table. P versus X was plotted on semilogarithmic paper using the log scale for X. Diameter range < 0.002 mm was taken as clay fraction.

3.5 Chemical analysis

3.5.1 Organic matter

5 g of a sample was oven-dried in a porcelain crucible at 100°C for three hours and then ashed at 400°C over-night. The weight loss on ignition was calculated and used as an estimate of the organic matter in the sample.

3.5.2 pH measurements

The pH of the sample was measured in deionized water, 0.1 M KCl and 0.01 M $CaCl_2$ solutions by mixing 4 g of dry sample with 10 ml each of the above solutions to produce a 1: 2.5 sample solution ratio (Michael, 1965). The solution mixture was mixed with a glass rod and allowed to settle over-night at room temperature. pH measurements were made using a PHB 82 Standard pH Meter.

3.5.3 Extraction of exchangeable K^+, Ca^{++}, Mg^{++} and soluble phosphorous

3.5.3.1 Ammonium acetate

50 g of dry sample was added to 500 ml of 1 M ammonium acetate buffer solution at pH 7.0 in plastic bottles with screw caps and gently shaken for 2 hrs at room temperature on a Stalproоukter shaking machine to insure the maximum extraction of cations. The extracts were filtered through folded filter papers (hard filtra), Allen (1989).

3.5.3.2 Ammonium lactate

5 g of dry sample was added to 100 ml of ammonium lactate acetic-acid solution at pH 3.95 in 113 ml glass bottles with screw caps and gently shaken for 1.5 hrs on a shaking machine. The extracts were filtered through hard filtra. 10 ml of each filtrate from (I) and (II) was transferred to 50 ml volumetric flasks and diluted with deionized water up to the mark, and stored for the

determination of exchangeable K^+, Ca^{++}, Mg^{++} and the readily soluble P in the sample.

3.5.4 Colorimetric determination of phosphorus

This method is based on the formation of a heteropolic acid complex (phosphomolybdic acid), when an acid molybdate reagent is added to a solution containing orthophosphate. Reduction of this complex gives the characteristic molybdenum blue colour (Murphy & Riley, 1962).

Reagents:

1. Sulphuric acid 5 N
2. 4% $(NH_4)_7Mo_7O_{24}.4H_2O$ solution stored in the dark or in a brown bottle.
3. Ascorbic acid solution ($C_6H_8O_6$) 1.75% (can not be kept longer than one day).
4. Potassium antimony tartrate solution is obtained by dissolving 0.275 g $K(SbO)C_4H_4O_6.0.5H_2O$ in deionized water and diluting to 100 ml (cannot be kept for more than a few weeks).
5. Mixed reagent: Mix 160 ml of (1), 50 ml of (2), 100 ml of (3) and 16 ml of (4). Make up to one litre with deionized water, mix and filter after 20 min to eliminate a blue colloidal precipitate which may form. The mixture can be kept only for one day.
6. Stock standard solution: Dissolve 1.9167 g of KH_2PO_4 in deionized water and dilute to one litre (1 ml contains 1 mg P_2O_5).
7. Working standard solutions: Dilute 10 ml of the stock standard solution to one litre. Transfer 10, 20, 40, 60, 80 ml of this solution to 200 ml volumetric flasks, fill up to the mark with deionized water and mix (200 ml of the working standard solutions contains 0.1, 0.2, 0.4, 0.6 and 0.8 mg P_2O_5, respectively). Store all the solutions in the dark.

Procedure: 20 ml of the reagent mixture was transferred to a 100 ml volumetric

flask, 20 ml of the first of the working standard solutions was added and the mixture was thoroughly mixed then left to stand for 20 min. The absorbance of the blue solution was measured in a 1 cm cuvet at 880 nm (the absorbance remains constant for at least 12 hrs). This procedure was repeated with each of the working standard solutions. The sample filtrates (see 3.5.3) were treated in the same manner.

A calibration curve was plotted from the readings of the working standards and the amount of P in the sample was calculated as:

$$mg\ P/g = \frac{C\ x\ 43.64\ x\ solution\ volume}{aliquot\ volume\ x\ 100\ x\ sample\ weight\ (g)}$$

where C = mg of P_2O_5 obtained from the calibration curve.

3.5.5 Determination of potassium by flame emission

Reagents:

1. Potassium stock solution: Dissolve 1.907 g KCl in distilled water and dilute to one litre (1 mg K/ml).
2. Working standard solutions: Dilute 100 ml of the stock solution to 1000 ml (100 ppm). Transfer 0, 1, 5, 10, 25, 50, 100 ml to 100 ml volumetric flasks and fill up to the mark with distilled water.
3. Working conditions: Wavelength (766 nm), slit-width (0.1 nm).

Procedure: After a warming up period , the photometer was set to zero deflection with the blank solution. Each of the working standards was then aspirated in turn. The sample solutions (see 3.5.3) were aspirated into the flame under the same conditions as the standards after appropriate dilutions. A

calibration curve was produced from the readings of the working standard solutions and the amount of potassium (ppm) in the sample was obtained.

Calculations:

$$K\ (mg/g) = \frac{ppm\ x\ solution\ volume}{aliquat\ volume\ x\ sample\ weight}$$

$$K\ \% = \frac{ppm\ x\ solution\ volume}{10^4\ x\ sample\ weight\ (g)}$$

3.5.6 Determinations by atomic absorption spectroscopy (AAS)

3.5.6.1 Calcium

Reagents:

1. Calcium stock solution: Dissolve 2.497 g dried $CaCO_3$ in a minimum volume of 1% HNO_3 and dilute to one litre (1 ml contains 1 mg Ca).

2. Working standard solutions: Dilute 20 ml of the stock solution to one litre with 1% HNO_3. Transfer 0, 5, 10, 25, 50, 75 ml to 100 ml volumetric flask and fill up to the mark with 1% HNO_3.

3. Lanthanum chloride solution (releasing agent to overcome the enhancement effect caused by the alkali like metals): Dissolve 25 g $LaCl_3.7H_2O$ in deionized water containing 1 ml of 2 M HCl and dilute to one litre.

4. Working conditions: Lamp current (3 mA), wavelength (422.7 nm), slit-width (0.2 nm).

Procedure: 20 ml of each of the working standard solutions and the sample filtrates (see 3.5.3) was separately placed in a 50 ml volumetric flask, and 4 ml of $LaCl_3.7H_2O$ solution was added to each flask. After a warming up period, the blank (zero ppm standard) was set to zero deflection. Sample solutions were

aspirated into the flame under the same conditions as the working standard solutions. A calibration curve was plotted from the readings of the standard solutions, and the amount of Ca (ppm) in the sample was determined (Adams and Passmore, 1966).

3.5.6.2 Magnesium

***Reagents*:**

1. Magnesium stock solution (100 ppm Mg): Dissolve 1.0136 g $MgSO_4.7H_2O$ in 1% HNO_3 and dilute to one litre.
2. Working standard solutions: Transfer 0. 1, 5, 10, 25, 30 ml of the stock solution to 100 volumetric flask and fill up to the mark with 1% HNO_3.
3. Lanthanum chloride solution (5000 ppm La): Dissolve 6.6837 g $LaCl_3.7H_2O$ in deionized water contains 1 ml of 2 M HCl and dilute to 500 ml.
4. Working conditions: Lamp current (3 mA), wavelength (285.2 nm), slit-width (0.5 nm).

Procedure: 20 ml of each of the working standard solutions and the sample filtrates (see 3.5.3) was separately placed in a 50 ml volumetric flask, and 4 ml of $LaCl_3.7H_2O$ solution was added to each flask. After a warming up period, the blank (zero ppm standard) was set to zero deflection. The sample solutions were aspirated into the flame under the same conditions as the working standard solutions. A calibration curve was plotted from the readings of the standard solutions, and the amount of Mg (ppm) in the sample was determined (Halls & Townshend, 1966).

3.6 Measurement of uranium, thorium and polonium by α-spectrometry

Methods for sample treatment and the radiochemical separation of natural uranium, natural thorium and ^{210}Po used in this study were based on procedures

described by Holm and Fukai (1977) and Lally (1992). The electrodeposition of U and Th was done using a method reported by Hallstadius (1984). Suitable amounts of isotopic tracers (^{232}U, ^{229}Th and ^{209}Po) were added to the sample prior to dissolution in aqua regia. After extraction into TBP from 8 M HNO_3 solution, thorium was recovered by back-extraction of the TBP phase with 1.5 M hydrochloric acid solution, and uranium with deionized water. Prior to extraction, the TBP was diluted with xylene to decrease the distribution coefficient of Th and facilitate its back-extraction to the aqueous phase. The thorium fraction was purified from any entrained uranium by dissolving it in 8 M nitric acid and passing it through an anion-exchange column in chloride form (DOWEX, AG 1-4X, 100-200 mesh). After washing the column with 8 M nitric acid, thorium was eluted with 9 M hydrochloric acid. Thorium and uranium in their respective solutions were electrodeposited onto a stainless steel disc from an ammonium sulphate electrolyte at a current of 1 A for one hour, after which the electrolyte was quenched with ammonia and the disc was dismantled. ^{210}Po in the sample was deposited onto a nickel disc from a diluted hydrochloric acid solution in an oven at 65 °C for two hours (Blanchard,1966). The interference of Fe^{+3} and Cr^{+6} that also deposit onto a nickel was eliminated by the addition of L-ascorbic acid (Flynn, 1968). Fuller details of yield determinants, sample preparation, extraction, and source preparation for α-spectrometric measurements are given below.

3.6.1 Isotopic tracers

3.6.1.1 Uranium

Three uranium isotopes, ^{232}U, ^{233}U and ^{236}U are most commonly used in alpha-spectrometric measurements as isotopic tracers for the determination of radiochemical yield and quantification of the isotopic composition of the natural

uranium isotopes (^{238}U, ^{235}U, ^{234}U). α-energies of ^{233}U (4.78 MeV and 4.82 MeV) are too close to the energies of ^{234}U (4.72 and 4.78 MeV) to be resolved by α-spectrometric techniques. Similarly, the energies of ^{236}U (4.47 and 4.52 MeV) interfere with those of ^{235}U (4.2 - 4.6 MeV). Therefore, in our measurements we have used ^{232}U, because its α-energies (5.26 and 5.32 MeV) are far from those of the naturally occurring isotopes of uranium and can be resolved without any spectral interference (**Fig. 3.7**). The only drawback of using ^{232}U is that the accompanying daughter nuclide, ^{228}Th, complicates the spectrum on standing for a long time after electrodeposition. However, in biological samples in which the amount of ^{235}U is insignificant, either ^{235}U or ^{236}U can be used as an isotopic tracer.

3.6.1.2 Thorium

Three isotopic tracers (radiochemical yield determinants) are commonly used; namely ^{228}Th, ^{229}Th and ^{234}Th. The ^{228}Th is only used when the ^{232}Th and ^{230}Th content of the sample is to be determined. If the sample itself contains relatively high concentrations of ^{228}Th, it could be measured by γ-spectrometry and then used as an isotopic tracer in α-spectrometric measurements of ^{232}Th and ^{230}Th. The disadvantages in using ^{228}Th as an isotopic tracer are the spectral interference that occurs from the rapid ingrowth of its daughter, ^{224}Ra (5.68 MeV), and the recoil problem that results in the contamination of the detectors after continuous operation. ^{234}Th is a β-emitter and so its chemical recovery must be determined by β-counting (Singh and Wrenn, 1979). The remaining isotope, ^{229}Th, which we have used in the current study, emits α-particles with energies ranging from 4.69 - 5.05 MeV which interfere slightly with the high energy part of ^{230}Th but it will not pose a problem if the spectrum resolution is well optimized (**Fig. 3.8**). The advantages of using ^{229}Th as a tracer for the

radiochemical measurement of the other thorium isotopes are as follows: (a) an increase in accuracy is associated with the simultaneous α-spectrometric measurements of the tracer and the other nuclides being determined, (b) the long half-life of ^{229}Th (7340 yrs), requires neither repeated preparation nor correction for decay, and (c) ^{229}Th is an α-emitter as are the naturally occurring thorium isotopes of interest; accordingly the α-spectrum provides as part of the measurement a determination of radiochemical yield, thereby saving time, and minimizes the handling and separate measuring techniques.

3.6.1.3 Polonium

^{208}Po and ^{209}Po are commercially available as isotopic tracers for radiochemical measurement of naturally occurring ^{210}Po. The α-energy of ^{208}Po (5.11 MeV) interferes with that of ^{210}Po at 5.3 MeV. ^{209}Po emits an α-particle of 4.88 MeV, is preferable from the spectral interference point of view and it was the tracer used throughout this work. The radioactive half-life of ^{209}Po is long (102 yr) decay correction thus not being required.

3.6.2 Calibration of isotopic tracers

The stock solutions of ^{232}U, ^{229}Th and ^{209}Po tracers used were calibrated against standard solutions of $UO_2(NO_3)_2$. $6H_2O$, Th $(NO_3)_4$. $5H_2O$ and digest solutions of certified reference material, CANMET uranium-thorium ore DH-1a (Dension Mines Limited, Elliot, Ontario, Canada). The certified value of ^{210}Pb in HD-1a was used for recalibrating the ^{209}Po tracer solution. Uranyl and thorium nitrates were dried to constant weight at 105 °C, and their exact content of water of crystallisation was determined by heating to a constant weight at 500 °C. Th and U standard solutions were prepared by dissolving a known amount of uranyl or thorium nitrate in2 M HNO_3 as follows:

(I) U-standard: 0.0527 g of dry $UO_2(NO_3)_2$. $6H_2O$ was placed in a volumetric flask and dissolved in 1000 g of 2 M HNO_3 (1 g contains 305.78 mBq ^{238}U = [Z x H x m x 12.33 mBq]/ [M x V]), where Z is the atomic weight, H is an isotopic abundance (99.27% ^{238}U by mass), m is the mass of the uranyl nitrate taken, M is the molecular weight of the uranyl nitrate, V is the volume of the solvent and the factor 12.33 mBq is the activity of 1 μg of ^{238}U.

(II) Th-standard: 0.0866 g of Th $(NO_3)_4$. $5H_2O$ was dissolved in 972 g of 2 M HNO_3 (1 g contains 146.7 mBq ^{232}Th. The activity of 1μg ^{232}Th = 4.047 mBq.

3.6.3 Sample preparation

A known amount of a sample (1 g for soil and marine sediments, 0.2 g for rock phosphate and 5-10 g for biological samples) was placed in an appropriately sized beaker and small amounts (**see Table 3.1**) of ^{232}U, ^{229}Th and ^{209}Po tracers were added, the amount of the tracer to be added being governed by the specific activity of the tracer solution and the activity level of the sample. Just enough HNO_3 to immerse the sample was then added and the beaker was covered with a watchglass and evaporated on a sand bath until nearly dry. The residue was digested and brought to near dryness twice with 20 ml of aqua regia (1 HNO_3 : 3 HCl). Finally, the residue was dissolved in 10 ml of HNO_3 and evaporated to near dryness. This fraction is now ready for sequential extraction of polonium, thorium and uranium.

Biological samples for U and Th determination were first ashed at 450 °C overnight, whereas for polonium the samples were wet ashed with HNO_3 in the presence of H_2O_2. The acid mixture was occasionally added to the sample on a sand bath until frothing ceased and then evaporated till nearly dry. The residue was treated as outlined above. Similarly, we have wet ashed the biological samples with HNO_3-$HClO_4$ mixture. The main part of the organic material was

first decomposed with nitric acid after which perchloric acid was added and the remaining nitric acid removed by boiling. This method of wet oxidation proved effective, but because of the danger of explosion, it requires a special fume-hood equipped with a water system.

Table 3.1

Specific activity of the tracer and the amounts added to the samples

Tracer	Activity	Amount of tracer added (g)			
	mBq/g	Soil	Sediment	Phosphate	Biological
^{232}U	62.1	O.5	0.5	1.0	0.5
^{229}Th	153	0.4	0.4	0.4	0.4
^{209}Po	426	0.3	0.3	0.3	0.3

3.6.4 Sequential extraction of polonium, thorium and uranium

3.6.4.1 Polonium

The residue in the beaker (**3.6.3**) was dissolved in 10 ml of 8 M HNO_3 and filtered into a 250 ml separatory funnel. The beaker was rinsed with 10 ml of 8 M HNO_3 and the solution was transferred to the same separatory funnel. 5 ml of TBP (tri-butylphosphate, $C_{12}H_{27}O_4P$) was added to the separatory funnel and shaken for 2 min on a shaker. The aqueous phase was separated and transferred to the beaker. The organic phase was extracted twice with 10 ml of 8 M HNO_3, shaken for 2 min each time and the aqueous phase was separated and transferred to the same beaker. The collected aqueous phase was evaporated on a sand bath untill nearly dry. The residue was dissolved and brought to near dryness twice

with 5 ml of HCl then redissolved in 2 ml of concentrated HCl and diluted with 5 ml of deionized water. A small amount of L-ascorbic acid ($C_6 H_8 O_6$) was added, and the solution was filtered into a deposition cell mounted with a polished nickel disc after pre-testing the cell/disc interface for possible leaks (the deposition cell used is described below). The beaker was rinsed with 5 ml of deionized water and filtered into the plating cell which was placed in an oven at 65 °C and stirred with a constant-speed stirrer for 2 hours. The plated nickel disc was dismantled and rinsed with a diluted ammonia solution (10 ml of ammonia in 1 litre of deionized water) and then with methanol. The edge of the disc was touched with tissue paper to absorb the film of methanol and then dried on a hot plate covered with aluminium foil.

3.6.4.2 Thorium

20 ml of xylene (C_8H_{10}) and 15 ml of 1.5 M hydrochloric acid were added to the organic phase in the separatory funnel (TBP), shaken for 2 min and the aqueous phase was separated and transferred to a beaker. The back-extraction procedure was repeated twice with 15 ml of 1.5 M HCl and the aqueous phase was transferred to the same beaker. The aqueous phase collected was evaporated on a sand bath until nearly dry. The residue was dissolved and evaporated to near dryness twice with 5 ml of HNO_3. A column was packed with an anion exchange resin in chloride form (DOWEX AG, 1-4X, 100-200 mesh) and washed with 15 ml of 8 M HNO_3. Thorium solution was passed through the column and discarded. The column was washed with 50 ml of 8 M HNO_3 and the Th was eluted from the resin bed with 50 ml of 9 M HCl and then evaporated until nearly dry. This fraction is now ready for electrodeposition.

3.6.4.3 Uranium

15 ml of deionized water was added to the organic phase in the separatory funnel (TBP), shaken for 2 min and the aqueous phase was separated and transferred to a beaker and acidified with few drops of HCl. The back-extraction procedure was repeated once more with 15 ml of deionized water. The aqueous phase was collected in the same beaker and evaporated on a sand bath to near dryness. This fraction is now ready for electrodeposition.

3.6.5 Electrodeposition of thorium and uranium

Apparatus: An electropolished stainless steel disc was fitted in the cap of c.20 ml polyethylene scintillation vial. The bottom of the vial has been cut off and a hole drilled through the centre of the cap for electrical connection to the cathode (disc). The disc, which has an exposed area of c.2.3 cm^2, was rinsed with acetone and deionized water prior to use. The assembly was checked for leakage by filling it with deionized water and leaving it standing for some time on paper. The anode, a platinum spiral, was introduced through the bottom of the vial and fitted around 5 mm from the cathode. The solution is not stirred during electrolysis.

Procedure: 1 ml of 0.3 M Na_2SO_4 was added to the solution containing thorium or uranium and completely dried on a sand bath. 300 µl of H_2SO_4 was added to the residue and the beaker was warmed and the solution swirled until the residue was completely dissolved. 4 ml of deionized water and 2 drops of 0.2% thymol blue indicator were added to the solution and titrated aganist concentrated ammonia dropwise to a yellow/orange end point. The solution was transferred to the electroplating cell mounted with a stainless steel disc after pre-testing the cell/stainless steel disc interface for possible leaks and the beaker was rinsed with 5 ml of 1% H_2SO_4. The pH of the solution was adjusted to fall within the

range of 2.1 - 2.4 with drops of ammonia, or if the end point is overstepped, 20% H_2SO_4 acid was added dropwise to achieve the pH required in the plating solution (different pH papers give different readings, the range given above refers to Merck's paper 9540 for pH 0-2.5). The thorium or uranium was electroplated at a current of 1 A for 1 hour, at the end of the hour the electrolyte was quenched with 1 ml of ammonia about 1 min prior to switching off the current. The disc was dismantled and washed with a dilute ammonia solution (10 ml concentrated ammonia in 1 litre deionized water) and then with acetone. The edge of the disc was touched with tissue paper to absorb the film of acetone and then dried on a hot plate covered with aluminium foil.

Complete dryness (step 1 above) is essential, since this effectively disposes of nitric acid and HCl acid left from the preceding sample preparation . The Na_2SO_4 serves as a carrier during this procedure preventing the actinide atoms from being adsorbed onto the walls of the beaker.

3.6.6 Alpha- spectrometry system

The α-spectrometry system used in the current study was based in all on 24 silicon ion-implanted and silicon surface- barrier detectors with 100 mm depletion depth and 300 mm^2 sensitive area. The detectors are connected to an ND6600 multi-channel analyzer via different routings (all Nuclear Data). Multiple ADC's (Analog-to-Digital Convertors) in combination with the routers receive the pulses from the detectors and the information, i.e. pulse height translated to a channel number, is stored in an MCA which provides 512 channels per detector. The energy calibration was carried out using ^{233}U and ^{241}Am sources. Detector counting efficiency, i.e. the factor representing that fraction of the total radiation emitted by the source which is recorded by the detector, was obtained by measuring ^{233}U and ^{241}Am sources made in the

laboratory by electroplating on a stainless steel disc. It was compared with a calibrated source in geometry used since it is dependent on the area of the detector, the active area of the source and the source-detector distance. Counting efficiency was calculated as

$$\varepsilon\ (\%) = \frac{A\ counted\ (cpm)}{A\ calibrated\ (cpm)}\ x\ 100$$

With 300 mm^2 detectors, the efficiency obtained was on the average 24-25%. Since isotopic tracers (radiochemical yield determinants) were used the effects of counting time and the detector efficiency cancelled out each other. Therefore, the detector efficiency is not needed in the sample activity calculation but it is essential for the chemical yield determination.

The system's lower limit of detection (LLD) depends mainly on the detector variable background which is caused by recoil of the daughter nuclides, ^{224}Ra and ^{228}Th from the ^{232}U tracer solution, diffusion of loosely bound nuclides and evaporation of volatile nuclides of polonium. The background of the system was measured with new stainless steel discs and the counts per 1000 minutes within the energy intervals occupied by nuclides of interest were recorded and used as a correction to activity measurements. The detector resolution, which represents the ability of the detector to separate lines of different energies, is measured in terms of the *full line width at half maximum* (FWHM). The FWHM was measured using ^{233}U as calibration source and it was found to be 4-5 channels (30-40 keV).

3.6.7 Quantitative analysis of U, Th and Po α-particle spectra

The typical α-particle spectra of natural uranium, natural thorium and polonium

obtained using ^{232}U, ^{229}Th and ^{209}Po as the tracers are shown in **Fig. 3.7 - 9.** Peaks representing the α-particle groups of the principal nuclides of interest and their short-lived daughters are indicated. The α-energies of the uranium, thorium and polonium isotopes and their half-lives are given in **Table 3.2.** For quantitative analysis, the count rates for the constituent radionuclides were obtained by integrating the counts under each peak. As can be seen, the shape of the spectrum is an important consideration, since a non-Gaussian tail is almost present on the low-energy side of an α-peak which makes the lower-energy lines of weak intensity and difficult to resolve. The tail is usually extends to zero energy and for a thin α- source the peaks are almost Gaussian and the correction of integrated nuclide count rates for low energy tail are negligible

The analysis of the uranium spectrum is straightforward in the sense that the peaks of ^{238}U, ^{235}U, ^{234}U and ^{232}U are well resolved. Once the integration limits are set for each peak, and the integration carried out, the only correction required is that due to the background count rate, provided the sources are counted soon after electrodeposition, otherwise, the shorter-lived nuclide ^{228}Th grows in rapidly yielding peaks which can not be resolved from the peaks of ^{232}U. The count rate correction for this interference was performed. 29% of the ^{228}Th group lies under the ^{232}U peak and the 71% branch of the ^{228}Th (5.42 MeV) peak receives the 5% component of its daughter ^{224}Ra group. If we assume that C_1, C_2, and C_3 are the measured count rates from the integration of the ^{232}U, ^{228}Th and ^{224}Ra peaks in the uranium spectrum respectively then the corrected count rate C'_1 for ^{232}U peak can be obtained from:

$$C'_2 = [C_2 - (0.05/0.95) \text{ X } C_3] \qquad (1)$$

$$C'_1 = [C_1 - (0.29/0.71) \text{ X } C'_2] \qquad (2)$$

Substituting equ. (1) into equ. (2) gives:

$$C'_1 = C_1 (0.4085\ C_2 - 0.0215\ C_3) \qquad (3)$$

The thorium spectrum is complicated by the rapid ingrowth of the 5% ^{224}Ra group under the ^{228}Th peak. Only background correction is needed for peaks identified as ^{232}Th, ^{230}Th and ^{229}Th. The correction of the ^{228}Th count rate due to the 5% of its daughter ingrowth was carried out first by obtaining the 95% ^{224}Ra count rate from the main ^{224}Ra peak. After the appropriate background correction, this count rate was used to calculate 5% component in the total background corrected ^{228}Th count rate. In the polonium spectrum only the background substraction is required.

Table 3.2

Half-lives and α-energies of uranium, thorium and polonium isotopes

Isotope	Half-life	α-energy (MeV)
^{232}U	72 y	5.32 (68%) - 5.27 (32%)
^{234}U	2.47 x 10^5 y	4.77(72%) - 4.72 (28%)
^{235}U	7.1 x 10^8 y	4.58(8%), 4.4(57%), 4.37(18%)
^{238}U	4.51 x 10^9 y	4.2 (75%) - 4.15 (25%)
^{228}Th	1.19 y	5.43 (71%) - 5.34 (29%)
^{229}Th	7340 y	5.05(7%),4.97(10%),4.9(11%) 4.84 (58%), 4.81 (11%)
^{230}Th	8 x 10^4 y	4.68 (76%) - 4.62 (24%)
^{232}Th	1.41 x 10^{10} y	4.01 (76%) - 3.95(24%)
^{209}Po	102 y	4.88 (99.74%)
^{210}Po	138.5 d	5.3 (100%)

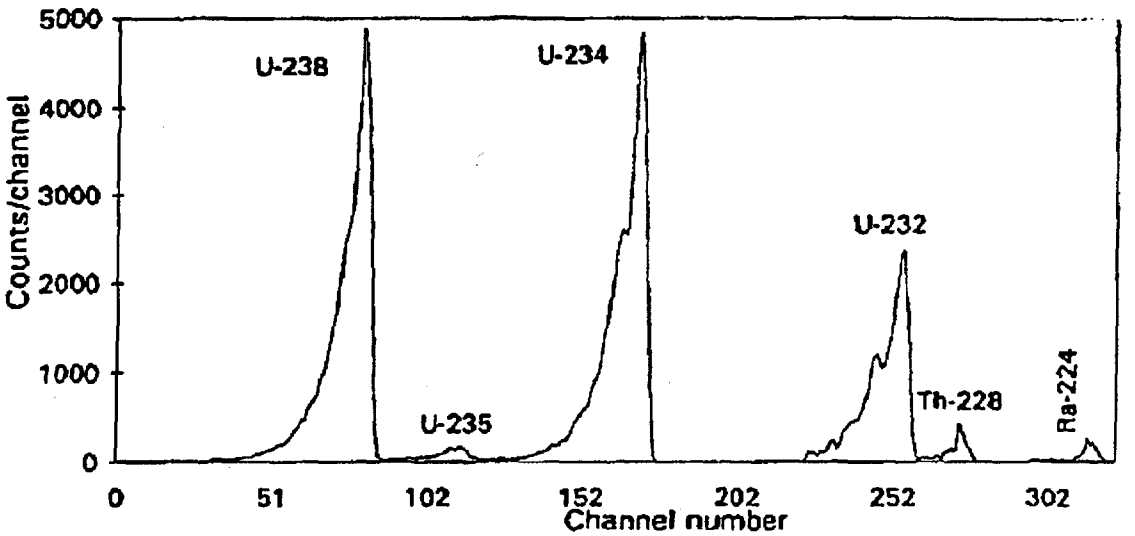

Fig. 3.7: α-particle spectrum of natural uranium separated from the Uro rock phosphate with added ^{232}U as a tracer

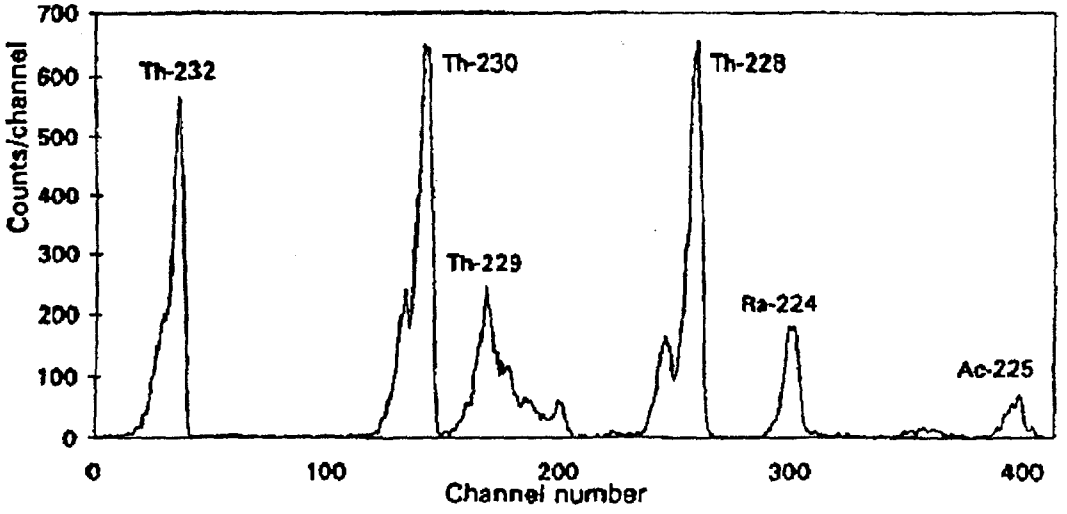

Fig. 3.8: α-particle spectrum of natural thorium separated from the Arkuri soil with added ^{229}Th as a tracer

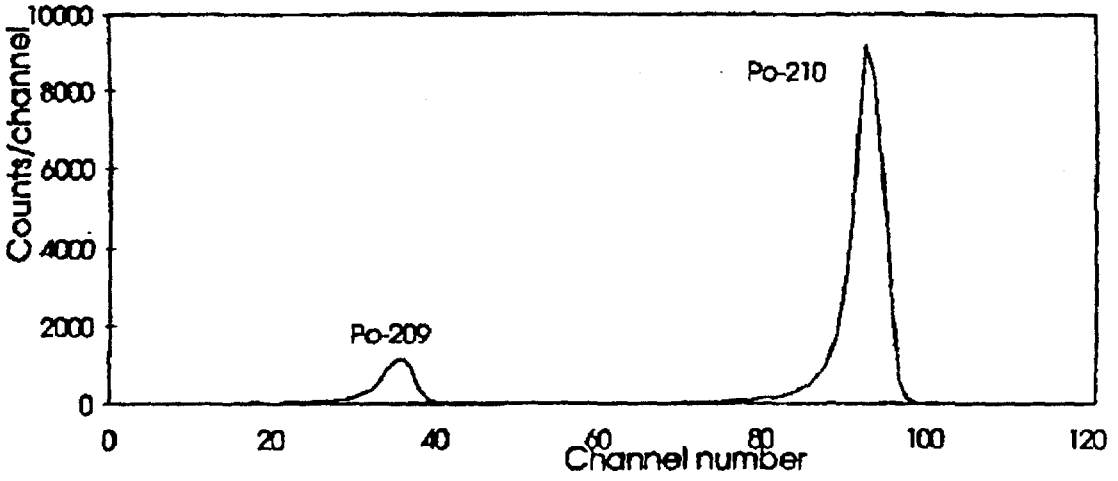

Fg. 3.9: α-particle spectrum of ^{210}Po separated from the Uro rock phosphate with added ^{209}Po as a tracer

3.6.8 Calculation of the α-activity in the samples

Given the corrected count rates for each peak in the sample α-spectrum, the activity (A) of each radionuclide in the sample was calculated as:

$$A = \frac{sample_{counts} \; x \; A^{\circ} \; (mBq)}{tracer_{counts} \; x \; sample \; weight \; (g)} \qquad Bq/kg$$

where A° is the initial activity of the added tracer. The calculated activity of ^{210}Po in the sample was corrected for half-life decay by dividing it by the factor ($e^{-(\ln 2/138.5 \; d \; . \; \Delta t)}$) where Δt is the time elapsed between deposition and the counting start date.

3.6.9 Chemical yield calculation

The chemical yield or extraction recovery of uranium, thorium and polonium was obtained from the observed ^{232}U, ^{229}Th and ^{209}Po tracer count rates in their respective spectra. The percentage chemical yield (Y%) is calculated from:

$$Y\% = \frac{A}{A^{\circ}} \; x \; 100$$

where A° is the initial activity of the added tracer and A is the fraction of the tracer activity that is actually deposited on the disc and is given by:

$$A = \frac{tracer \; count \; rate}{counting \; efficiency \; x \; counting \; time \; (\text{sec})} \qquad Bq$$

We have used the average counting efficiency of 25%. The counting time

required to improve the validity of the measurements depends on the activity of the sample which also governs the amount of tracer to be added. The minimum counting time used was 3 days. Chemical recoveries of ^{232}U, ^{229}Th and ^{209}Po tracers added to the samples are shown in **Table 3.3 - 5**.

A fundamental assumption in radiochemical yield calculation is that no fractionation occurs between different isotopes of the same element during the electrodeposition process and the preceding chemical separation steps. The possibility of isotopic separations even under equilibrium conditions should always be borne in mind, since the relative isotopic mass differences may result in considerable divergencies in chemical behaviour under same circumstances, but as the mass differences become smaller, the separation factors also decrease.

Table 3.3

Chemical recovery of ^{229}Th tracer added to the samples

No.	Activity on disc (Bq)	Added tracer activity (Bq)	Recovery %
1	0.299	0.313	96
2	0.050	0.051	98
3	0.061	0.064	95
4	0.206	0.226	91
5	0.064	0.072	89
6	0.186	0.212	88
7	0.049	0.058	84
Average			91.57

Table 3.4

Chemical recovery of ^{232}U tracer added to the samples

No.	Activity on disc (Bq)	Added tracer activity (Bq)	Recovery %
1	0.028	0.044	64
2	0.026	0.041	63
3	0.035	0.050	70
4	0.034	0.051	67
5	0.031	0.051	61
6	0.030	0.050	60
7	0.031	0.049	63
Average			64

Table 3.5

Chemical recovery of ^{209}Po tracer added to the samples

No.	Activity on disc (Bq)	Added tracer activity (Bq)	Recovery %
1	0.158	0.302	52
2	0.236	0.429	55
3	0.104	0.169	62
4	0.143	0.151	95
5	0.139	0.169	82
6	0.103	0.158	65
Average			68.5

3.7 Measurement of ^{226}Ra, ^{228}Ra, ^{40}K and ^{137}Cs by γ-spectrometry

The ^{226}Ra, ^{228}Ra, ^{40}K and ^{137}Cs activity in the samples was measured using a γ-spectrometry system equipped with a P-type high-purity germanium (HPGe) and coaxial Lithium-drifted Germanium Ge (Li) detectors connected to an ND6600 MCA. The detectors were calibrated for different geometries using Amersham mixed radionuclide standards. Samples were sealed in 60-180 ml polyethylene containers with plastic covers and set aside to allow gaseous ^{222}Rn (half-life, 3.8 days) and its short-lived decay products (^{214}Pb & ^{214}Bi) to reach equilibrium with the long-lived ^{226}Ra precursor in the sample. At the end of the ingrowth period the samples were counted for 2-5 days (depending on their activity levels) so as to validate the measurements within the 5% standard deviation at the 95% confidence interval. ^{226}Ra and ^{228}Ra were analysed through their progeny peaks: ^{214}Bi (609 keV) and ^{214}Pb (352 keV) and ^{228}Ac (911 keV). The activity of ^{40}K and ^{137}Cs was measured directly via 1461 keV and 662 keV peaks, respectively. In order to determine the background distribution around the detectors, an empty polyethylene container was counted in the same manner as the samples for the different geometries.

3.7.2 γ- activity calculation

A graphic log/log plot of efficiency curve as a function of γ-energy was plotted for 60 ml and 180 ml geometry for the different detectors using the Amersham mixed radionuclide standard. An acid diluted mixed radionuclide standard solution was mixed with a mixture of Dowex 1-X8 anion exchange and Dowex WX8 cation exchange resins in a beaker. The resin mixture was wetted so as to improve activity distribution and thoroughly mixed and dried. A small portion of the dried resin (1-2 g) was weighed and placed in a 5 cm^3 beaker. The activity concentration in this sample was measured 30 cm from the detector and regarded

as a point source. A well calibrated point source was measured at the same source-detector distance, and from this the activity concentration in the resin was calculated. Calibration samples were then prepared by mixing weighed portions of the resin with sugar. γ-energies, branching ratios and the half-lives of the radionuclides used for system calibration are given in **Table 3.6**. The influence of sample geometry on the counting efficiency of the specific nuclide's energy is shown in **Fig. 3.10 -12**. The counting efficiency (ϵ) of the specific nuclide's energy was calculated by the formula:

$$\varepsilon = \frac{counts\ /\ second}{\gamma\text{-}emitted\ /\ second} = \frac{counts\ /\ second}{activity\ x\ branching\ ratio}$$

From the standard efficiency calibration curves, the counting efficiencies of the γ-lines of interest viz.^{214}Pb (352 keV), ^{214}Bi (609 keV), ^{228}Ac (911 keV), ^{40}K (1461 keV) and ^{137}Cs (662 keV) were taken and the activity concentration (A) of each radionuclide in the sample was calculated using the formula:

$$A = \frac{counts\ /\ second}{\varepsilon\ x\ branching\ ratio\ x\ sample\ mass\ (g)} \quad Bq/g$$

The absolute transition probability by gamma-decay through the selecled energies (i.e. branching ratio) and the counting efficiencies in ddifferent geometries are shown in **Table 3.7.**

Table 3.6

γ-energies, branching ratios and the half-lives of the radionuclides used for γ-system calibration

Nuclide	Energy (KeV)	Half-life	Branching ratio %
^{241}Am	59.5	432.7 y	36.3
^{109}Cd	88	463 d	3.6
^{57}Co	122	271 d	85.6
^{139}Ce	166	137.66 d	79.9
^{203}Hg	279	46.6 d	81.5
^{113}Sn	392	115 d	64.17
^{137}Cs	661.66	30 y	84.62
^{88}Y	898	106.61 d	94.0
	1836		99.35
^{60}Co	1173.24	1929 d	99.90
	1332.5		99.98

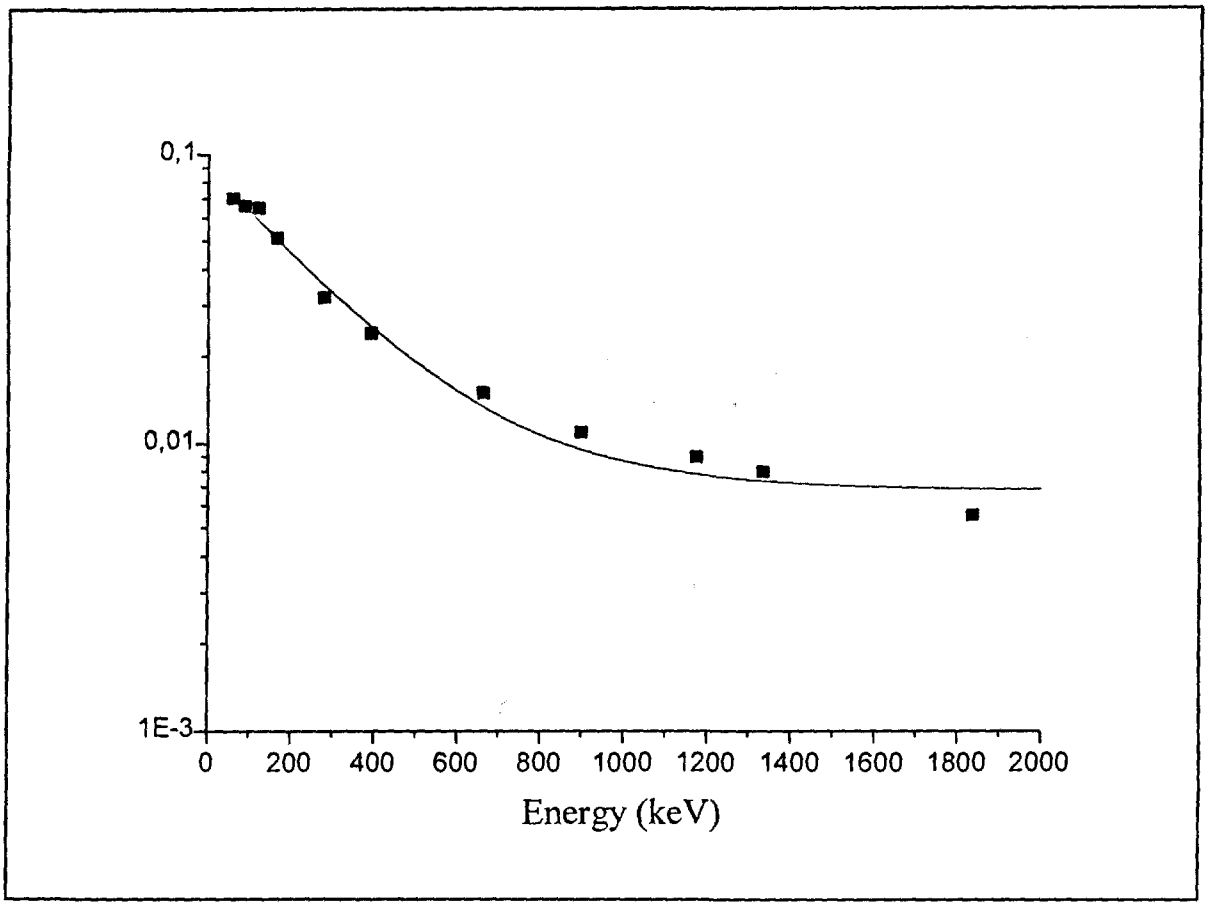

Fig. 3.10: Log/linear efficiency curve as a function of γ-energy for a 105 cm^3 coaxial Ge (Li) detector measured in a 60 ml polyethylene container

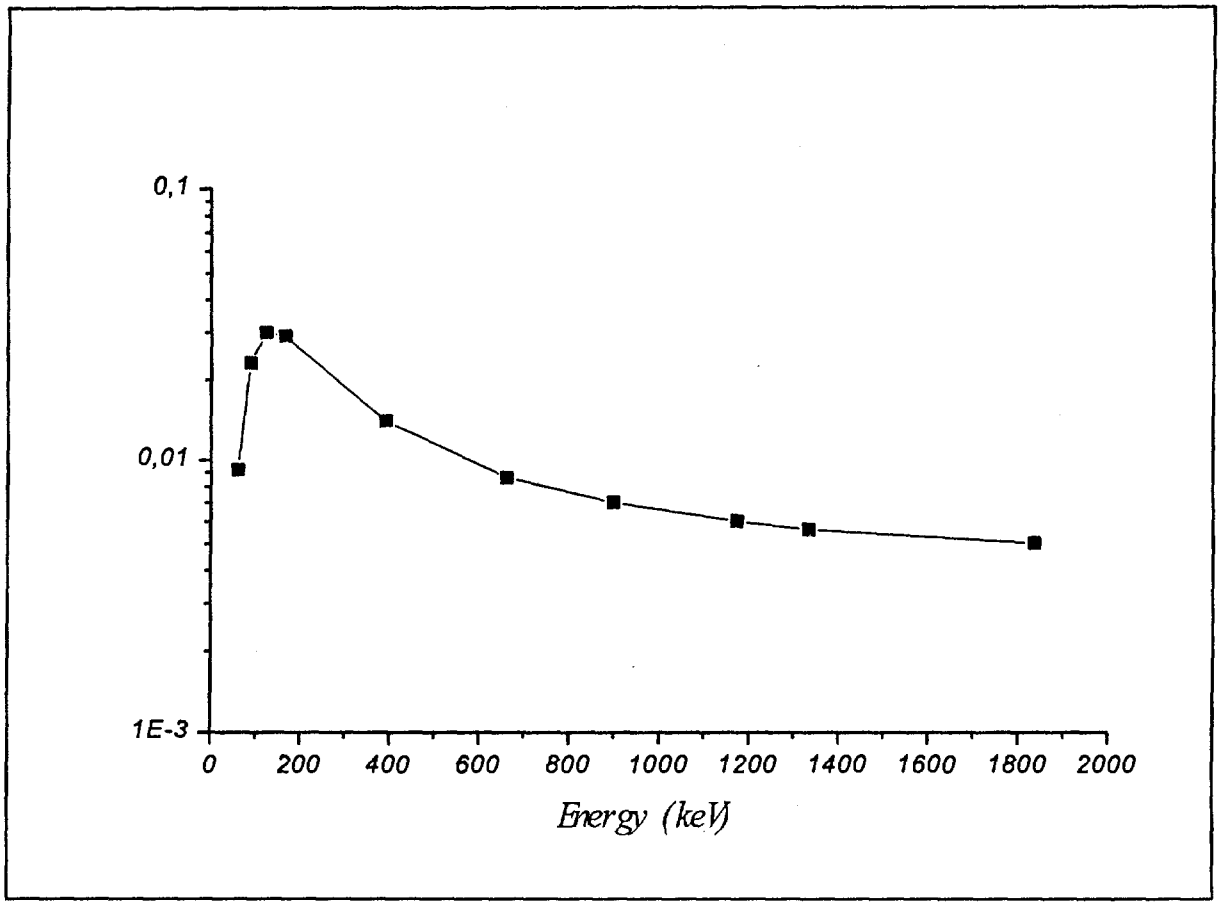

Fig. 3.11: Log/linear efficiency curve as a function of γ-energy for a 105 cm^3 coaxial Ge (Li) detector measured in a 180 ml polyethylene container

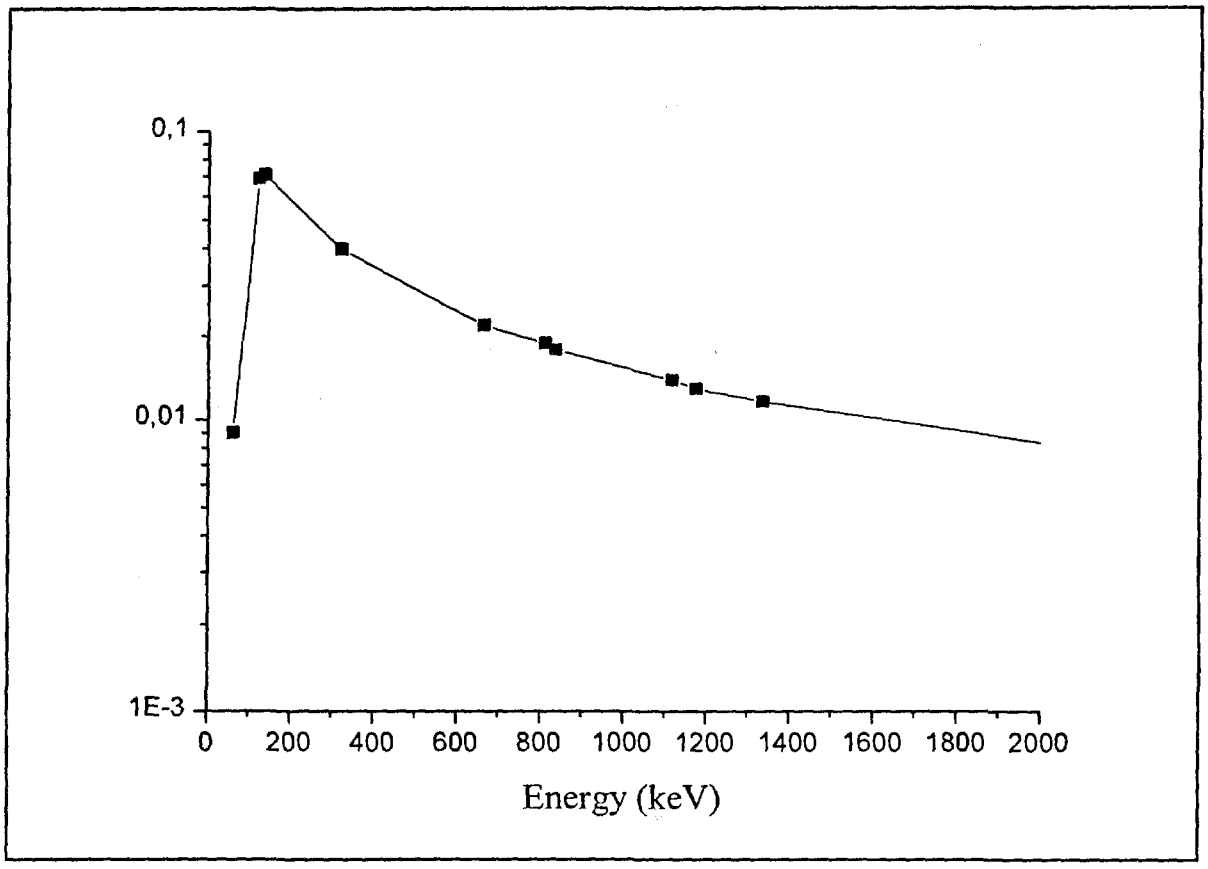

Fig. 3.12: Log/linear efficiency curve as a function of γ-energy for a p-type HPGe detector measured in a 60 ml polyethylene container

Table 3.7

The counting efficiencies of the selected energies in different sample geometries and their branching ratios (P_γ)

Nuclide	Energy keV	Counting efficiency (%)			
		P_γ (%)	60 ml 92 cm^3 Ge(Li)	180 ml 105 cm^3 Ge(Li)	60 ml HPGe
^{214}Pb	295	19.2	0.044	0.016	0.044
	352	37.1	0.026	0.015	0.038
^{214}Bi	609	46.1	0.016	0.009	0.023
	1120	15.04	0.0095	0.0056	0.014
	1760	15.92	0.0065	0.0035	0.009
^{228}Ac	911	29	0.011	0.0065	0.016
^{40}K	1461	10.7	0.0075	0.004	0.012
^{137}Cs	662	84.62	0.015	0.0085	0.022

3.8 Measurement of exchangeable ^{226}Ra by liquid scintillation

50 grams of dry sample was added to 500 ml of 1 M ammonium acetate solution at pH 7.0 in a plastic bottle with a screw cap and gently shaken for two hours on a shaking machine to insure maximum extraction. The extract was filtered through a folded filter papers (hard filtra). 400 ml of the filtrate was evaporated to dryness on a hot plate at 55 °C and the residue ashed by stepwise increasing the temperature up to 400 °C. The ash was dissolved in 25 ml of boiling 7.2 M HNO_3. The solution was transferred to a 113 ml glass bottle with a screw cap. 6 ml of n-hexane and three glass beads were added and the bottle was filled up with deionized water leaving 0.5 to 1 ml below the screw cap for air bubbles to gurad aginst a sudden rise in temperature or pressure. The bottles were tightly closed and stored in a laying position for a period of four weeks at room temperature to allow the ingrowth of gaseous ^{222}Rn (half-life, 3.8 days) and its short-lived decay products (^{214}Bi & ^{214}Pb) to reach equilibrium with the ^{226}Ra precursor in the sample. Bottles for determining background counts as well as standard (6.10 Bq of ^{226}Ra) were prepared on the same occasion and set aside as members of the sample series for the same period. At the end of the ingrowth period the three phases (aqueous-organic-air) in the bottle were equilibrated by vigorous shaking for one hour and left standing for 15 minutes phase separation period. An aliquot of 3 ml of organic n-hexane phase was transferred to the counting polyethylene vial containing 10 ml of scintillation solution (LIPOLUMA). This operation and the closing of the vial was carried out within ten seconds to reduce the loss of ^{222}Rn by evaporation to minimum. Samples were left standing for two hours to allow the build-up of short-lived ^{222}Rn daughters to attain equilibrium with their progenitor (^{222}Rn) and the counting of the series was then started. Samples were counted for their α-activity for 40 min using a microcomputer-based liquid scintillation counter

(Scint Varuhuset AB). The counting efficiency was determined at the start of the series using a standard ^{226}Ra solution. For the purpose of checking the decay time in the system counting was started and ended with the blank and the standard samples (Eriksson, 1987). The measurement error was 4%.

The following basic programme was used for the calculation of the radium activity concentration and the measurement error:

```
10 'RACONT
20 CLOSE #1
25 INPUT "NAME OF DATA FILE", RA1$
30 OPEN RA1$ FOR APPEND AS #1
40 INPUT "EXP CODE", A1$
50 INPUT "DATE OF MEASUREMENT", A2$
60 INPUT "TR.CPM 1=",C1
70 INPUT "TR.CPM 2=",C2
80 INPUT "BG.CPM 1=",C3
90 INPUT "BD.CPM 2=",C4
100 INPUT "GIVE TOTAL NUMBER OF MEASURED SAMPLES=", N1
110 M1=6.1: REM THE STANDARD SAMPLES CONTAIN 6.1 Bq RA-226
115 A3$="T1/2 CONSTANT FOR THE MEASUREMENT TIME USED="
120 PRINT #1, A1$, A2$
130 REM INPUT "KG/SAMPLE=",P1: REM (USED IF THE WEIGHT IS A CONSTANT)
135 REM P1=P1*.95: REM (WEIGHT TIMES FRACTION OF DRY MATTER IN SAMPLE)
140 A1=(C1-C3): A2=(C2-C4): H=(C4-C3)/N1
150 L1=(LOG(A1/A2))/N1:C5=M1/A1
160 REM C6=C5/P1
165 INPUT "1ST NO OF THE SERIES IS=", N2:REM USED IF Nos ARE A SEQUENCE
170 N3=N2-1:REM USED IF THE Nos ARE A SEQUENCE
175 PRINT #1,"No","NET CPM","BQ/KG","MEASUREMENT ERROR IN %"
180 PRINT "THE No OF THE SAMPLE IS",N3+1:REM USED IF THE Nos ARE A SEQU
185 REM INPUT "GIVE No OF THE SAMPLE", N3
190 INPUT "KG/SAMPLE=",P1
195 P1=P1*.95:REM (WEIGHT TIMES FRACTION OF DRY MATTER IN SAMPLE)
197 C6=C5/P1
200 INPUT "GIVE CPM=(IF THE SERIES IS ENDED ANSWER -1)",X:
205 N3=N3+1: F=X-(C3+(N3-N2)*H)
210 E=EXP((N3-N2)*L1):B=C6*F*E
```

```
215 IF X=-1 THEN 270
220 FE=(SQR((X+F)*40)/(F*40))*100
230 REM REM PRINT "No",N3; "NET CPM=",F;"RA CONTENT=",B"BQ/KG",
240 PRINT #1, N3, F, B, FE
260 GOTO 180
270 PRINT #1, A3$; L1:PRINT #1,"INCREASE IN THE BACKGROUND, CPM=";H
275 CLOSE #1
280 END
```

Note: If constant weight of the samples is used the lines 130, 190, 195 and 197 should be preceded by "rem" so that they will be skipped.

3.9 Determination of maximum emanation power

10 g of dry sample was placed in 113 ml storage bottle with 100 ml of 0.01 M NaOH solution. The bottles were gently shaken to ensure wetting and left open overnight. The bottle was then closed and shaken vigorously to achieve maximum dispersion of the soil aggregates. Procedure as above (see 3.8).

Chapter 4

RESULTS AND DISCUSSION

The main physical and chemical parameters of the soil samples are shown in **Table 4.1**. The pH_{aq} ranged from 6.5 - 8.3. The average content of organic matter (OM%) as estimated by loss of weight on ignition was low, ranging between 0.06 and 0.22%. The exchangeable ^{226}Ra fraction constituted 19 -24% of the total amount of the radium. On the average, the maximum emanation power (surfacial radium) was found to be 26.4 Bq/kg.

The activity concentration of ^{238}U, ^{232}Th, ^{226}Ra, ^{228}Th, ^{228}Ra and ^{40}K in the soil samples, and the corresponding external exposure due to the γ-radiation from the ground as estimated using the formula derived by Probonas and Kritidis (1993), **see Appendix**, are presented in **Table 4.2**. The average contents of ^{238}U, ^{232}Th and ^{40}K were found to be 20.1 ± 16.4, 19.1 ± 8.1 and 280.3 ± 137.6 Bq/kg dry weight, respectively. It is estimated that in areas with a normal radiation background, the world average value for U and Th activity concentrations in soil is 25 Bq/kg and 370 Bq/kg for ^{40}K (UNSCEAR, 1982). However, the share of ^{40}K within the radioactivity of soil is a clear-cut function of the stable potassium content of the soil.

The estimated external exposure value lies within the range of 23.16 to 107.78 nGy/h with an average value of 45.4 ± 21.33 nGy/h, which is slightly lower than the world average outdoor exposure value of 55 nGy/h (UNSCEAR, 1988). Adopting the conversion factor of (H μSv/y = 6.13 D nGy/h) as recommended by UNSCEAR (1982) on an assumed value of 100% outdoor exposure, the average exposure obtained from the concentration values of natural radionuclides in soils corresponds to the annual dose equivalent of 277.99

μSv/y. The average dose equivalent rate received from the cosmic rays measured on the Nile at Khartoum is 295 μSv/y, using GR-200A dosemeters (Ibrahim, 1996). The most important aspect of exposure to cosmic rays is the variation with altitude. If the variations in cosmic radiation with altitude are ignored, the total dose equivalent for the whole country amounts to 573 μSv/y. For the calculation of the population-weighed mean of the dose equivalent rate, the estimates of exposure based on soil measurements do not apply to urban areas since the building materials used in urban areas significantly affect the external exposure (Probonas and Kritidis, 1993). A common feature of any environmental radiation measurements is the considerable variation in soil radioactivity with location depending on soil physicochemical parameters. In these measurements, the highest natural radionuclide concentrations were observed in the soils from Arkuri and Dumper in the western part of the country. The corresponding external radiation exposures are 92.2 and 107.8 nGy/h, respectively. The soil-forming rocks in these areas comprise groups of igneous and metamorphic rocks, the most extensive rock units in this so-called basement complex being granites which have given rise to soils with relatively high uranium content. It may be in place to recall that high background radiation areas are defined as those where the external γ-radiation from the ground exceeds 230 nGy/h over extensive areas (Malanca et al. 1993). In fact, soil radioactivity has a direct influence on living components in the given environment, as the radionuclides within the soil exert a direct radiation load. However, the radiation dosage sustained by the living organisms because of the natural radioactivity of the soil (external irradiation) is usually much smaller than the inner radiation load caused by the incorporated (inhaled or ingested) radionuclides. Here we should born in mind that, the natural gamma radiation of the soil is the function of its humidity, as higher moisture content decreases

the intensity of radiation exposure (Andras, 1993).

The activity concentrations of the fallout nuclide ^{137}Cs and ^{235}U in the soil samples are presented in **Table 4.3**. ^{137}Cs activity ranged from 0.8 to 18.5 Bq/kg dry weight with an average value of 4.94 ± 4.29 Bq/kg. We have calculated the exposure from concentration values of U and Th daughter nuclides. ^{137}Cs and ^{235}U activity concentrations were omitted since they contribute very little to the total exposure from the environmental background (Green et al. 1989). On the basis of daughter/parent activity concentration ratios in **Table 4.3** it is obvious that the radioactive disequilibrium exists in both uranium and thorium decay series. However, the $^{234}U/^{238}U$ (0.81 - 1.35) and $^{228}Th/^{232}Th$ (0.6 - 2.14) activity ratios does not greatly deviate from the unity in most of the soil samples analysed. Further along the ^{238}U decay series, The values for $^{226}Ra/^{238}U$ and $^{230}Th/^{238}U$ ratios were found to range from 0.32 - 7.13 and 0.19 - 1.8, respectively. Studies on disequilibrium in surface materials have shown that many soils show $^{234}U/^{238}U$ activity ratios less than unity and $^{230}Th/^{238}U$ much less than unity due to loss of uranium which is more soluble in oxidizing surface waters than thorium (Rosholt et al., 1966). Other soils, often organic rich, have $^{234}U/^{238}U$ is greater than unity as a result of upward migration of uranium leached from lower down in the profiles.

Little has been published on $^{226}Ra/^{238}U$ disequilibrium in soils. Megumi (1979) suggest that soils typically have $^{226}Ra > ^{238}U$ due to preferential loss of uranium from soils and extreme Ra/U activity ratios of up to 32 have been found in mountain tundra soils (Shuktomova et al., 1983). Recent studies of Australian soils have also shown $^{238}U < ^{226}Ra$ (Dickson and Wheller, 1992). The typical of U-Ra disequilibrium is possibly related to the stability of the minerals hosting uranium. In soils where uranium is contained in easily weathered minerals, uranium can be readily leached but if it is resident in resistant minerals only

^{226}Ra formed by radioactive decay and located in radiation damaged mineral sites is available for leaching.

The main physical and chemical characteristics of the Uro and Kurun rock phosphates are presented in **Table 4.4**. The samples showed a mean pH_{aq} of 6.9 and 7.3 respectively, and were thus neutral to basic. The average content of organic matter (OM%) as estimated by loss of weight on ignition was low, viz.0.24% for Uro and 0.08% for Kurun rock phosphate on a dry weight basis. On the average, the exchangeable ^{226}Ra fraction constituted 0.06% (Uro) and 0.29% (Kurun) of the total amount of the radium. The maximum emanation power (surficial radium) of the rock phosphates dispersed in water was found to be 299 Bq/kg (Uro) and 39 Bq/kg (Kurun). It should be realized that one part of this fraction of radium will be fixed on the surface of the soil particles and that one part consists of the exchangeable radium fraction that contaminates the calcium source of plants. The value for Kurun rock phosphate is close to the average maximum emanation we have obtained for soils in Sudan, viz.26 Bq/kg which means that the extent of contamination that could be expected for the calcium source of the plants grown using Kurun ground rock fertilizer is negligible.

Activity concentrations of natural radionuclides from ^{238}U and ^{232}Th decay series, and of ^{40}K in Uro and Kurun rock phosphates are summarized in **Table 4.5-8**. Uranium and its decay products are the principal contributors of radioactivity in both the rock phosphate deposits, with activity concentrations ranging from 4031 - 13745 Bq/kg (Uro) and 146 - 686 Bq/kg (Kurun). The highest activity levels were measured in grey coloured rock phosphate samples. The equivalent mass concentrations of uranium in the Uro and Kurun rock phosphates were found to lie within the range of 100 - 1117 ppm and 12 - 56 ppm, respectively. Uranium exploration has shown that concentrations of

uranium in ore of minable grade usually range from 1000 - 5000 ppm, and that concentrations greater than 100 ppm are of potential interest depending on the size of the deposit and the presence of other recoverable minerals (IAEA, 1979). The uranium mass concentrations in Uro rock phosphate lie within the range that could be recovered economically as a by-productof phosphate industry (Bouwer et al. 1978).

The radiation effects in the air are normally expressed in terms of the exposure rate or the absorbed dose rate in air. Factors for converting radionuclide activity in soil or bedrock into the ground component of absorbed dose rates in air (1 m above ground surface) has been estimated from photon transport calculation applied to infinite soil or bedrock and air media. Dose rate conversion factors (DRCF) in air are known for unit specific activity in soil for ^{40}K, ^{232}Th and ^{226}Ra (UNSCEAR, 1982 and 1993). These calculations were made under the assumption of radioactive equilibrium between radionuclides in Th- and U-decay series, and homogeneous concentration in the first metre of soil (density = 1.4 gcm^{-3}). However, under surface and near-surface geological conditions a closed chemical system may not exist. The process of weathering provides for both the introduction and removal of material. Dose rate factors in air 1 m above ground for rocks (density = 2.4 gcm^{-3}) were not calculated because the factors for converting natural radionuclide concentration into radiation exposure are nearly identical for rocks and soil (IAEA, 1990). In the case of equal concentrations in soil and rock, an expected higher unit dose rate from rock (caused by higher activity in the same volume) is reduced by attenuation in more dense rock material. It has to be noticed that main dose rate contribution from radionuclides in U-decay series arises from decay products of the noble gas, ^{222}Rn. Independent of the degree of radioactive disequilibrium between uranium and radium, dose rate in air is a

function of ^{226}Ra concentration in soil or bedrock (Barisic, 1994). Absorbed dose rates in air 1 m above the area of Uro and Kurun rock phosphate deposits as estimated using dose rate conversion factors (DRCF) adopted by UNSCEAR (1993) are presented in **Tables 4.9** and **4.10**. The exposure rates lie within the range of 574 - 7108 nGy/h in Uro and 75 - 402 nGy/h in Kurun rock phosphate deposit area. In southern Kerala and Tamil Nadu (India), recognized high background area, the absorbed dose rates in air reach 6000 nGy/h (UNSCEAR, 1988), which compared well with the levels found in Uro phosphate deposit area. It may be in place to recall that high background radiation areas are defined as those where the external gamma-radiation from the ground is greater than 230 nGy/h over extensive areas (Malanca et al., 1993).

Untreated rock phosphates have been used as plant fertilizers in many parts of the world at rates ranging from 300 to 600 kg/hectare (Makweba, 1993). The external radiation exposure in the gricultural land may arise from the extensive use of ground rock phosphate fertilizers. Assuming an average annual fertilizer intensity of 300 kg per hectare (10^4 m^2), it can be deduced that an average of c.123.93, 120.63, 120.24, 0.22 and 1.77 Bq/m^2 of ^{238}U, ^{226}Ra, ^{210}Po, ^{232}Th and ^{40}K respectively will be distributed per unit arable land from Uro rock fertilizer (**Table 4.11**). On the other hand, the contribution of radionuclides contained in Kurun rock phosphate fertilizer to the natural radioactivity of arable land is comparatively insignificant. For radionuclides deposited on soil the activity will usually be transported downwards into the soil by water infiltration and by ploughing, and the resulting soil layer between the source and the receptor locations will provide greater shielding than the air above ground alone (Kocher & Sjoreen, 1985). It must be considered, however, that radium may be bound to the soil matrix to a relatively high extent over many years, as is known for the

other alkaline earth ions so that annual fertilizing with rock phosphate would result in an accumulation of radium in the soil. Uranium would not accumulate to the same extent in the soil, since it is partially leached from the upper layers by rain water (UNSCEAR, 1966). Thorium may be disregarded because of its very low concentration in the rock phosphate fertilizers. There is no accumulation of ^{40}K in the soil as the result of using phosphate fertilizers (Pfister et al. 1976). Unlike electropositive uranium, thorium, radium and potassium, which can be adsorbed on the surface of clay minerals, polonium is amphoteric and its behaviour in the soil is difficult to be predicted. It should be remembered that the polonium content in plants should be interpreted with caution since some of it enters the biological-cycle from the atmosphere.

If a circular area of 100 hectares (10^6 m^2) of land fertilized with Uro and Kurun ground rock phosphates at the rate of 300 kg/ha. Assume that the fertilizers are homogeneously distributed in the soil down to the mean ploughing depth of 20 cm, and that the activity remains in the soil until removal by radioactive decay. By using the formula derived by Pfister et al. (1976) for estimating external radiation exposure caused by phosphate fertilizers (**see Appendix**), the radionuclides deposited on the ground from Uro and Kurun rock fertilizers would yield an additional external radiation exposure of 23.41 X 10^{-9} and 2.59 X 10^{-9} Gy/h at one m above the ground level, respectively. In comparison to the average outdoor exposure due to the terrestrial γ-radiation as determined from the nationwide survey on soil natural radioactivity in Sudan, viz. 45.4 nGy/h, it is evident that the additional external radiation exposure for the population due to fertilization with ground rock phosphate is negligible. However, the amount of fertilizer applied on a farm will determine how much external radiation a farmer would be exposed to during work. Nevertheless, handling and storage would lead to direct external radiation; inhalation of radon

and of rock phosphate dust may increase the internal exposure considerably. **Pfister and Pauly (1980)** have estimated that the effective dose to workers who handle rock phosphate during industrial operation involving phosphate ore is 200 μSv/year. UNSCEAR (1993), data on the annual effective dose to an average member of the public resulting from the extraction and processing of earth materials shows that phosphate industry is dominating (0.04 - 10 μSv/year).

In terms of the mean activity concentrations distributed per unit area given above from the practice of applying 300 kg/ha of ground rock phosphate fertilizer annually, if complete retention in soils is assumed over a period of 10 years then the total uranium, radium and polonium activity imparted to the soil with Uro and Kurun rock fertilizers, would amount to a mean of 1240, 1210 and 1202 Bq/m^2 and 120, 130 and 120 Bq/m^2 respectively. The natural uranium and radium content of unfertilized soils in Sudan lies within the range of 5.6 - 77.4 Bq/kg and 7.9 - 101.3 Bq/kg respectively, except for some areas with an unusually high uranium content which indicates that after the intensive use of rock fertilizers, the α-activity of the soils will increase, in particular with Uro rock phosphate. The extent of the uptake by crops and the possible effects on humans due to ingestion of food containing high α-emitting nuclides is related to the pH of the fertilized soils, the types of crops grown in soils fertilized with rock phosphates and the Ra/Ca ratio in the soil. As can be seen in **Table 4.4** the extractability of the nutrient elements increases tremendously in acid media and so it can equally well be inferred that more uranium, radium and polonium will be available for plant uptake when the ground rock fertilizers are applied to acidic soils. Consideration must therefore be paid to the fact that in problem areas that require nutrient supplement, soils are usually acidic. Research in New Zealand, Australia and England has shown that the α-activity of wheat grains

increases after intensive fertilizing with superphosphate, and being highest on acidic soils (Marsden, 1964). It should be remembered that because of the manufacturing process involved, superphosphate has only about half the activity of the parent rock phosphate (i.e, radium is precipitated with solid by-product phosphogypsum as insoluble sulphate). These various measurements do, however, indicate the possible increase in the natural α-activity of food products as the result of phosphate fertilizers, but it is not suggested that the amounts obtained constitute anything in the nature of a hazard to health. However, inspite of well established evidence of increased uptake of radionuclides by foodstuffs after spreading phosphate fertilizers in acid soils, most of the recent studies that have considered the radiological aspects of the agricultural use of phosphogypsum have generally concluded that the increased risk is low, both from the increased radon flux from the soil and uptake by plants (Lindeken, 1980; Lindeken and Coles, 1978; Roessler, 1984, 1988).

The radionuclide content of rock phosphates has been reported in several publications (e.g. Boothe, 1977; Roessler et al. 1979; IAEA 1990; Hussein 1992). In comparing the radioactivity of materials that contain Ra, Th and K a common index termed radium equivalent activity (Hamilton, 1971) is required to obtain the total activity. Since 98% of the radiological effects of the uranium series are produced by radium and its daughter products, the contribution from the ^{238}U and the other ^{226}Ra precursors is usually ignored (Beretka and Mathew, 1985) so that the Ra_{eq} of a sample can be expressed as: $Ra_{eq} = A_{Ra} + A_{Th} X\ 1.43 + A_K X\ 0.077$, where A is the specific activity in pCi/g. Comparisons of Ra_{eq} of Uro and Kurun rock phosphates with those of some other countries calculated on the basis of the above formula are shown in **Table 4.12**. The Ra_{eq} of rock phosphates originating from different regions shows considerable variation which are related to the type of rock phosphate, the highest concentrations of

natural radionuclides have usually been observed in sedimentary phosphates, while low values are reported for igneous phosphates (UNSCEAR, 1993).

Based on the daughter/parent specific activity ratios given in **Table 4.13** and **Table 4.14**, radioactive equilibrium exists within uranium decay series in both Uro and Kurun rock phosphate ores. In most of the samples the values for $^{234}U/^{238}U$, $^{230}Th/^{238}U$, $^{226}Ra/^{238}U$ and $^{210}Po/^{238}U$ are not much differ from unity. Whereas ^{228}Th is found in considerable excess over its precursor^{232} Th. We tend to consider that the differences in geochemical properties alone between ^{232}Th and the intermediate^{228} Ra cannot fully account for the extent of this departure from the equilibrium state, and attribute the ^{228}Th excess to the input of ^{228}Ra, the more soluble intervening nuclide, from the surrounding areas by rain washout.

The prevalence of radioactive equilibrium between U-Ra and Po-U in a such large gross of surface rock phosphate samples signifies that both Uro and Kurun phosphate deposits are intact rock being of low porosity and extremely low permeability. If the structure is slightly porous, radioactive disequilibrium will be induced either by loss of radium in water percolating through the rock due to its greater solubility over parent uranium or by diffuse of radon gas out a deposit. However, under such situation both addition and substraction of radium are possible. Since low porosity/permeability is one of the important characteristics of the hard rock that influence the design of waste repositories and sealing systems (IAEA, 1992), Uro and Kurun phosphate deposits can further be investigated as a possible radioactive waste disposal media. However, it is recognized that it may be difficult to balance the need for data against the repository performance requirements, further investigations should maximize the understanding of their mass properties (geology, geometry and mechanical) and site hydrology.

The results of the analyses of the natural and artificial radionuclide of the Red Sea coastal sediments are shown in **Table 4.15 -16**. For natural radionuclides the ranges of activity concentrations measured differ widely, as thier presence in the marine environment depends on their physical, chemical and geochemical properties and the pertinent environment in the biological process. The average concentrations of ^{238}U, ^{226}Ra, ^{210}Po, ^{230}Th, ^{232}Th, ^{228}Th and ^{40}K obtained were 29.6 ± 16.3, 11.6 ± 15.2, 33± 29.1, 6.6 ± 4.6, 6 ± 6.1, 48.4 ± 20.9 and 158.3 ± 161.9 Bq/kg dry weight, respectively. Apart from the study of uranium-series disequilibrium in sediments by Ku (1969) in the Red Sea hot-brine area, no data has appeared in the literature for radionuclide concentrations in the Red Sea sediments. The values obtained for ^{226}Ra, ^{228}Th and ^{232}Th are fairly low compared to those in coastal marine sediments in the Bay of Bengal (Sharif et al., 1994) and the north-west Pacific Ocean (Yang et al., 1986). The concentrations for ^{238}U, ^{234}U and ^{40}K are similar to the average activity of each of the radionuclides in the marine sediments from the Ghazaouet Bay on the western coast of Algeria (Noureddine and Baggoura, 1997), and from some other areas of the world, as reported by Fukai and Yokoyama (1982), whereas the average concentration of ^{210}Po is low. Generally sediments from Port Sudan harbour area show higher concentrations of ^{226}Ra and ^{210}Po relative to those collected from the fringing reefs. Since the concentrations of all the radionuclides of uranium and thorium series, and ^{40}K of the coastal sediments are generally comparable to those in Sanganeb atoll which is 30 km off-shore to the north-east of Port Sudan harbour (**Fig. 3.4**), both anthropogenic and terrestrial influx from the hinterland in the data is negligible.

As regards the artificial radioactivity, ^{137}Cs is considered in this study in order to ascertain if there has been any fallout of ^{137}Cs in the Red sea coastal zone.

The presence of ^{137}Cs in the sediments was evident, its activity ranged from 0.16 to 10.1 Bq/kg dry weight with an average value of 4.1 ± 3.96 Bq/kg which is less than the values from the pre-Chernobyl period cited in the literature for sediments from different regions of the world (IAEA, 1973 and Livingston et al., 1977). When the sediments are compared locationwise with respect to ^{137}Cs content, those collected from the Port Sudan harbour area show relatively high values. It should be in place to recall that, this coastal region is free from any direct radioactive waste discharges. The average concentration of ^{137}Cs in the Sudanese soil is 4.12 Bq/kg which is in good agreement with the average value found in the coastal sediments (Sam et al., 1997).

Table 4.17 provides activity concentration ratios of $^{235}U/^{238}U$, $^{234}U/^{238}U$, $^{232}Th/^{238}U$, $^{228}Th/^{232}Th$ and $^{230}Th/^{232}Th$ found in the sediments. The $^{235}U/^{238}U$ activity ratios lie within the range of 0.015 - 0.051 with an average value of 0.034, which corresponds to 74% of detrital value of this ratio (0.04657). However, the average $^{234}U/^{238}U$ activity ratio is 1.15, indicating scavenging of ^{234}U from the water column. The value obtained is identical with the disequilibrium ratio that is often found on ocean floors in different regions of the world (Schimmield and Price 1988; Ku 1969). The organic surface layer of the coastal sediments also gave similar values for $^{234}U/^{238}U$ (Joshi and Ganguly, 1976). From $^{238}U/^{232}Th$ activity ratios, ^{238}U activity is seen to be on the average 40 times higher than the ^{232}Th activity concentration in the sediments. Unlike ^{232}Th, the total ^{238}U measured in the sediments consists of two components: authigenic derived from sea water and detrital present in terrestrially derived mineral phases (i.e, $\sum U = U_a + U_d$). To differentiate authigenic from detrital uranium, Huh et al. (1987) estimated the detrital uranium (U_d) from the measured ^{232}Th, which is essentially all detrital as U_d = ($^{238}U/^{232}Th$) X ^{232}Th. The average ^{232}Th concentration measured in the sediment

was 6.02 Bq/kg, given a $(U/Th)_d$ value of 0.58, an average authigenic uranium content of 3.49 Bq/kg or 12% of the total uranium can be deduced. Anderson (1982) suggested that particulate authigenic uranium is primarily formed in surface sea water, but is rapidly remineralized in deep water. Therefore, the $^{238}U/^{232}Th$ ratios in surface marine sediments should be representative of that in detrital phases. In contrast to ^{228}Th, both ^{232}Th and ^{230}Th activity concentrations in the sediments are extremely low, as can be seen from $^{228}Th/^{232}Th$ activity ratios which lie within the range of 2.85 - 98.09 with an average value of 25.56. Such a high $^{228}Th/^{232}Th$ activity ratio implies that the rate of sedimentation was rapid, and that the sampled sediments are young surficial sediments. This is because the bottom sediments older than 10 years were found to have $^{228}Th/^{232}Th$ ratio of less than unity as the results of ^{228}Ra migration and decay of initial excess ^{228}Th (Koide et al. 1973; Ku 1976). The $^{228}Th/^{232}Th$ activity ratio has therefore been used as a geochronometer in dating coastal marine sediments deposited during the last decade or so, providing that the sedimentation rate is rapid enough to allow the delineation of decreasing excess ^{228}Th with depth.

Although the size of the data is limited, correlation between ^{238}U and ^{232}Th activity concentrations in sediments collected along one transect across the area of the fringing reefs at Port Sudan (**Fig. 4.1**) shows that the ^{238}U content is higher in sediments in shallower water, while for ^{232}Th the trend is not clear. The higher values observed for uranium probably reflect the good correlation of uranium with biogenic material, since the surface sediments in the biologically rich environments such as fringing reefs are highly associated with organic matter.

The activity concentrations of uranium and thorium isotopes, ^{226}Ra, ^{210}Po, ^{40}K and ^{137}Cs measured in seagrass, green algae (*Halimeda* and *Cystoseria*) and

brown algae (*Padina* and *Sargassum*) are given in **Tables 4.18-19**. Marine species considered in this work were collected from the area of the fringing reefs at Port Sudan. It would be desirable to sample in other parts of the Red Sea as well to check whether radionuclide content varies according to location. On the basis of individual data there is no great variation with regard to natural radionuclide content. ^{210}Po concentration in algae ranged from 13.7 Bq/kg (*Halimeda*) to 36.4 Bq/kg (*Sargassum*). These levels are significantly higher in contrast to ^{210}Po content in algae from the Syrian coast (Othman et al., 1994), and Baltic Sea (Skwarzec et al., 1988). Nevertheless, the detection of activity levels for ^{137}Cs in algae (0.33 - 1.32 Bq/kg) and its undetectability in seagrass and sediments taken from the same sampling depth confirms the fact that algae are the effective bioindicators for monitoring marine radioactivity levels. The distribution of fallout radioactivity in the marine environment is often investigated by using indicator organisms. Algae are known to be responsive to the soluble phase of constituents in the ambient medium but they donot respond to elements associated to particulate matter (Pentreath, 1985). The concentrations in the algae should then be correlated to the concentrations of the dissolved constituents and not to the total concentration. ^{137}Cs is readily accumulated by biota, presumably because of its chemical similarity to potassium which takes active part in the exchange processes with the surrounding medium. Studies has shown that only a minor part of the total ^{137}Cs c.0.006% present in seawater is bound to the particulate material (Duursma, 1972). Similarly, in the Irish Sea less than 0.1% of ^{137}Cs was found retained on a 0.22 μ millepore filter (Hetherington and Harvey, 1978). Thus, ^{137}Cs seems to be one of the more conservative isotopes which are released to the marine environment through human activities and algae could give indications of its variation.

The content of organic matter (OM%) in the sediments, as estimated by loss of weight on ignition, varies from 6.65-28.89% on a dry weight basis (Port Sudan) and 7.76-25.89% (Sawakin). These values should be considered high.

A set of 20 sediments, collected at various points in Port Sudan harbour (**Fig. 3.5**), were analysed for uranium and thorium isotopes and the results are presented in **Table 4.20** and **4.21**. The range of values observed for ^{238}U activities were 2.71-13.42 Bq/kg and for ^{222}Th 3.62 - 18.73 Bq/kg dry weight. These activity concentrations can be compared with ranges of 1.8 - 6.5 BqU/kg and 4.1-12.1 BqTh/kg dry weight for the sandy sediments of the Irish Sea (McCartney et al., 1992), 2.6 - 24.2 BqTh/kg and 3.6 - 32.3 BqU/kg for coastal sediments in the United Kingdom (McDonald et al., 1991) and 3 - 11 BqU/kg for sediments in the North Sea (Nedwell et al., 1993). The maximum activity concentrations for ^{238}U and ^{232}Th in the sediments of the Suez Canal have been reported to be 16 Bq/kg and 15.5 Bq/kg, respectively (El Tahawy et al., 1994), very similar to the levels found in this study. $^{235}U/^{238}U$ activity quotients lie within the range of 0.031 - 0.068 with an overall mean of 0.045 ± 0.009, which is the same as the detritus concentration value of this ratio (0.046) while $^{234}U/^{238}U$ activity quotients vary from 1.01-1.24 with an overall mean of 1.13 ± 0.06. This can be compared with the range of 1.12 - 1.14 in coastal sediments from the west coast of India (Joshi and Ganguly, 1976)). Detrital particles of rivers have ratios of 0.9 - 1.0, and seawater has a fairly constant value of 1.15 due to preferential mobilization of ^{234}U during weathering (Thurber, 1962 and Cochran, 1982). Therefore, a value slightly greater than unity is typical of sediments owing to the scavenging of ^{234}U from the water column. $^{232}Th/^{238}U$ activity quotient ranges from 0.4- 4.5 with an average value of 2.4±1.17. With the exception of sample 4 and 6 (**Fig. 3.5**) which are taken from the main harbour entrance, $^{232}Th/^{238}U$ activity quotients are much greater than unity. This

can be attributed to the fact that, in addition to the greater abundance of thorium in the earth's crust. It has long been established that thorium is a particularly insoluble element in natural waters and is usually found associated with solids. Therefore, this ratio is typically much below unity in waters and above unity in solid particles. In our previous study with sediments from the fringing reefs area just north of Port Sudan harbour, ^{238}U activity concentration was found to be on the average 40 times higher than that of ^{232}Th. This excess of ^{238}U is probably attributed to the organic and mineral biogenic material which is always associated with the sediments in biologically productive shallow-waters of fringing reefs. This is because in a such highly productive waters, sedimentation rates are usually high and reducing conditions lead to the transformation of uranium to the more insoluble uranus form.

Sawakin harbour is situated c. 60 km south of Port Sudan harbour. **Tables 4.22** and **4.23** present the results of uranium and thorium isotopes and their activity quotients in seven samples collected from Sawakin harbour. As can be seen the activity concentrations for ^{238}U lie within the range 3.87 - 24.79 Bq/kg with an overall mean of 13.52 ± 6.85 Bq/kg and 1.13 - 10.04 Bq/kg with an average value of 5.65 ± 3.57 Bq/kg for ^{232}Th. In the metalliferous sediments of the Red Sea hot-brine area, the activity levels reported for uranium and thorium were 6-31 ppm (36-372 Bq/kg) and 0.1-0.5 ppm (0.4-2.0 Bq/kg), respectively (Ku, 1969). It is obvious that the sediments from Sawakin exhibit high ^{238}U values relative to ^{232}Th as compared with Port Sudan where the reverse is true. This is shown by $^{232}Th/^{238}U$ activity quotient which is less than unity in most of the samples. This opposite trend with respect to $^{232}Th/^{238}U$ activity quotients in these two sets of sediments probably reflects a variation in the physicochemical composition. Keating et al. (1996), reported that the highest ^{238}U activity in Whitehaven harbour was found in the sediments containing the

highest percentage of silt fraction. It is well known that many radionuclides, in common with stable metals, are concentrated in the finer-grained sediments due to large surface area and mineralogical effects (Assinder et al., 1997). Since ^{232}Th is essentially detrital, another possible explanation for relatively excess ^{238}U activity in Sawakin harbour sediments is the remineralization of particulate authigenic uranium (i.e. concentration in excess of that expected from the composition of the earth crust). Anderson (1982) showed that remineralization of uranium fixed to the organic matter in surface sea water is possible except in areas of high organic carbon flux. In general, sediments from harbours at Port Sudan and Sawakin exhibit low activity levels for uranium, thorium and their decay products comparable to marine sediments from some other regions of the world, e.g. in Greek coastal areas (Florou and Kritidis, 1991), the northwest Pacific Ocean (Yang et al., 1986), coastal sediments from the Bay of Bengal (Sharif et al., 1994), and the Algerian coast (Noureddine and Baggoura, 1997). The Red Sea sediments are rich in carbonate as reported by Said (1990). However, we donot have enough evidence on whether these carbonates are detrital or authigenic in nature, but from the low activity values obtained for uranium one can speculate that they are detrital in origin. According to Girdler (1966), the shallower parts on either sides of the Red Sea are down-faulted continental blocks covered initially by carbonate sediments and evaporites and subsequently by coral layers and unconsolidated sediments. It has been well documented that the marine deposits (clays) of detrital origin are depleted in uranium relative to thorium (Huh and Kadko, 1992; Ku et al., 1968 and Heye, 1969). In all samples of the Sawakin the activity quotients for $^{234}U/^{238}U$ are slightly greater than unity (1.09 - 1.18).

The activity concentrations of ^{232}Th, ^{230}Th and ^{228}Th in the sediments of both harbours are listed in **Tables 4.21** and **4.23**. It should be in place to recall that,

the concentrations of other decay-series nuclides in sediments depend in part on the concentrations of uranium and thorium as their supporting sources and in part on whether there is a flux out or into the sediments. In all sediment samples analysed, the $^{228}Th/^{232}Th$ activity quotient is greater than unity. While $^{230}Th/^{232}Th$ and $^{228}Th/^{230}Th$ activity quotients show different trends. In Port Sudan, $^{230}Th/^{232}Th$ ratios are around unity and $^{228}Th/^{230}Th$ is greater than unity. Whereas in the Sawakin harbour sediments $^{230}Th/^{232}Th$ is much greater than unity, with the exception of two samples (Nos 30 and 31, **Fig. 3.6**) collected from the nearshore which show a value close to unity. The values for $^{228}Th/^{230}Th$ are widely scattered ranging from 0.23-1.38. Moore (1967) has concluded that, $^{228}Th/^{232}Th$ and $^{230}Th/^{232}Th$ ratios are usually close to unity in detrital river particles and, consequently, in nearshore sediments. In constructing the budget of uranium series nuclides, Huh and Kadko (1992) have observed that nearly all of the ^{230}Th produced by ^{234}U decay in the water column is removed to sediments; less than 0.02% remains in water column. In general, the anomalous behaviour is to be expected of thorium isotopes in a coastal sediments since the activity concentration of authigenically produced and particle-reactive radionuclides such as ^{228}Th and ^{230}Th is a function of sedimentation rate, being high and largely unsupported in freshly deposited sediments. A feature which also implies a short residence time in seawater. The sedimentation rates in coastal regions are known to be two to three orders of magnitude higher than in the open sea so that it is not uncommon for ^{228}Th to appear in considerable excess of the parent ^{232}Th in coastal sediments as well as wide scattering data of ^{230}Th which could possibly be explained by change in the sediment accumulation rate.

These activity concentration ratios illustrate that the order of alpha-emitting thorium isotopes in sediments from Port Sudan is: $^{228}Th > ^{232}Th > ^{230}Th$ and

$^{230}Th > ^{228}Th > ^{232}Th$ for the Sawakin harbour. The order basically reflects the position of ^{230}Th in the uranium decay series versus ^{228}Th and ^{232}Th which are in the thorium decay series. This is shown by the activity concentrations of the parent isotopes which has the order: Th > U in Port Sudan sediments and the reverse is true for the Sawakin.

Figures **4.2** and **4.3** show the relationship between ^{238}U activity concentrations in Port Sudan and Sawakin sediments with depth and organic matter content, respectively. The trend in each of these figures is that ^{238}U activity concentration increases with depth and organic matter content. Accumulation of uranium in organic- rich sediments has been well documented from sediment and water column studies (Todd et al., 1988). On the other hand, this proportional increase in uranium concentration with respect to the depth is indicative of remineralization of uranium derived from the dissolved state in seawater and the absence of any anthropogenic or terrestrial influx from the hinterland to the sediments, whereas ^{232}Th data show no correlation with both depth and organic matter content in the sediments (**Fig. 4.4**). With regard to remineralization it is important to notice that in the Red Sea evaporation far exceeds precipitation and runoff.

Table 4.1

The main physicochemical parameters of the sampled soils

Parameter	Range	Mean value
pH_{aq}	6.5 - 8.3	7.4
pH_{KCl}	6.3 - 7.9	6.9
pH_{CaCl2}	6.6 - 7.9	7.1
OM%	0.06 - 0.22	0.12
Clay %	17 - 86	44.6
Sand %	0.1 - 49.4	19.9
Exchangeable ^{226}Ra (Bq/kg)	2.3 - 22	9.3
Emanation power (Bq/kg)	2.5 - 46.3	26.4
Acetate soluble ions mg/100 g:		
Calcium	67.6 - 132.2	91.3
Magnesium	4.4 - 30.8	13.6
Potassium	8.3 - 19.1	13.5
Phosphorus	0.7 - 3.6	1.6

Table 4.2

Activity concentration of ^{238}U, ^{232}Th, ^{226}Ra, ^{228}Th, ^{228}Ra and ^{40}K in soil samples (Bq/kg dry weight) and the corresponding external radiation exposure

Location	^{238}U	^{232}Th	^{226}Ra	^{228}Th	^{228}Ra	^{40}K	I (nGy/h)
Arkuri	77.44	43.19	63.15	43.88	35.30	688.00	92.19
El Ban Jadeed	35.78	19.64	35.96	19.32	28.35	204.47	43.94
Alain	20.24	17.14	84.72	16.17	31.39	168.27	66.37
Al Molbus	15.44	26.02	28.04	15.61	28.35	98.09	33.38
Dumper	15.51	18.78	114.2	40.25	101.29	91.81	107.78
Sawani	16.31	13.63	22.87	19.91	21.33	204.56	35.38
Khour Abeyyid	26.92	14.51	22.49	11.87	21.65	166.62	30.29
Jebel Kordofan	8.72	15.24	23.95	17.67	29.64	241.32	38.92
Al Qa'a	23.39	19.12	21.62	28.28	27.22	340.00	46.11
Kh. Abu Habil	27.68	31.45	20.55	30.25	22.14	180.04	37.79
Uro	30.61	7.60	9.66	7.76	7.94	276.55	23.19
Ad Duwem	13.56	23.19	20.05	20.93	28.67	298.89	40.68
Blue Nile	10.78	18.65	27.28	17.61	24.13	306.85	42.35
Um Dom	10.89	15.81	17.95	13.12	21.87	248.58	32.11
Dongola	6.05	11.89	17.38	13.52	19.02	346.01	35.51
Kassala	9.56	17.12	13.04	20.52	24.54	422.25	41.30
El Qash	5.60	9.93	11.54	12.93	15.10	323.68	30.19
Aroma	7.42	13.93	14.77	12.57	21.71	439.14	38.77
Average	20.11	19.10	31.62	20.12	28.31	280.29	45.35
STD	16.39	8.08	27.04	9.46	18.72	137.56	21.33
Minimum	5.60	7.60	9.66	7.76	7.94	91.81	23.16
Maximum	77.44	43.19	114.2	43.88	101.29	688.00	107.78

Table 4.3

Activity concentration of ^{235}U, ^{137}Cs (Bq/kg, dry weight) in soils and daughter/parent activity ratios within U and Th decay chains

Location	^{235}U	^{137}Cs	$^{234}U/^{238}U$	$^{230}Th/^{238}U$	$^{226}Ra/^{238}U$	$^{228}Th/^{232}Th$	$^{228}Ra/^{232}Th$
Arkuri	3.33	3.79	1.35	0.61	0.82	1.02	0.81
El Ban Jadeed	1.22	3.80	1.14	0.78	1.00	0.80	1.40
Alain	0.88	18.54	1.21	1.45	4.25	0.94	1.82
Al Molbus	0.71	0.80	1.09	1.80	1.87	0.60	1.08
Dumper	0.69	7.05	1.09	1.06	7.13	2.14	5.32
Sawani	0.41	1.23	1.07	1.18	1.44	1.46	1.50
Khour Abeyyid	0.68	ND*	1.19	0.81	0.82	0.82	1.47
Jebel Kordofan	0.35	3.59	1.13	1.44	2.66	1.16	2.00
Al Qa'a	0.72	7.09	1.04	0.66	0.96	1.48	1.42
Kh. Abu Habil	1.01	1.32	0.82	1.31	0.75	0.96	0.71
Uro	1.11	8.36	1.02	0.19	0.32	1.02	1.00
Ad Duwem	0.59	1.57	1.04	1.29	1.43	0.90	1.26
Blue Nile	0.33	ND	1.23	1.45	2.45	0.94	1.26
Um Dom	0.36	ND	0.91	1.27	1.64	0.83	1.38
Dongola	0.37	3.32	1.03	1.50	2.83	1.14	1.58
Kassala	0.34	4.72	1.05	1.40	1.30	1.19	1.47
El Qash	0.42	2.42	0.81	1.33	2.00	1.30	1.50
Aroma	0.15	6.47	1.05	1.57	2.14	0.90	1.57
Average	0.76	4.94	1.07	1.17	1.99	1.08	1.59
STD	0.69	4.29	0.13	0.39	1.55	0.34	0.96
Minimum	0.15	0.80	0.81	0.19	0.32	0.60	0.71
Maxmum	3.33	18.54	1.35	1.8	7.13	2.14	5.32

ND*= undetectable

Table 4.4

The main physicochemical parameters of Uro and Kurun rock phosphates

Parameter	Uro phosphate	Kurun phosphate
pH_{aq}	6.9	7.3
pH_{KCl}	6.4	6.8
pH_{CaCl2}	6.4	6.8
OM%	0.24	0.08
Exchangeable ^{226}Ra (Bq/kg)	2.3	1.3
Emanation power (Bq/kg)	299.1	38.6
AC- A L soluble ions mg/100 g		
Calcium	60 - 151	191 - 216
Magnesium	0.6 - 8.0	0.6 - 6.8
Potassium	2.0 - 88.5	3.5 - 100.8
Phosphorus	0.8 - 6.2	1.6 - 3.9

AC = ammonium acetate buffer solution, AL = ammonium lactate acetic-acid

Table 4.5

Activity concentration of uranium and its decay products in Uro rock phosphate

Sample number	Colour	^{238}U Bq/kg	^{234}U Bq/kg	^{230}Th Bq/kg	^{226}Ra Bq/kg	^{210}Po Bq/kg	eU ppm
Uro1	brown	1342	1564	1768	1389	1490	109
Uro2	brown	3143	3248	3405	3226	2916	256
Uro3	grey	8567	8067	8137	7151	6561	697
Uro4	grey	13745	14877	12487	15377	15084	1117
Uro5	grey	1762	1793	1755	1539	1773	143
Uro6	brown	2391	2620	3028	1972	2091	194
Uro7	brown	2209	2232	2392	1701	2153	180
Uku8	brown	2469	2459	2219	1761	2244	201
Uro11	brown	4332	4584	4723	3709	4134	352
Uro12	brown	2587	3712	4088	4878	4055	210
Uku24	brown	1575	1599	1573	1243	1471	128
Uro25	grey	2182	2080	2024	2112	1823	177
Uku26	grey	4571	4612	4468	4031	4441	372
Uku27	grey	10099	9103	8695	8862	8439	821
Uku28	brown	2796	3183	3439	2569	2444	227
Uro29	brown	5240	5630	6080	5523	5793	426
Uku30	grey	1225	1232	1261	1322	1226	100
	Mean	4131	4270	4208	4021	4008	336
	STD	3395	3427	2973	3552	3399	276
	Min	1225	1232	1261	1243	1226	100
	Max	13745	14877	12487	15377	15084	1117

1 µg U = 12.3 mBq

Table 4.6

Activity concentration of natural thorium, ^{235}U and ^{40}K in Uro rock phosphate

Sample number	Colour	^{232}Th Bq/kg	^{228}Th Bq/kg	^{235}U Bq/kg	^{40}K Bq/kg
Uro1	brown	7.36	230.27	51.71	104.71
Uro2	brown	0.88	199.60	118.47	54.92
Uro3	grey	1.03	114.78	318.49	48.25
Uro4	grey	18.99	121.98	492.09	29.14
Uro5	grey	0.76	155.05	66.55	43.21
Uro6	brown	10.43	101.62	93.13	125.47
Uro7	brown	4.01	154.56	85.75	92.27
Uku8	brown	10.91	186.42	92.03	97.30
Uro11	brown	5.17	105.87	164.86	78.59
Uro12	brown	11.29	170.68	79.59	13.65
Uku24	brown	6.53	230.40	61.73	78.02
Uro25	grey	4.68	224.28	80.23	87.47
Uku26	grey	8.08	123.60	190.17	52.81
Uku27	grey	22.31	146.30	465.28	27.48
Uku28	brown	6.62	196.09	107.49	40.49
Uro29	brown	2.29	176.29	180.95	58.37
Uku30	grey	5.89	196.05	8.17	27.00
	Mean	7.48	166.69	156.28	62.27
	STD	5.8	41.9	13.61	30.80
	Minimum	0.76	101.62	8.17	13.65
	Maximum	22.31	230.40	492.09	125.47

Table 4.7

Activity concentration of uranium and its decay products in Kurun rock phosphate

Sample number	Colour	^{238}U Bq/kg	^{234}U Bq/kg	^{230}Th Bq/kg	^{226}Ra Bq/kg	^{210}Po Bq/kg	eU ppm
Ku1	grey	622.81	625.25	685.94	527.49	648.09	50.65
Ku2	black	146.47	149.37	151.54	152.96	87.10	11.91
Ku3	black	357.54	347.44	389.14	412.69	293.88	29.07
Ku4	black	227.94	229.68	249.30	240.13	166.81	18.53
Ku5	brown	569.38	570.80	847.38	617.77	756.44	46.29
Ku6	grey	307.99	330.71	346.64	350.00	417.94	25.04
Ku7	grey	358.94	353.62	387.49	342.80	308.38	29.18
Ku8	grey	686.19	667.69	720.52	706.04	717.29	55.78
Ku9	brown	328.87	241.68	355.90	819.89	395.37	26.74
Ku10	black	245.48	242.10	254.53	204.13	235.82	19.95
Ku11	black	234.56	257.89	263.05	284.07	197.25	19.07
Ku12	grey	631.02	623.65	665.61	531.00	634.90	51.30
	Mean	393.09	386.66	443.09	432.41	404.83	31.96
	STD	176.80	175.9	216.50	200.50	220.70	14.40
	Min	146.47	149.37	151.54	152.96	87.10	11.91
	Max	686.19	667.69	847.38	819.89	756.44	55.78

Table 4.8

Activity concentration of natural thorium, ^{235}U and ^{40}K in Kurun rock phosphate

Sample number	Colour	^{232}Th Bq/kg	^{228}Th Bq/kg	^{235}U Bq/kg	^{40}K Bq/kg
Ku1	grey	2.04	113.89	22.06	57.49
Ku2	black	4.23	147.81	6.01	331.55
Ku3	black	16.35	148.91	18.16	73.81
Ku4	black	16.37	137.74	11.12	289.62
Ku5	brown	4.12	191.34	22.55	67.31
Ku6	grey	6.82	153.12	11.89	64.25
Ku7	grey	6.14	87.73	12.42	85.58
Ku8	grey	1.93	50.22	27.62	71.02
Ku9	brown	5.80	232.84	12.75	290.04
Ku10	black	3.09	77.60	9.09	70.19
Ku11	black	11.45	178.03	11.26	237.24
Ku12	grey	4.49	61.07	22.63	58.00
	Mean	6.90	131.69	15.63	141.34
	STD	4.90	53.10	6.40	105.10
	Minimum	1.93	50.22	6.01	57.49
	Maximum	16.37	232.84	26.62	331.55

Table 4.9
Absorbed dose rate in air 1 m above Uro rock phosphate area

Nuclide	Concentration (Bq/kg)		DRCF (nGy/h per Bq/kg)	Dose rate (nGy/h)	
	Mean	Range		Mean	Range
^{40}K	62.3	13.7 - 125.5	0.0414	2.58	0.58 - 5.23
^{232}Th	7.5	0.8 - 22.3	0.623	4.98	0.49 - 13.71
^{226}Ra	4021	1243 - 15377	0.461	1854	573 - 7089
Total				1862	574 - 7108

Table 4.10
Absorbed dose rate in air 1 m above Kurun rock phosphate area

Nuclide	Concentration (Bq/kg)		DRCF (nGy/h per Bq/kg)	Dose rate (nGy/h)	
	Mean	Range		Mean	Range
^{40}K	141.3	57.5 - 331.6	0.0414	5.84	2.4 - 13.74
^{232}Th	6.9	1.9 - 16.4	0.623	6.23	1.25 - 9.97
^{226}Ra	432	153 - 820	0.461	199	71 - 378
Total				211	75 - 402

Table 4.11

The mean activity concentration of radionuclides in Uro and Kurun rock phosphate distributed per unit area (Bq/m^2)

Radionuclide	Uro rock phosphate	Kurun rock phosphate
^{238}U	123.93	11.79
^{235}U	4.69	0.47
^{234}U	128.24	11.59
^{230}Th	126.24	13.29
^{226}Ra	120.63	12.97
^{210}Po	120.24	12.14
^{232}Th	0.22	0.21
^{228}Th	5.00	3.95
^{40}K	1.77	4.24

Table 4. 12

Comparison of equivalent radium activity of Uro and Kurun rock phosphates with those of some other countries

Country	Ra_{eq} Bq/kg
Uro	1245 - 15417
Kurun	160 - 862
Abu Zaabal (Egypt)	568
Morocco	1616
Tanzania (Minjingu)	5942
Togo (Taiba)	1143
USA (Idaho)	777 - 1332 *
USA (Florida)	318 - 1406 *
Western Europe	1406

* radium only 1 pCi/g = 37 Bq/kg

Table 4.13

Daughter/parent specific activity ratios in Uro rock phosphate

Sample No.	$^{234}U/^{238}U$	$^{230}Th/^{238}U$	$^{226}Ra/^{238}U$	$^{210}Po/^{238}U$	$^{228}Th/^{232}Th$
Uro1	1.02	0.99	0.87	1.01	204.01
Uro2	0.95	0.93	0.97	0.84	47.92
Uro3	1.01	0.98	0.88	0.97	15.29
Uro4	0.99	0.89	0.71	0.91	17.09
Uro5	1.06	1.09	0.86	0.95	20.48
Uro6	1.44	1.58	1.89	1.57	15.12
Uro7	1.07	1.16	1.05	1.12	76.98
Uku8	0.94	0.95	0.84	0.77	111.44
Uro11	1.08	0.91	1.12	1.09	6.42
Uro12	0.90	0.86	0.88	0.84	6.56
Uku24	1.01	1.03	1.08	1.00	33.29
Uro25	1.17	1.32	1.04	1.11	31.29
Uku26	1.03	1.08	1.03	0.93	226.82
Uku27	1.09	1.23	0.83	0.88	9.74
Uku28	1.01	1.08	0.77	0.98	38.54
Uro29	1.02	0.99	0.79	0.93	35.28
Uku30	1.14	1.23	0.92	0.87	29.62
Mean	1.05	1.08	0.97	0.98	54.46
Std	0.11	0.18	0.26	0.17	64.32
Min	0.90	0.86	0.71	0.77	6.42
Max	1.44	1.58	1.89	1.57	226.82

Table 4.14

Daughter/parent specific activity ratios in Kurun rock phosphate

Sample No.	$^{234}U/^{238}U$	$^{230}Th/^{238}U$	$^{226}Ra/^{238}U$	$^{210}Po/^{238}U$	$^{228}Th/^{232}Th$
Ku1	1.00	1.10	0.85	1.04	55.83
Ku2	1.02	1.04	1.04	0.59	34.94
Ku3	0.97	1.09	1.15	0.82	9.12
Ku4	1.01	1.09	1.05	0.73	8.41
Ku5	1.00	1.49	1.09	1.33	46.44
Ku6	1.07	1.13	1.14	1.36	22.45
Ku7	0.99	1.08	0.96	0.86	14.29
Ku8	0.97	1.05	1.03	1.05	26.02
Ku9	0.74	1.08	2.49	1.20	40.15
Ku10	0.99	1.04	0.83	0.96	25.11
Ku11	1.09	1.12	1.21	0.84	15.56
Ku12	0.99	1.06	0.84	1.01	13.60
Mean	0.99	1.11	1.14	0.98	25.99
Std	0.08	0.12	0.43	0.22	14.71
Min	0.73	1.03	0.83	0.59	8.41
Max	1.09	1.49	2.49	1.36	55.83

Table 4.15

Activity concentration of natural uranium and its decay products in the Red Sea coastal sediments (Bq/kg)

Location	Depth m	^{238}U	^{235}U	^{234}U	^{226}Ra	^{210}Po
Fringing reef area	1.00	53.04	2.33	61.99	2.69	4.79
	1.25	48.25	1.85	54.42	3.06	5.07
	1.50	43.95	1.53	54.69	2.92	5.46
	6.00	45.77	1.48	51.19	2.42	4.55
	7.00	34.58	1.06	33.39	3.24	12.52
	16.0	37.22	1.11	40.28	3.99	20.72
	19.5	36.68	0.98	41.50	3.81	21.66
Open sea	100	24.88	1.26	29.51	6.29	48.43
Main harbour entrance	32.0	9.19	0.39	11.92	13.31	50.76
North harbour	13.0	13.54	0.54	15.96	13.39	94.68
South harbour	17.0	7.47	0.36	8.37	59.89	81.80
	15.0	6.51	0.10	7.07	13.18	60.31
Sanganeb atoll	3.00	49.99	1.78	58.04	2.78	3.74
	750	18.44	0.58	20.19	9.37	49.58
Trinkitat Mersa		14.67	0.28	18.65	33.98	18.48
	Mean	29.61	1.04	33.81	11.62	33.01
	STD	16.29	0.64	18.69	15.17	29.02
	Min	6.51	0.10	7.07	2.42	3.74
	Max	53.04	2.33	61.99	59.89	94.68

Table 4.16

Activity concentration of thorium isotopes, ^{40}K and ^{137}Cs found in the Red Sea coastal sediments (Bq/kg)

Location	Depth m	^{232}Th	^{228}Th	^{230}Th	^{40}K	^{137}Cs
Fringing reef area	1.00	1.13	34.55	4.21	31.15	ND
	1.25	0.38	14.63	3.31	23.86	ND
	1.50	1.32	42.72	3.86	29.10	ND
	6.00	0.78	20.26	1.53	34.83	0.16
	7.00	0.88	16.15	1.71	52.94	0.49
	16.0	1.82	63.79	2.83	71.09	ND
Open sea	19.5	0.93	55.70	2.40	71.10	ND
	100	7.11	71.54	7.67	202.28	4.66
Harbour entrance	32.0	14.32	58.75	12.57	421.73	10.09
North harbour	13.0	13.16	73.67	12.05	514.95	ND
South harbour	17.0	10.22	66.56	12.96	76.78	8.35
	15.0	11.62	60.61	7.86	431.52	9.64
Sanganeb atoll	3.00	0.22	21.58	1.19	31.59	0.23
	750	7.05	72.00	11.25	234.93	1.79
Trinkitat Mersa		19.29	54.89	14.23	138.95	ND
	Mean	6.02	48.44	6.64	158.39	4.09
	STD	6.09	20.92	4.64	161.89	3.96
	Min	0.22	14.63	1.53	23.86	0.16
	Max	19.29	73.67	14.23	514.95	10.09

ND = Undetectable

Table 4.17

Activity ratios of ^{235}U / ^{238}U, ^{234}U / ^{238}U, ^{232}Th / ^{238}U, $^{228}Th/^{232}Th$ and $^{230}Th/^{232}Th$ in the Red Sea coastal sediments

Location	Depth m	^{235}U / ^{238}U	^{234}U / ^{238}U	^{238}U / ^{232}Th	$^{228}Th/^{232}Th$	$^{230}Th/^{232}Th$
Fringing reef area	1.00	0.044	1.17	46.93	30.58	3.73
	1.25	0.034	1.13	126.97	38.50	8.71
	1.50	0.035	1.24	33.29	32.36	2.92
	6.00	0.032	1.12	58.68	25.97	1.96
	7.00	0.031	0.97	39.29	18.35	1.94
	16.0	0.029	1.08	20.45	35.05	1.55
	19.5	0.027	1.13	39.44	59.94	2.56
Open sea	100	0.051	1.19	3.49	10.06	1.08
Main harbour entrance	32.0	0.042	1.29	0.64	4.10	0.88
North harbour	13.0	0.039	1.18	1.03	5.59	0.92
South harbour	17.0	0.048	1.12	0.73	6.51	1.27
	15.0	0.015	1.09	0.56	5.23	0.68
Sanganeb atoll	3.00	0.036	1.16	227.23	98.09	5.41
	750	0.031	1.09	2.62	10.21	1.59
Trinkitat Mersa		0.019	1.27	0.76	2.85	0.74
	Mean	0.034	1.15	40.14	25.56	2.39
	STD	0.009	0.078	59.93	25.10	2.09
	Min	0.015	0.97	0.56	2.85	0.68
	Max	0.051	1.29	227.23	98.09	8.71

Table 4.18

Activity concentration of natural uranium and its decay products in Seagrass and algae collected from the fringing reef area at Port Sudan at depths ranging from 0.5 to 1.5 m

Species name	^{238}U Bq/kg	^{235}U Bq/kg	^{234}U Bq/kg	^{230}Th Bq/kg	^{226}Ra Bq/kg	^{210}Po Bq/kg
Halimeda	29.39	0.95	34.30	0.79	8.19	13.69
Cystoseira	17.29	0.69	13.34	1.35	3.69	32.57
Padina	20.59	0.68	23.27	2.08	4.99	15.04
Sargassum	11.87	0.42	13.63	0.62	9.63	36.37
Seagrass	21.22	0.76	23.62	1.06	7.65	22.68

Table 4.19

Activity concentration of natural thorium, ^{40}K and ^{137}Cs in Seagrass and algae collected from the fringing reef area at Port Sudan at depths ranging from 0.5 - 1.5 m (Bq/kg)

Species name	^{232}Th	^{228}Th	^{40}K	^{137}Cs
Halimeda	0.29	6.02	78.79	0.33
Cystoseira	0.61	6.67	827.49	0.85
Padina	0.61	7.14	538.68	ND
Sargassum	0.25	6.17	719.18	1.32
Seagrass	0.28	1.06	823.32	ND

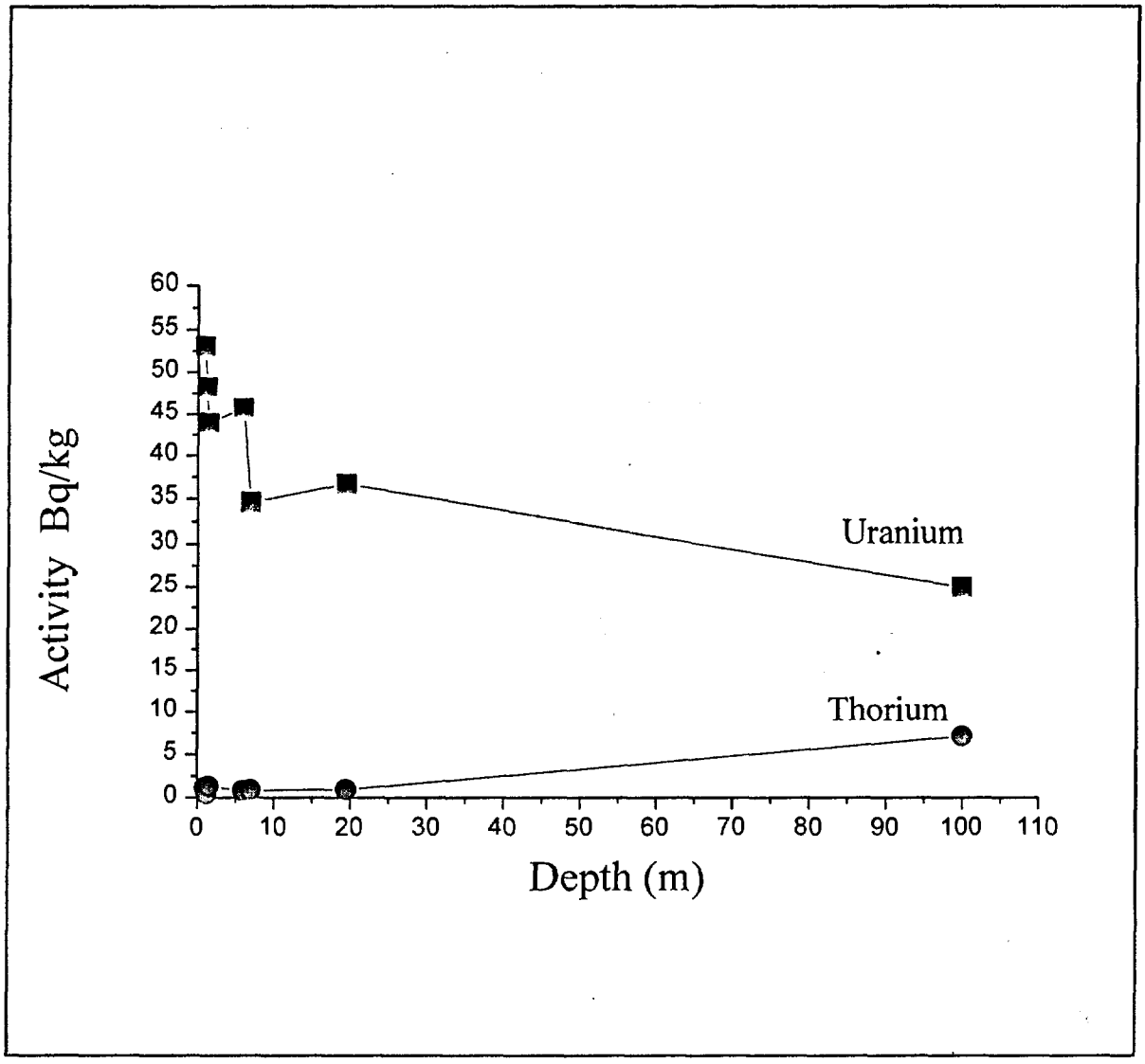

Fig. 4.1: Activity concentration of ^{238}U and ^{232}Th in the sediments collected from the fringing reefs area at Port Sudan vs depth

Table 4.20: Activity concentrations (Bq/kg dry weight) and activity quotients of uranium isotopes and Th/U in Port Sudan harbour sediments

Sample No.	Depth m	OM%	^{238}U	^{235}U	^{234}U	$^{235}U/^{238}U$	$^{234}U/^{238}U$	Th/U
1	65	27.22	8.95	0.38	9.51	0.042	1.06	1.09
2	168	13.86	7.29	0.26	8.82	0.035	1.21	1.53
3	110	19.43	8.59	0.31	9.17	0.036	1.07	2.18
4	57	20.99	7.06	0.31	8.05	0.044	1.14	0.51
5	74	12.92	6.78	0.29	7.52	0.043	1.12	1.81
6	35	28.89	13.42	0.46	14.87	0.034	1.12	0.40
7	33.5	8.44	4.01	0.20	4.42	0.050	1.10	2.88
8	25	12.77	4.99	0.20	5.32	0.041	1.01	1.24
9	22	10.29	3.95	0.22	4.56	0.057	1.15	3.17
10	24	7.77	3.12	0.15	3.54	0.049	1.13	4.03
11	12	6.81	3.31	0.16	3.94	0.048	1.19	3.73
12	3.0	9.38	3.37	0.15	3.83	0.045	1.14	2.97
13	16	7.59	2.71	0.13	3.04	0.047	1.12	4.30
14	19	6.65	3.50	0.24	4.22	0.068	1.20	4.55
15	26	11.05	4.74	0.23	5.23	0.047	1.10	2.25
16	21.5	11.13	4.63	0.14	5.52	0.031	1.19	2.62
17	18.5	12.36	4.90	0.20	5.37	0.042	1.09	2.58
18	14	11.78	6.23	0.26	7.72	0.042	1.24	1.93
19	18	16.21	6.09	0.23	7.18	0.038	1.18	2.05
20	11	11.36	4.34	0.28	4.78	0.065	1.10	2.24
Mean	38.63	13.35	5.59	0.24	6.33	0.045	1.13	2.40
STD	39.97	6.31	2.58	0.08	2.83	0.009	0.06	1.17
Min	3.0	6.65	2.71	0.13	3.04	0.031	1.24	0.40
Max	168	28.89	13.42	0.46	14.87	0.068	1.24	4.55

Table 4.21: Activity concentrations (Bq/kg dry weight) and activity quotients of thorium isotopes in Port Sudan harbour sediments

Sample No.	Depth m	^{232}Th	^{230}Th	^{228}Th	$^{228}Th/Th$	$^{230}Th/Th$	$^{228}Th/^{230}Th$
1	65	9.76	9.26	13.65	1.39	0.95	1.47
2	168	11.18	11.18	15.92	1.42	1.00	1.42
3	110	18.73	16.94	21.73	1.16	0.90	1.28
4	57	3.62	5.15	9.28	2.56	1.42	1.80
5	74	12.29	11.25	16.74	1.36	0.92	1.49
6	35	5.38	7.20	9.81	1.82	1.34	1.36
7	33.5	11.54	10.48	16.89	1.46	0.91	1.61
8	25	6.18	6.83	10.72	1.73	1.11	1.57
9	22	12.51	12.11	15.90	1.27	0.97	1.31
10	24	12.58	11.84	19.58	1.56	0.94	1.65
11	12	12.34	11.73	18.09	1.47	0.95	1.54
12	3.0	10.00	9.44	14.32	1.43	0.94	1.52
13	16	11.66	10.26	16.96	1.45	0.88	1.65
14	19	14.94	14.23	21.64	1.36	0.89	1.53
15	26	10.65	12.23	16.59	1.56	1.15	1.36
16	21.5	12.12	12.68	15.23	1.26	1.05	1.20
17	18.5	12.63	15.94	16.74	1.33	1.26	1.05
18	14	12.02	12.72	17.00	1.41	1.06	1.34
19	18	12.47	13.56	14.49	1.16	1.09	1.07
20	11	9.72	10.56	13.18	1.36	1.09	1.25
Mean	38.6	11.17	11.28	15.72	1.48	1.04	1.42
STD	39.9	3.35	2.88	3.36	0.30	0.15	0.19
Min	3.0	3.62	5.15	9.28	1.16	0.88	1.05
Max	168	18.73	16.94	21.73	2.56	1.42	1.80

Table 4.22: Activity concentrations (Bq/kg dry weight) and activity quotients of uranium isotopes and Th/U in Sawakin harbour sediments

Sample No.	Depth m	OM%	^{238}U	^{235}U	^{234}U	$^{235}U/^{238}U$	$^{234}U/^{238}U$	Th/U
25	40	16.93	12.42	0.47	14.15	0.038	1.14	0.31
26	91	19.34	14.14	0.64	16.43	0.045	1.16	0.38
27	38.5	13.68	24.79	0.89	26.90	0.036	1.09	0.08
28	13.5	7.76	15.34	0.58	17.49	0.038	1.14	0.07
29	15	25.89	17.17	0.65	18.94	0.038	1.10	0.47
30	16	15.68	6.92	0.32	7.53	0.047	1.09	1.45
31	5.5	12.29	3.87	0.19	4.58	0.048	1.18	2.40
Mean	31.36	15.94	13.52	0.53	15.15	0.041	1.13	0.74
STD	29.37	5.73	6.85	0.23	7.42	0.005	0.036	0.87
Min	5.5	7.76	3.87	0.19	4.58	0.036	1.09	0.07
Max	91	25.89	24.79	0.89	26.90	0.048	1.18	2.40

Table 4.23: Activity concentrations (Bq/kg dry weight) and activity quotients of thorium isotopes in Sawakin harbour sediments

Sample No.	Depth m	^{232}Th	^{230}Th	^{228}Th	$^{228}Th/Th$	$^{230}Th/Th$	$^{228}Th/^{230}Th$
25	40	3.79	7.10	6.16	1.62	1.87	0.87
26	91	5.37	8.93	10.27	1.91	1.66	1.15
27	38.5	1.89	35.27	7.68	4.06	18.66	0.23
28	13.5	1.13	14.87	5.58	4.94	13.16	0.38
29	15	8.05	13.02	12.29	1.53	1.62	0.95
30	16	10.04	9.99	13.81	1.38	0.99	1.38
31	5.5	9.29	9.32	11.13	1.19	1.00	1.19
Mean	31.36	5.65	14.07	9.56	2.38	5.57	0.88
STD	29.37	3.57	9.71	3.15	1.49	7.25	0.43
Min	5.5	1.13	7.10	5.58	1.19	0.99	0.23
Max	91	10.04	35.27	13.81	4.94	18.66	1.38

OM% = Organic matter content

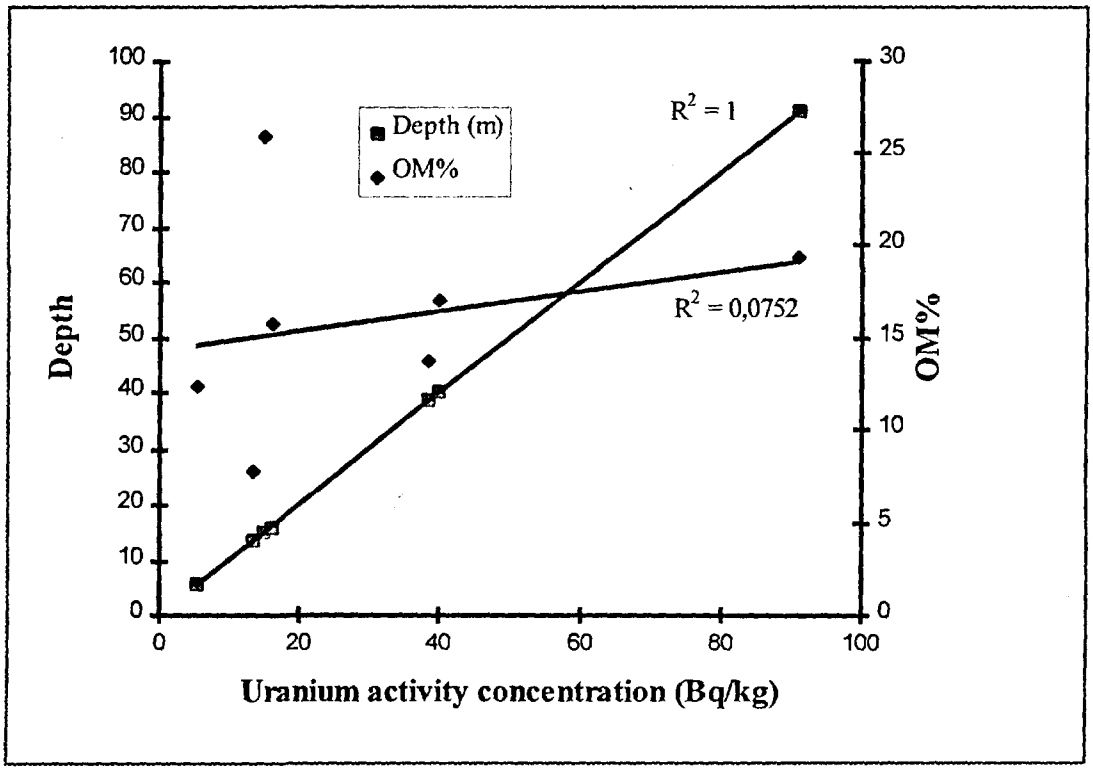

Fig. 4.2: ^{238}U activity concentration in Port Sudan harbour sediments plotted against depth and organic matter

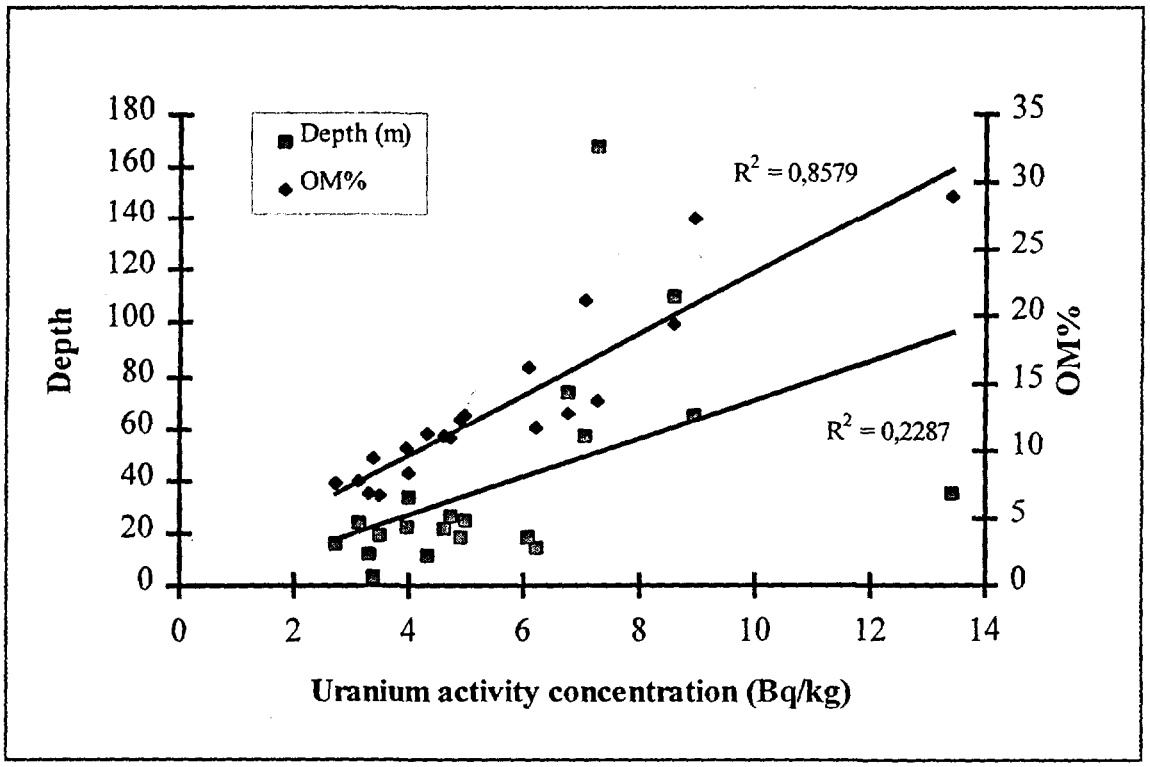

Fig. 4.3: ^{238}U activity concentration in Sawakin harbour sediments plotted against depth and organic matter content

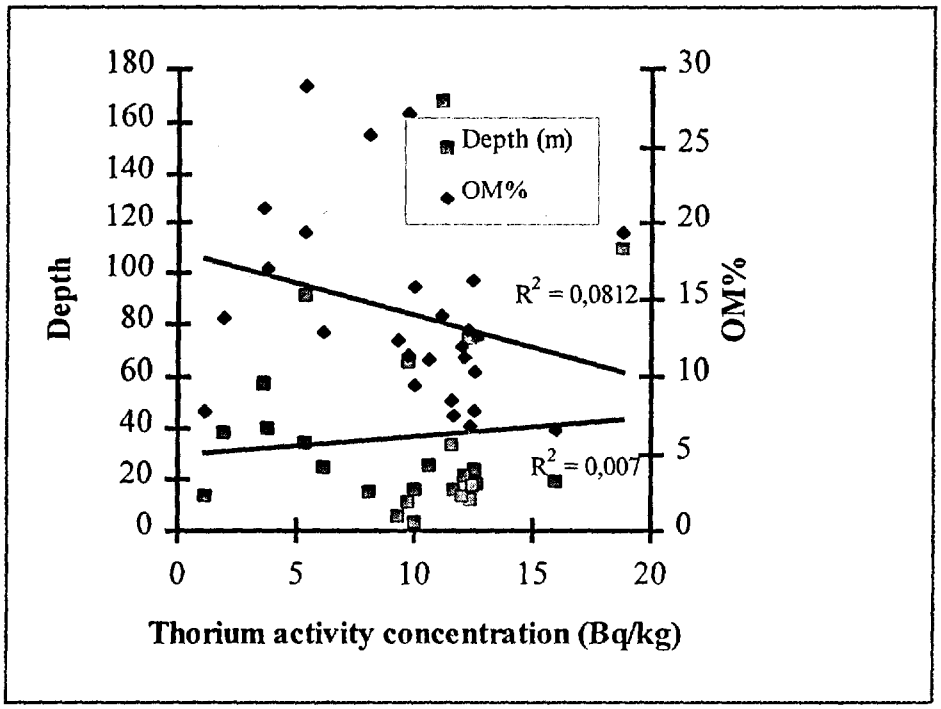

Fig. 4.4: ^{232}Th activity concentration in sediments of Port Sudan and Sawakin plotted against depth and organic matter content

CONCLUSIONS

The external radiation exposure from the ground has been calculated from the measurements of radionuclide activity concentrations in soil from various locations in Sudan. The exposure ranges from 23 nGy/h (at Uro) to 108 nGy/h (at Dumper). The maximum values observed are significantly lower than the extreme values reported in Brazil and India (UNSCEAR,1977).The ranges of ^{238}U, ^{232}Th, ^{226}Ra, ^{228}Th, ^{228}Ra and ^{40}K concentrations in soils are fairly normal compared with those reported for regions of the world. However, owing to the relatively high radionuclide content of soils at Dumper and Arkuri, these districts merit further radiological surveys with regard to outdoor and indoor exposure measurements. Although no data is available on the level of man-made radioactive contamination that might have reached the country prior to the Chernobyl accident in 1986, the small amounts of the fallout nuclide ^{137}Cs measured show that only long-lived radionuclide from the previous atmospheric nuclear explosions remain in the soil. Further study is necessary in order to draw a detailed radiation map of Sudan.

^{238}U and its decay products primarily contribute to the high natural radioactivity of phosphate deposits at Uro and Kurun in the eastern part of the Nuba Mountains. ^{232}Th, ^{235}U and ^{40}K occur in low concentrations and hence they contribute relatively little to the radioactivity of the ore matrix. The additional external radiation exposure for the farmers due to the fertilization with Uro and Kurun ground rock phosphates is negligible compared to the mean terrestrial radiation exposure in the country. However, high occupational radiation exposures are to be expected for persons engaged in the production of

fertilizers or working in fertilizer storehouses owing to inhalation of radon and phosphate fertilizer dust. Assuming complete retention of uranium, radium and polonium the α-activity of the soils will increase after the intensive use of fertilizers especially with Uro rock phosphate. The availability for plant uptake will increase when the fertilizers are applied to acidic soils but any possible effect on humans due to ingestion of food containing high activity of α-emitting nuclides requires further investigation. However, from the estimates given above it can be concluded that the contribution of natural radionuclides contained in rock phosphate fertilizers to the internal radiation exposure of the population should also be low compared with that from other natural radiation sources. The data also indicate a need for further radiological assessments of the communities living in the vicinity of the Uro and Kurun phosphate deposits, where the assessment should incorporate factors implied by using drinking water drawn from underground water supplies and by the use of rocks from these areas as building material. These rock phosphate deposits can further be investigated as a possible radiowaste depository medium because the daughter/parent activity concentration ratios in uranium series indicate the properties of hard rock that influence the design of waste repositories and sealing systems.

Basic information on the concentration levels of natural and man-made radionuclides in the sediments and biota from the Sudanese Red Sea coastal waters have been obtained. The Salient features in sediments of the fringing reefs include the following:

1. High uranium content relative to thorium.
2. Typical oceanic $^{234}U/^{238}U$ disequilibrium ratio of 1.15, on the average.

3. Extremely high $^{228}Th/^{232}Th$ activity ratios.

4. High $^{230}Th/^{232}Th$ activity ratio.

These features collectively suggest that the rate of sedimentation is rapid and that fractions of ^{234}U, ^{228}Th and ^{230}Th have been scavenged from the seawater.

On the other hand the maximum activity concentrations found for ^{238}U and ^{232}Th in the sediments from Port Sudan and Sawakin harbours are comparable to those reported for the Suez Canal sediments though the level of radioactivity in these sediments is generally low compared with coastal marine sediments from some other regions of the world. The general trend in the two sets of the sediment data is that the Th/U activity quotient is greater than unity in Port Sudan and less than unity in Sawakin with the exception of two nearshore samples. A value greater than unity for Th/U ratio, is a feature suggesting high sedimentation rate relative to normal pelagic sediments which represent 80% of the ocean floor and not a significant sink for uranium. Uranium activity concentration show a well-defined positive correlation with both depth and organic matter content of sediments, whereas Th activity is independent. There is a need of further study to determine the effect of grain-size on the level of radionuclides which might be a cause of the observed variations.

The presence of the anthropogenic radionuclide ^{137}Cs in the sediment and the marine species was evident. Although none is available on its levels in this coastal region in the pre-Chernobyl era, the levels measured indicate that it is originated from the previous atmospheric nuclear explosions in the fifties and early sixties because only the long-lived isotope is measurable. Among the marine species analysed, the brown algae *Sargassum* shows slightly higher uptake for both ^{210}Po and ^{137}Cs.

Chapter 5

BIBLIOGRAPHY

Aarkrog, A. Source terms and inventories of anthropogenic radionuclides. *In:* Radioecoloy: Lectures in Environmental Radioactivity, pp. 21 (ed. Holm, E.). World Scientific Publishing Co., Utopia Press, Singapore, 1994.

Adams, P. B. and Passmore, W. O. Critical factors in the determination of the alkaline earth elements in glass by atomic absorption spectrometry. *Anal. Chem.* **38**(4), 630 (1966).

Alan, M. The book of seaweeds, Gordon and Cremonesi Publishers, QK572.9 77-30049 (1977).

Allen, S. E. Chemical Analysis of Ecological Materials. Blackwell Scintific Publications, (1989).

Anderson, R. F. Concentration, vertical flux and remineralization of particulate uranium in seawater. *Geochim. Cosmochim. Acta*, **46**, 1293-1299 (1982).

Andras, S. S. Radioecology and Environmental Protection. Ellis Horwood Limited, England, 1993.

Assinder, D. J., S. M. Mudge and G. S. Bourne. Radiological assessment of the Ribble estuary-1. Distribution of radionuclides in surface sediments. *J. Environ. Radioactivity*, **36**(1):1-19 (1997).

Bagnall, K. W. Chemistry of the rare earth radioelements. Academic Press, New York, (1957).

Barisic, D. Dose rate conversion factors, soil thickness and their influence on natural background dose rate in air above carbonate terrains. *J. Environ. Radioactivity*, **31**(1), 51-70 (1994).

Beretka, J. and Mathew, P. J. Natural radioactivity of Australian building materials, industrial wastes and by-products. *Health Physics*, **48**(1), 280-282 (1985).

Blanchard, L. Rapid determination of lead-210 and polonium-210 in environmental samples by deposition on nickel. *Anal. Chem.*, **38**(2), 189 (1966).

Bril, K. and Holzer, S. Determination of uranium in zirconium ores. A modification of the stannichloride method. *Anal. Chem.*, **33**, 55-8 (1961).

Bock, R. and Bock, E. Separation of inorganic mixtures by partition between two solvents. V. preparation of pure thorium and cerium compounds by extraction with organic solvents. *J. Inorg. Chem.*, **263**, 146-68 (1950).

Boothe, G. F. The need for radiation controls in the phosphate and related industries. *Health Physics*, **32**, 285-290 (1977).

Bouwer E. J., Johon W. M. and McDowel J. W. Uranium assay of phosphate fertilizers and other phosphatic materials. *Health Phys.*, **34**, 345-352 (1978).

Brinkman, K. The geology and mineralization of basement complex in the northeast Nuba Mountains, Sudan, 34pp. Hanover (1986).

Butler, F. E. and Hall, R. M. Determination of actinides in biological samples with bidentate organophosphorus extractants. *Anal. Chem.*, **42**, 1073 (1970).

Callahan, C. M. Ultra-violet determination of uranium in concentrated HCl acid. *Anal. Chem.*, **33**, 1660-4 (1961).

Choppin, D. I. and Rydberg, J. Nuclear chemistry, theory and applications, pp. 429-438. Pergamon Press, Oxford, 1980.

Chow, S. N. and Carwswell, D. J. Effect of phosphate ion on the ion-exchange and solvent extraction properties of thorium. *Australian J. App. Sci.*, **14**, 193-7 (1963).

Cochran, J. K. The oceanic chemistry of the U- and Th-decay series nuclides. In *U-series disequilibrium: Applications to environmental problems*, eds M. Ivanovich and R. S. Harmon. Clarendon Press, Oxford, pp. 384-430 (1982).

Cochran, J. K. The oceanic chemistry of the uranium- and thorium-series nuclides. In *Uranium-series Disequilibrium: Applications to earth, Marine and Environmental Sciences*, M. Ivanovich and R. S. Harmon (Eds). Clarendon Press, Oxford, pp. 334-395 (1992).

Coggle, J. E. Biological effects of radiation (2nd edition), International Publications Service, Tayler and Francis Inc., New York (1983).

Cook, G.B., Duncan, J. F. Modern radiochemical practice, Chapter 1. Clarendon Press, Oxford (1952).

Coomber, D. I. Radiochemical Methods in Analysis, pp.175-218. Plenum press, New York (1975).

Cotton, F. A. and G. Wilkinson. Advanced Inorganic Chemistry: A Comprehensive Text (5th edition), 1145p. Interscience Publishers, New York, 1988.

Culler, F. L. Reprocessing of nuclear fuel and blanket materials by solvent extraction. Pro. Int. Conf. Peaceful Uses of Atomic Energy, Geneva, paper P/822, **9**, pp.464-83. UN, New York, 1956.

Cutter, G. A., K. W. Bruland and R. W. Risbrough. Deposition and accumulation of plutonium isotopes in Antarctica. *Nature* **279**, 628-629 (1979).

Day, P.R. Particle fractionation and particle-size analysis. *In*: C. A. Black, D. D. Evans, J. L.White, L. E. Ensminger and F. E. Clark (Editors), Methods of Soil Analysis. *Agronomy* **9**(1), 914-926 (1965).

DeRegge, P. and Boden, R. Radiochemical analysis techniques: review of chemical separation techniques applicable to α-spectrometric measurements. *Nuclear Instruments and Methods in Physics Research*, **223**, 181-187 (1984).

Dickson, B. L., Meakins, R. L. and Bland, C. J. Evaluation of radioactive anomalies using radium isotopes in ground-water. *J. Geochem. Expl.*, **19**, 195-205 (1983).

Dickson, B. L. And G. E. Wheller. Uranium-seriés disequilibrium in exploration geology. *In*: M. Ivanovich and R. S. Harmon (Eds), Uranium-series Disequilibrium: Applications to Earth, Marine and Environmental Sciences, Chapter 20, pp.704, Clarendon Press, Oxford, (1992)

Duursma, E. G. Geochemical aspects and applications of radionuclides in the sea. Oceanogr. *Mar. Biol. Ann. Rev.*, **10**, 137-223 (1972).

Eakins, J. D. and Morrison, R. T. A new procedure for the determination of lead-210 in lake and marine sediments. *Int. J. Appl. Rad. Isot.*, **29**, 536 (1978).

Eakins, J. D. The application of radiochemical separation procedures to environmental and biological materials. *Nuclear Instruments and Methods in Physics Research*, **223**, 194-199 (1984).

El-Tahawy, M. S., M. A. Farouk, N. M. Ibrahim and S. A. M. El- Mongey. Natural and artificial radionuclides in the Suez Canal bottom sediments and stream water. *Radiat. Phys. Chem*, **44** (½):87-89 (1994).

Eriksson, Å. A convenient method for determination of radium in environmental samples. *International Agrophysics*, **3**(3), 157-163 (1987).

Figgins, P. E. The radiochemistry of polonium. Nuclear Science Series, NAS-NS3037, 1961.

Fisher, N. S., Burns, K. A., Cherry, R. D. and Heyrand, M. Accumulation and cellular distribution of ^{241}Am, ^{210}Po and ^{210}Pb in two marine algae. *Marine Ecol.*, **11**, 233-7 (1983).

Fleischer, R. L. Alpha recoil damage: relation to isotopic disequilibrium and leaching of radionuclides. *Geochim. Cosmochim. Acta*, **52**, 1459-66 (1988).

Flynn, W. W. The determination of low levels of ^{210}Po in environmental materials. *Anal. Chim. Acta*, **43**, 221-227 (1968).

Folsom, T. R., Mohanrao, G. J., and Winchell, P. Fallout caesium in surface sea-water off the california coast by gamma-ray measurements. *Nature* **187**, 480 (1960).

Friedlander, G., J. W. Kennedy, E. S. Macias and J. M. Miller. Nuclear and Radiochemistry (3rd edition), 684 p. John Wiley and Sons, New York, 1981.

Fukai, R. and Yokoyama, Y. Natural radionuclides in the environment. *In*: The Handbook of Environmental Chemistry, **1**/part B. Springer, Berlin, pp. 47-60 (1982).

Fuller, M. J. Inorganic ion-exchange chromatography on oxides and hydrous oxides. *Chromatog. Revs.*, **14**(1), 45-76 (1971).

Gamal, M. The geology and structure of El Biteria area, northeast Nuba Mountains, M.Sc Thesis, Department of Geology, University of Khartoum, Sudan (1987).

Gascoyne, M. Geochemistry of the actinides and daughters. *In*: M. Ivanovich and R.

S. Harmon (Eds), Uranium-series Disequilibrium: Applications to Earth, Marine and Environmental Sciences, Chapter 2, pp.34. Clarendon Press, Oxford, (1992).

Gascoyne, M. and Schwarcz, H. P. Radionuclide migration over recent geologic time in a granitic pluton. *Isot. Geol. Sci.*, **59**, 75-85 (1986).

Girdler, R. W. In: "the world rifts systems" (T.N., Irvine, ed.). *Geol. Surv. Can. Ottawa*, paper 6614, 65-77 (1966).

Goldschmidt, V. M. Geochemistry. Clarendon Press, Oxford (1954).

Green, B. M. R., Lomas, P. R., Bradley, E. J. and Wrixon, A. D. Gamma radiation levels outdoor in Great Britain. London: HMSO; NRPB-R191 (1989).

Halls, D. J., Townshend, A. A study of some interferences in the atomic absorption spectrophotometric of magnesium. *Anal. Chim. Acta*, **36**, 278-285 (1966).

Hallstadius L. A method for the electrodeposition of actinides. *Nuclear Instruments and Methods in Physics Research*, **223**, 266-267 (1984).

Hamilton, E. I. The relative radioactivity of building materials. Am. Ind. *Hyg. Ass. J.*, **32**, 398 (1971).

Harada, K., Burnett, W. C., Larock, P. A. and Cowart, J. B. Polonium in Florida ground-water and its possible relationship to the sulphur cycle and bacteria. *Geochim. Cosmochim. Acta*, **53**, 143-50 (1989).

Harrey, B. R. and Lovett, M. B. The use of yield tracers for the determination of α-emitting activities in the marine environment. *Nuclear Instruments and Methods in Physics Research*, **223**, 224-234 (1984).

Head, J. H. Minimum detectable photopeak areas in Ge(Li) spectra. *Nucl. Instrum. Methods* **98**, 419 (1972).

Hetherington, J. A. and Harvey, B. R. Uptake of radioactivity by marine sediments and implications for monitoring metal pollutants. *Mar. Pollut. Bull.* **9**, 102-106 (1978).

Heye, D. Uranium, thorium and radium in ocean water and deep-sea sediments. *Earth Planet. Sci. Lett.*, **6**:112-16 (1969).

Heyrand, M. and R. D. Cherry. Polonium-210 and lead-210 in marine food chains. Mar. Biol. **52**, 227-236 (1979).

Hirayama, F., Y. Yuasa, A. Tani, M. Naito and K. Miyamaru. A method for rapid radiochemical analysis of transuranium elements in nuclear facilities. *Nucl. Instr. Meth. Phys. Res.* **223**, 188-193 (1984).

Holm, E. and Fukai, R. Method for multi-element α-spectrometry of actinides and its application to environmental radioactivity studies. *Talanta*, **24**, 659-664 (1977).

Holm, E., Ballestra S. and Fukai, R. A method for ion-exchange separation of low levels of americium in environmental materials. *Talanta*, **26**, 791 (1979).

Holm, E. Sources and distribution of anthropogenic radionuclides in marine environment. *In*: Radioecoloy: Lectures in Environmental Radioactivity, pp. 63 (ed. Holm, E.). World Scientific Publishing Co., Utopia Press, Singapore, 1994.

Huh, C. A. and Kadko, D. C. Marine sediments and sedimentation processes. *In*: M. Ivanovich and R. S. Harmon (Eds), Uranium-series Disequilibrium: Applications to Earth, Marine and Environmental Sciences, Chapter 13, pp. 460-486. Clarendon Press, Oxford (1992).

Huh, C-A, Zahnle, D. L., Small, L. F., and Noshkin, V. E. Budgets and behaviours of uranium and thorium series isotopes in Santa Monica Basin sediments. *Geochim. Cosmochom. Acta*, **51**, 1743-54 (1987).

Hussein, E. M. Radioactivity of phosphate ore, superphosphate and phosphogypsum in Abu-Zaabal phosphate plant, Egypt. *Health Physics*, **67**(3), 280-282 (1994).

IAEA. Gamma- ray surveys in uranium exploration. Tech. Rep. Series No.**186**. *International Atomic Energy Agency*, Vienna, Aústria (1979).

IAEA. The environmental behaviour of radium,Vol.**2**. Technical Rep. Series No.**310**. *International Atomic Energy Agency*, Vienna, Austria (1990).

IAEA. The use of gamma-ray data to define the natural radiation environment. The *International Atomic Energy Agency*, IAEA-TECDOC-566, Vienna, Austria (1990).

IAEA. Radioactive contamination of the marine environment (Proceedings of a symposium, Seatle, USA, 10-14 July 1972). *International Atomic Energy Agency*,

Vienna, Austria, xii, pp. 786 (1973).

IAEA. Performance of engineered barriers in deep geological repositories.Technical Reports Series No. **342**. *International Atomic Energy Agency*, Vienna, Austria (1992).

Ishimori, T. Separation of radium D, E and F by ion exchange. *Bull. Chem. Soc. Japan*, **28**, 432-5 (1955).

IAEA. Measurement of radionuclides in food and the environment: A Guidebook. Technical Reports Series No. **295**. *International Atomic Energy Agency*, Vienna, Austria (1989).

Ivanovich, M. Uranium series disequilibria applications in geochronology. *In*: Uranium Series Disequilibrium: Applications to Environmental Problems (eds. Ivanovich, M. and Harmon, R. S). Clarendon Press, New York, 1992.

Jaakkola, T. Radiochemical separations. *In*: Radioecology: Lectures in Environmental Radioactivity (E. Holm, ed.), pp. 233. World Scientific, Utopia Press, Singapore (1994).

Jaworowski, Z. Radioactive lead in the environment and in the human body. *At. Energy Rev.* 7, 3-34 (1969).

Jaworowski, Z. Natural and man-made radionuclides in the global atmosphere. *IAEA Buttetin* **24**, 35-39 (1982).

Jenkins, I. L. and Mckay, H. A. C. Partition of uranyl nitrate between water and organic solvents. VI. salting-out by a second nitrate. *Trans. Faraday Soc.*, **50**, 107-19 (1954).

Joshi, L. U., and Ganguly, A. K. Anomalous behaviour of uranium isotopes in coastal marine environment of the west coast of India. *Geochim. Cosmochim. Acta*, **40**, 1491-96 (1976).

Keating, G. E., McCartney M., and C. M. Davidson. Investigations of the technological enhancement of natural decay series radionuclides by the manufacture of phosphates on the Cumbrian coast. *J. Environ. Radioactivity*, **32**(1-2):53-66 (1996).

Keller, C. Radiochemistry, Ellis Horwood Series in Physical Chemistry, Ellis Horwood Ltd, England (1988).

Kennedy, J., Davis, R. V. and Robinson, B. K. Separation of heavy metals with acid alkylphosphate and phosphonate resins. AERE Report C/R1986 (1956).

Khalil, A. S. M. Fishes in the mangrove ecosystem of the Sudan area, Sudanese Red Sea: population ecology, community structure and species diversity. Unpublished M.Sc thesis, University of Khartoum, Sudan (1994).

Khopar, S. M. and De, A. K. Distribution of some metal ions in the system of bis-(2-ethylhexyl)-590-orthophosphoric acid vs nitric-oxalic acid solution. *J. Atomic Energy Soc. Japan*, **2**, 585-90 (1960).

Kigoshi, K. Alpha-recoil thorium-234: dissolution into water and the $^{234}U/^{238}U$ disequilibrium in nature. *Science*, **173**, 47-8 (1971).

Knab, D. Determination of americium in small environmental samples. *Anal. Chem.* **51**, 1095 (1979).

Ko, R. and Weiller, M. R. Spectrographic determination of thorium in uranium ore. *Anal. Chem.*, **34**, 85-7 (1962).

Kocher, D. C. and Sjoreen, A. L. Dose-rate conversion factors for external exposure to photon emitters in soil. *Health Physics*, **48**(2), 193-205 (1985).

Koide, M., R. Michel, E. D. Goldberg, M. M. Herron and C. C. Langway Jr. Depositional history of artificial radionuclides in the Ross Ice Shelf, Antarctica. *Earth Planet. Sci. Lett.* **44**, 205-223 (1979).

Koide, M. and E. D. Goldberg. $^{241}Pu/^{239+240}Pu$ ratios in polar glaciers. *Earth Planet. Sci. Lett.* **54**, 239-247 (1981).

Koide, M., K. K. Bertine, T. J. Chow and E. D. Goldberg. The $^{240}Pu/^{239}Pu$ ratio, a potential geochronometer. *Earth Planet. Sci. Lett.* **72**, 1-8 (1985).

Koide, M., Bruland, K. W. and Golgberg, E. D. $^{228}Th/^{232}Th$ and ^{210}Po geochronologies in marine and lake sediments. *Geochim. Cosmochim. Acta*, **37**, 1171-87 (1985).

Knoll, G. F., Radiation detection and measurement (2nd edition), John Wiley and Sons, New York (1989).

Korkish, J. Modern methods for the separation of rarer metal ions. Pergamon, Oxford

(1969).

Kraus, K. A. and Nelson, F. Anion-exchange studies of the fission products. Pro. Int. Conf. Peaceful Uses of Atomic Energy, Geneva, 7, 113-25 (1956).

Krishnawami, S., D. Lal, J. M. Martin and M. Meybeck. Geochronology of lake sediments. *Earth Planet. Sci. Lett.* **11**, 407-414 (1971).

Ku, T. L., W. S. Broecker and N. Opdyke. Comparison of sedimentation rates measured by paleomagnetic and the ionium methods of age determination. *Earth Planet. Sci. Lett.*, **4**:1-16 (1968).

Ku, T. L. Uranium series isotopes in sediments from the Red Sea hot-brine area. *In*: E. T. Degenes and D. A. Ross (Eds), Hot-brines and recent heavey metal deposits in the Red Sea, pp.512-24. Springer-Verlag, New York (1969).

Ku, T. L. The uranium series methods of age determination. *Ann. Rev. Earth planet. Sci.*, **4**, 347-80 (1976).

Langmuir, D. Uranium solution-mineral equilibria at low temperatures with sedimentary ore deposits. *Geochim. Cosmochim. Acta*, **42**, 547-69 (1978).

Lally, A. E. and Gloven, K. M. Source preparation in α-spectrometry. *Nuclear Instruments and Methods in Physics Research*, **223**, 259-265 (1984).

Lally, A. E. Chemical procedures. In: M. Ivanovich and R. S. Harmon (Eds), Uranium-series Disequilibrium: Applications to Earth, Marine and Environmental Sciences, Chapter 4, pp. 95. Clarendon Press, Oxford (1992).

Lavrukhina, A. K. Chemical analysis of radioactive materials, London Iliffe Books Ltd (1967).

Leung, K. C., Lau, S. Y. and Poon, C. B. . Gamma- radiation dose from radionuclides in Hong Kong soil. *J. Environ. Radioactivity*, **11**, 279-290 (1990).

Lindeken, C. L. (1980). Radiological considerations of phosphogypsum utilization in agriculture. *In: Proceedings of the International Symposium on Phosphogypsum*, Lake Buena Vista, FL, Borris, D. P. And Boody, P. W. (Eds), Florida Institute of Phosphate Research, pp. 459-80.

Lindeken, C. L., and D. G. Coles (1978). The radium-226 content of agricultural gypsum. *In: Radioactivity in Consumer Products*. Moghissi, A., Carter, M., and Barker, R. (Eds), U.S. Regulatory Commission Report No. NUREG/CP-0001, pp. 369-75.

Livingston, H. D., Bowen V. T. and Burke J. Fallout radionuclides in Mediterranean Sea. Rapp. *Comm. Int. mer.*, **24**, 37-40 (1977).

Love, D. L. and Greendale, A. E. Polarographic determination of technetium and ruthenium radionuclides in fission products. *Anal. Chem.*, **32**, 780 (1960).

Makweba, M. M. The natural radioactivity of the rock phosphates, phosphatic products and their environmental implications. *Sci. Total Environ.*, **133**, 99-110 (1993).

Malanca, A., Pessina, V. and Dallara, G. Assessment of the natural radioactivity in the Brazilain State of Rio Grande Do Norte. *Health Physics*, **65** (3), 298 (1993).

Marsden, F. R. S. Radioactivity of some rocks, soils, plants and bones. *In*: Adams, J. A. S. and Lowder, W. M. (Eds.), The natural radiation environment, pp. 807-824. Chicago, IL, The University of Chicago Press, (1964).

Martell, E. A. Transport patterns and residence times for atmosphric trace constituents vs altitude. Advances in Chemical Series No. 93. Radionuclides in the Environment, pp.139-157 (1970).

Martin, D. B. and Pope, D. G. Separation of tervalent lanthanides from actinides by extraction chromatography. *Anal. Chem.*, **54**, 2552 (1982).

Mayer, S. W., Tompkins, E. R. Ion exchange as a separation method. IV. A theoretical analysis of the column separations process. *J. Am. Chem.Soc.* **69**, 2866-74 (1947).

Mckay, H. A. C. Principles of radiochemistry, pp. 73-82. Butterworth, London (1971).

McCartney, M., P. J. Kershaw, D. J. Allington, A. K. Young and D. Turner. Industrial sources of naturally occurring radionuclides in the eastern Irish Sea. *Radiation Protection Dosimetry*, **45**(1/4):711-714 (1992).

McDonald, P., Cook, G. T., and M. S. Baxter. Natural and artificial radioactivity in

coastal regions of UK. In *Radionuclides in the study of marine processes*. Ed. P. J. Kershaw and D. S. Woodhead. Elsevier Applied Science, London, pp. 329-39 (1991).
Meinke, W. W. United States Atomic Energy Commission Report AECD-2739 (1964).

Michael, P. Hydrogen-ion activity. *In*: C. A. Black, D. D. Evans, J. L. White, L. E. Ensminger and F. E .Clark (Editors), Methods of Soil Analysis. *Agronomy* **9** (2), 914-926 (1965).

Moore, W. S. Amazon and Mississippi river concentrations of uranium, thorium and radium isotopes. *Earth Planet. Sci. Lett.*, **2**: 231-4 (1967).

Morcos, S. A. Physical and chemical oceanography of the Red Sea. Oceanog. *Mar. Biol. Ann. Rev.* **8**, 73-202 (1970).

Myrick, T. E., Berven, B. A. and Haywood, F. F. Determination of concentrations of selected radionuclides in surface soil in the United States. *Health Physics*, **35** (3), 613-642 (1983).

Murphy, J. and Riley, A. A modified single solution method for the determination of phosphate in natural waters. *Anal. Chem. Acta*, **27**, 31-36 (1962).

Möbius, S. Experiments for training in nuclear and radiochemistry. School for Nuclear Technology, Karlsruhe, GMBH, ISSN0303-4003 (1988).

Naokes, J. E., F. Schönholer and H. Polash (Eds), Proc. Int. Conf. Advances in liquid scintillation spectrometry, Vienna, Austria (1992).

Nedwell, D., Parkes, S., Upton, A. And D. J. Assinder. Seasonal fluxes across the sediment-water interface, and processes within North Sea sediments. *Phil. Trans. R. Soc. Lond. A*, **343**:519-29 (1993).

Nemodruck, A. A. and Verotinitskaya, I. E. Extraction luminescence method for determination of uranium in soils, silts, plants and animal tissues. *Anal. Chem.*, **17**, 481-5 (1962).

Othman, I., T. Yassine and I. S. Bhat. The measurement of some radionuclides in the marine coastal environment of Syria. *The Science of the Total Environment*, **153**, 57-60 (1994).

Overman, R. T. And H. M. Clark. Radioisotope techniques, Chapter 9, pp. 344. McGraw-hill Book Company, New York (1960).

Pasternack, B. S. And N. H. Harley. Detection limits for radionuclides in the analysis of multi-component gamma-spectrometer data. *Nucl. Instrum. Methods* **91**, 533-540 (1971).

Parks, G. A. and Pohl, D. C. Hydrothermal solubility of uraninite. *Geochim. Cosmochim. Acta*, **52**, 863-75 (1988).

Pennington, W., R. S. Cambray and E. M. Fisher. Observations of lake sediments using fallout ^{137}Cs as atracer. *Nature* **242**, 324-326 (1973).

Pennington, W., Cambray, R. S., Eakins, J. D., and Harkness, D. D. Freshwater Biol. **6**, 317 (1976).

Pentreath, R. J. Alpha-emitting nuclides in the marine environment. *Nucl. Instr. Meth. Phys. Res.* **223**, 493-510 (1984).

Pentreath, R. J. General review of literature relevant to coastal water discharges. In: Behaviour of radionuclides released into coastal waters. IAEA-TECDOC-329, 17-66 (1985).

Pfister, H. And H. Pauly (1980). Occupational dose from natural radionuclides in phosphate fertilizers. *Radiat. Environ. Biophys.*, **16**(2).

Pfisher, H., Philipp, G. and Pauly, H. Population dose from natural radionuclides in phosphate fertilizers. Rad. and Environm. Biophys. **13**, 247-261 (1976).

Pfeifer, V. and Hecht, F. Extraction of uranium. Microchim. Acta, **3**, 378-89 (1960).

Probonas, M. and Kritidis, P. The exposure of the Greek population to natural gamma radiation of terrestrial origin. *Radiation Protection Dosimetry*, **46**(2), 123-126 (1993).

Quindos, L. S., Fernandez, P. L., Soto, J., Rodenas, C. and Gomez, J. Natural radioactivity in Spanish soils. *Health Physics*, **66**(2), 194 (1993).

Ritchie, J. C., J. R. McHenery and A. C. Gill. Dating recent reservoir sediments. Limnol. *Oceanogr.* **18**, 254-263 (1973).

Robbins, J. A. Geochemical and geophysical applications of radioactive lead. In: The biochemistry of lead in the environment, pp. 285-393 (ed. Nriagu, J. O.). Elsevier, North Holland, 1978.

Roos P., Holm E., Persson R. B. R. Comparison of AMP precipitate method and impregnated $Cu_2[Fe(CN)_6]$ filters for the determination of radiocaesium concentration in natural waters. *Nuclear Instruments and Methods in Physics Research*, **A 339**, 282-286 (1994).

Roessler, C. E. (1984). The radiological aspects of phosphogypsum. *Proc. of the Seminar on Phosphogypsum*, Miami, Florida Institute of Phosphate Research, pp. 11-36.

Roessler, C. E. (1988). Radiological assessment of the application of phosphogypsum to agricultural land. *In: Proceedings of the second International Symposium on Phosphogypsum*, G. M. Lloyd (Ed.), Florida Institute of Phosphate Research, Miami, Florida, pp. 5-23.

Roessler, C. E., Smith, Z. A., Bolch, W. E., and Prince, R. J. Uranium and radium-226 in Florida phosphate materials. *Health Phys.*, **37**, 269-277 (1979).

Roser, F. X., Kegel, G. and Cullen, T. L. Radioactivity of some high-background areas in Brazil. *In*: adams, J. A. S. and Lowder, W. M., eds. The natural radiation environment, pp. 855-72. Chicago, IL, The University of Chicago Press (1964).

Rosholt, J. N., Doe B. R. And M. Tatsumoto. Evaluation of the isotopic composition of uranium and thorium in soil profiles. *Geol. Soc. Am. Bull.*, 77, 987 - 1004 (1966).

Said, R.The geology of Egypt. Published for the Egyptian General Petroleum Corporation, CONOCO, Hurghada Inc. And repsol Exploration. Balkema, Rotterdam (1990).

Sam, A. K. and Eriksson, Å. Radium uptake by vegetation grown in Western Sudan. *J. Environ. Radioactivity*, **29**(1), 27-38 (1995).

Sam, A. K. and Holm, E. The natural radioactivity in phosphate deposits from Sudan. *Sci. Total Environ.*, **162**, 173-178 (1995).

Schönholer, F. Liquid scintillation spectrometry in environmental measurements. *The Science of the Total Environment*, **173/174**, 29-40 (1995).

Sedlet, J. Actinium, astatine, francium, polonium and protactinium. *In*: Treatise on Analytical Chemistry, Part II. Systematic Analytical Chemistry of the Elements, Vol.4, pp. 219-366 (eds. Kollhoff, I. M. and Elving, P. J.). Interscience Publishers, New York, 1964.

Sharif, A. K. M., A. B. Bilkis, S. Roy, M. D. H. Sikder, K. M. Idriss Ali and S. Safiullah. Concentrations of radionuclides in coastal sediments from the Bay of Bengal. *The Science of the Total Environment*, **158**, 1-8 (1994).

Shimmield, G.B. and Price, N. B. The scavenging of ^{230}Th and ^{231}Pa during pulsed hydrothermal activity at 20 °S, East Pacific Rise. Geochim. *Cosmochim. Acta*, **52**, 669-77 (1988).

Skwarzec, B. And L. Falkowski. Accumulation of ^{210}Po in selected species of Baltic invertebrates. *J. Environ. Radioactivity*, **8**, 99-109 (1988).

Shuktomova, I. I., Titaeva, N. A., Taske, A. I. And R. M. Aleksakhin. Behaviour of uranium, thorium and radium in mountain tundra soils. *Soviet Soil Sci.*, **51**, 51 - 56 (1983).

Sill, C. W. and D. G. Olson. Sources and prevention of recoil contamination of solid state alpha detectors. *Anal. Chem.* **42**, 1596-1607 (1970).

Sill, C. W. Determination of thorium and uranium isotopes in ores and mill tailings by α-spectrometry. *Anal. Chem.* **49**, 618-621(1977).

Sill, C. W. and Williams, R. I. Preparation of actinides for α-spectrometry without electrodeposition. *Anal. Chem.*, **53**, 412 (1981).

Singh, N. P. and Wrenn, M. E. Tracers and methods for determining thorium and uranium in biological samples. *In*: Actinides in man and animals (Proc. of the Snowbird Actinide Workshop), pp. 53-68 (1979).

Stanner, D. A. and S. R. Aston. Factors controling the interactions of ^{137}Cs with suspended and deposited sediments in estuarine and coastal evironment. *In*: Impacts of Radionuclides Releases into the Marine Environment. IAEA-SM-248/141, pp. 131-141 (1981).

Strehlow, F. W. E. An ion-exchange selectivity scale of cations based on equilibrium distribution coefficients. *Anal. Chem.*, **32**, 1185-8 (1960).

Strehlow, F. W. E., Rethemeyer, R. and Bothma, C. J. C. Ion- exchange selectivity scale for cations in nitric and sulphuric acid media with a sulfonated polystyrene resin. *Anal. Chem.*, **37**, 106-11 (1965).

Swartz, D. H. and Arden, D. D. Geologic history of Red Sea area. *Bull. Am. Ass. Petrol. Geol.* **44**, 1621-1637 (1960).

Talvite, N. A. Electrodeposition of actinides for α-spectrometric determination. *Anal. Chem*, **44**, 280 (1972).

Titayeva, N. A., Taskayev, A. I., Ovshenkov, V. Y., Aleksakhin, R. M. and Shuktomova, I. I. Uranium, thorrium and radium isotope compositions in solid in prolonged contact with radioactive stratal water. *Geoch. Inter.*, **14**, 57-63 (1977).

Thurber, D. L. Anomalous $^{234}U/^{238}U$ in nature. *J. Geophys. Res.*, **67**:4518-20 (1962).

Todd, J. F., Elsinger R. J. And W. S. Moore. The distribution of uranium, radium and thorium isotopes in two anoxic fjords: Framvaren fjord (Norway) and Saanich Inlet (British Columbia). *Marine Chemistry*, **23**:392-415 (1988).

UNSCEAR. United Nations Scientific Committee on the Effects of Atomic Radiation. Sources and effects of ionizing radiation. Suppl. No. **16** (A/5216), pp 20. United Nations, New York, (1966).

UNSCEAR. United Nations Scientific Committee on the Effects of Atomic Radiation. Sources and effects of ionizing radiation. E77LX.1. 725 pp, United Nations, New York (1977).

UNSCEAR. United Nations Scientific Committee on the Effects of Atomic Radiation. Sources and Effects of Ionizing Radiation. Report to the General Assembly, with Scientific Annexes, United Nations, New York (1982).

UNCSEAR. United Nations Scientific Committee on the Effects of Atomic Radiation. Sources and effects of ionizing radiation. Report to the General Assembly, with Scientific Annexes, United Nations, New York (1988).

UNSCEAR. United Nations Scientific Committee on the Effects of Atomic Radiation. Sources and effects of ionizing radiation. Report to the General Assembly, with Scientific Annexes, United Nations, New York (1993).

Urry, W. D. Radioactive determination of small amounts of uranium. *Am. J. Sci.*, **239**, 191-203 (1941).

Vogel's. Textbook of Quantitative Inorganic Analysis (4th edition), Longman Group Ltd, 1978.

White, J. C., and Ross, W. J. Separations by solvent extraction with Tri-n-OctylPhosphine Oxide. Nuclear Science Series NAS-NS-3102, U.S. National Academy of Sciences (1961).

Wilson, O. J. Numerical calculation of the geometric efficiency of circular detector and surface source arrangements. Australian Radiation Laboratory, ARL/TR027 (1980).

Wood, D. F. and Mckenna, R. H. Determination of small amounts of uranium in hafnium, zirconium and zircaloy-2. *Anal. Chim. Acta*, **27**, 446-53 (1962).

Yamato, A. An anion exchange method for the determination of ^{214}Am and plutonium in environmental and biological samples. *J. Radioanal. Chem.*, **75**, 265 (1982).

Yang, H. S., Y. Nozaki, H. Sakai, Y. Nagaya and K. Nakamura. Natural and man-made radionuclide distributions in Northwest pacific deep-sea sediments: rates of sedimentation, bioturbation and ^{226}Ra migration. *J. Geochim.*, **20**, 29 (1986).

Yu-Ming Lin, Pei-Huo, Ching-Jiang Chen and Ching-Chung Huang. Measurements of terrestrial gamma radiation in Taiwan, Republic of China. *Health Physics*, **52**(6), 805-811 (1987).

*Bacon, M. P. And R. F. Anderson. Distribution of thorium isotopes between dissolved and particulate forms in the deep sea. *J. Geophysical Research*, **87**(C3): 2045-2056 (1982).

Bhat, S. G., Krishnaswami, S, Lal D. Rama and W. S. Moore. ^{234}Th/^{238}U ratios in the ocean. *Earth planet. Sci. Lett.*, **5**:483-91(1969).

Chen, J. H., Edwards R. L. And G. J. Wasserburg. ^{238}U, ^{234}U and ^{232}Th in seawater. *Earth and Planetary Science Letters*, **80**: 241-251(1986).

Kaufman A., Li, Y. H., and K. K. Turekian. The removal rates of ^{234}Th and ^{228}Th from water of the New York Bight. *Earth planet. Sci. Lett.*, **54**:385-92 (1981).

Murnane R., J. L. Sarmiento and M. P. Bacon. Thorium isotopes, particle cycling models, and inverse calculations of model rate constants. *J. Geophsical Research*, 99(C2): 3393-3405(1990).

Nozaki, Y and Y. Horibe. The water column distributions of thorium isotopes in the western north Pacific. *Earth and Planetary Science Letters*, **54**: 203-216 (1981).

Scott, M. R.Thorium and uranium concentrations and isotope ratios in river sediments. *Earth Planet. Sci. Lett.*, **4**:245-52 (1968).

Appendix

The dose rate due to the external γ- radiation of terrestrial origin was evaluated by use of the following equation:

$$D = 0.010\ A_1 + 0.506\ A_2 + 0.284\ A_3 + 0.421\ A_4 + 0.045\ A_5$$

where D is the absorbed dose rate in nGy/h and A_1, A_2, A_3, A_4 and A_5 are the specific activities in Bq/kg of the radionuclides ^{238}U, ^{226}Ra, ^{228}Ra, ^{228}Th and ^{40}K respectively. The external radiation exposure over the arable land due to the natural radionuclides contained in the rock phosphate fertilizers was obtained using the following formula:

$$D = 0.87\ (\sum \Gamma_i\ A_i)\ \pi\ \ln(1 + [R^2/\ a^2]) \qquad \text{rd/h}$$

where,

D is the γ- dose rate in air 1 m above the ground level in rd/h,

A_i the activity per unit area of the i-th γ-emitting radionuclide in Ci/m^2,

Γ_i the specific γ-dose rate constant for the γ-radiation of the i-th radionuclide in $R.m^2/Ci.h$; set equal to 0.826 $R.m^2/Ci.h$ for radium decay products and to 0.081 $R.m^2$ /Ci.h for ^{40}K, R the radius of the considered area, and a the height above the ground in m.

(1 Gy = 100 rd, 1 Ci = 3.7×10^{10} Bq).